SAE Aerospace
An SAE International Group

AEROSPACE INFORMATION REPORT

SAE AIR1168/13

Issued 1999-11
Reaffirmed 2006-03

Spacecraft Equipment Environmental Control

PREFACE

This document is one of 14 Aerospace Information Reports (AIR) of the Third Edition of the SAE Aerospace Applied Thermodynamics Manual. The manual provides a reference source for thermodynamics, aerodynamics, fluid dynamics, heat transfer, and properties of materials for the aerospace industry. Procedures and equations commonly used for aerospace applications of these technologies are included.

In the Third Edition, no attempt was made to update material from the Second Edition nor were SI units added. However, all identified errata were corrected and incorporated and original figure numbering was retained, insofar as possible.

The SAE AC-9B Subcommittee originally created the SAE Aerospace Applied Thermodynamics Manual, and, for the Third Edition, used a new format consisting of AIR1168/1 through AIR1168/10. AIR1168/11 through AIR1168/14 were created by the SAE SC-9 Committee.

The AIRs comprising the Third Edition are shown below. Applicable sections of the Second Edition are shown parenthetically in the third column.

AIR1168/1	Thermodynamics of Incompressible and Compressible Fluid Flow	(1A,1B)
AIR1168/2	Heat and Mass Transfer and Air-Water Mixtures	(1C,1D,1E)
AIR1168/3	Aerothermodynamic Systems Engineering and Design	(3A,3B,3C,3D)
AIR1168/4	Ice, Rain, Fog, and Frost Protection	(3F)

TO PLACE A DOCUMENT ORDER: **Tel: 877-606-7323 (inside USA and Canada)**
Tel: 724-776-4970 (outside USA)
Fax: 724-776-0790
Email: custsvc@sae.org
SAE WEB ADDRESS: **http://www.sae.org**

PREFACE (Continued)

AIR1168/5	Aerothermodynamic Test Instrumentation and Measurement	(3G)
AIR1168/6	Characteristics of Equipment Components, Equipment Cooling System Design, and Temperature Control System Design	(3H,3J,3K)
AIR1168/7	Aerospace Pressurization System Design	(3E)
AIR1168/8	Aircraft Fuel Weight Penalty Due to Air Conditioning	(3I)
AIR1168/9	Thermophysical Properties of the Natural Environment, Gases, Liquids, and Solids	(2A,2B,2C,2D)
AIR1168/10	Thermophysical Characteristics of Working Fluids and Heat Transfer Fluids	(2E,2F)
AIR1168/11	Spacecraft Boost and Entry Heat Transfer	(4A,4B)
AIR1168/12	Spacecraft Thermal Balance	(4C)
AIR1168/13	Spacecraft Equipment Environmental Control	(4D)
AIR1168/14	Spacecraft Life Support Systems	(4E)

F.R. Weiner, formerly of Rockwell International and past chairman of the SAE AC-9B Subcommittee, is commended for his dedication and effort in preparing the errata lists that were used in creating the Third Edition.

TABLE OF CONTENTS

LIST OF FIGURES

LIST OF FIGURES (Continued)

LIST OF FIGURES (Continued)

LIST OF TABLES

1. INTRODUCTION:

1.1 Scope:

This part of the manual presents methods for arriving at a solution to the problem of spacecraft inflight equipment environmental control. The temperature aspect of this problem may be defined as the maintenance of a proper balance and integration of the following thermal loads: equipment-generated, personnel-generated, and transmission through external boundary.

Achievement of such a thermal energy balance involves the investigation of three specific areas:

1. Establishment of design requirements.
2. Evaluation of properties of materials.
3. Development of analytical approach.

The solution to the problem of vehicle and/or equipment pressurization, which is the second half of major environmental control functions, is also treated in this section. Pressurization in this case may be defined as the task associated with the storage and control of a pressurizing fluid, leakage control, and repressurization. Although secondary to the thermal energy balance, the function of pressure control is nevertheless an important aspect of the overall environmental problem.

1.2 Environmental Control Systems:

Environmental control systems (ECS) must operate in a continuously changing radiant thermal energy exchange condition with the Sun, Earth, and space, and with variable internal equipment loads. Frequently, during the operational phase, concentrated amounts of energy must be dissipated from small components with small external surfaces. The internally generated heat loads may be cyclic but also random with respect to the orbit.

Some equipment such as actuators, attitude control devices, or storage tanks may be partially exposed and require special treatment. Other components will function properly only if pressurized, while in some instances pressurization is used as a means of eliminating the need for qualification in a hard vacuum. These installation techniques will introduce their own thermal control problems and contribute to the selection of a specific ECS configuration.

1.3 Nomenclature:

Wherever the same symbol is used in the text for different properties, the paragraph number is included in the definition as a convenience and to avoid ambiguity. Variations of symbol usage in an equation may be defined in the explanatory list following the equation. Thermoelectric nomenclature is listed separately in 4.6.4.1.

A	=	Heat transfer surface, ft^2 or in^2
a	=	$1-\frac{D_e}{D_0}$ = Taper parameter (4.6.1.6, Equation 101)
C	=	Specific heat, W-s/°F, Btu lb-ft^3
C	=	Parameter, dimensionless (Equations 24 to 27)
COP	=	Coefficient of performance, dimensionless
c_p	=	Specific heat capacity at constant pressure, Btu/lb-°F
c_v	=	Specific heat capacity at constant volume, Btu/lb-°F
D	=	Diameter, ft, in
E	=	Blackbody emissive power, Btu/h-ft^2 (4.4)
E	=	Planetary emission, Btu/h
E	=	Potential, Btu/h-ft^2 (4.4.6.1)
F	=	Configuration factor, dimensionless (4.4.6.1, Equation 63)
F	=	Fraction of vapor condensed in tube, dimensionless (4.6.1.6)
F	=	Wind force, lb (4.4.3.3)
°F/W	=	°F per watt (4.2.1.2) (Tables 5 and 6)
f	=	Fractional volume of insulation occupied by fibers, dimensionless (4.2, Equation 2)
f	=	Friction factor, dimensionless
f	=	Interchange factor, dimensionless
f	=	Mean friction factor, dimensionless (4.6.1)
G	=	Sum of all incident radiation, Btu/h-ft^2
G	=	Mass velocity, lb/s-ft^2 (5.2.3)
g	=	Gravitational force, in/s^2
g'	=	Artificial gravitational force, in/s^2
g_0	=	Gravitational acceleration on Earth, cm/s^2
gρ or ρg	=	Specific weight (density), lb/ft^3
$g\rho_f$	=	Fin specific weight, lb/ft^3
$g\rho_t$	=	Tube specific weight, lb/ft^3
H	=	Film heat transfer parameter, Btu/h-ft^2-°F (4.4.3.2, Equation 52)
H	=	Adiabatic head, ft
h	=	Altitude, miles (4.2)
h	=	Surface heat transfer coefficient, Btu/h-ft^2-°F (4.4.2.3)
h_c	=	Film condensation coefficient, Btu/h-ft^2-°F (4.6.1.6)
h_r	=	Radiation heat transfer coefficient, Btu/h-ft^2-°F
ID	=	Inside diameter, in
J	=	Radiosity, Btu/h-ft^2
K	=	Constant, dimensionless (4.4.2.3)
K	=	Fin thermal conductivity, Btu/s-ft-°F

1.3 (Continued):

K	=	Heat transfer coefficient, dimensionless (Equation 31)
K	=	Parameter for physical properties of fluid (4.6.1.2, Equation 89)
k	=	Thermal conductivity, Btu-ft/h-ft^2-°F
k'	=	Apparent thermal conductivity, Btu-ft/h-ft^2-°F
L	=	Fin length, ft (4.6.1)
L	=	Latent heat of evaporation, Btu/lb
M	=	Mach number, dimensionless
m	=	Molecular weight (5.2)
m	=	Fluid mass, lb
N	=	Number of parallel tubes (4.6.1.6)
N_s	=	Specific speed, dimensionless (4.6.3.4, Equation 122)
N_{Bo}	=	Bonde number $= \frac{D_h^2 \rho g k g_0}{\sigma}$ (4.6.1.1)
N_{We}	=	Weber number $= \frac{D_h \rho g V^2}{\sigma}$ (4.6.1.1)
N_{Re}	=	Reynolds number $= \frac{\rho V \delta}{\mu}$ (4.6.1.5)
n	=	Number of shields (4.2.2.1)
P	=	Pump power parameter, dimensionless (4.4.3.2)
P	=	Pressure, psi (4.4)
Q	=	Internal heat load rate, Btu/h (4.2)
Q	=	Heat input, Btu (4.2)
Q	=	Heat load, Btu/min (4.4.3.3), Btu/s (4.6.2.3)
Q_{abs}	=	Incident solar radiation absorbed, Btu/h-ft^2 (4.4.6.1)
Q_c	=	Cooling load, Btu/min (4.6.1)
Q_f	=	Volumetric flow rate, ft^3/min
Q_R	=	Condenser-radiator heat rejection rate, Btu/s (4.6.1.4)
q	=	Heat transfer rate, Btu/h (4.2.1.1 and 4.4.2.3)
q'	=	Heat transfer rate/unit area, Btu/h-ft^2
Q/V_1	=	Refrigeration effect/unit volume of refrigerant, Btu/ft^3 (4.6.2.2)
R	=	Universal gas constant, ft-lb/lb-°R
R	=	Earth radius, miles
R	=	Reflected solar energy from planet, Btu/h-ft^2
R_R	=	Radiation resistance, h-°F/Btu (4.4.6.1, Equation 80)
R_T	=	Combined conduction and radiation resistance, h-°F/Btu (4.4.6.1, Equation 81)
r	=	Pressure ratio, dimensionless (4.6.1 and 4.6.3.2)
r	=	Albedo, dimensionless
r	=	Parameter, dimensionless (Equation 6)
S	=	Solar radiation, W/ft^2 (4.2.2.1)
S	=	Solar constant = 430 Btu/h-ft^2 (Figure 20)
S	=	Entropy, Btu/°R
T	=	Temperature, absolute, °R

1.3 (Continued):

t	=	Temperature, °F, °C
u	=	Velocity, ft/h
u	=	Volume flow, ft^3/h (4.4.3.3)
V	=	Axial velocity, ft/s
W	=	Weight, lb
W	=	Combined tube and fin weight, lb
w	=	Weight flow, lb/h (4.4.2.3)
w	=	Net heat flow per unit area, W/ft^2 (4.2.2.1, Equation 9, Figure 16)
X	=	Tube length, ft (4.6.1.5)
Y	=	Expansion factor, dimensionless
Y	=	Blade twist, dimensionless (4.6.1.2, Equation 88)
Z_0	=	Combined figure of merit, 1/K (4.5.5, Equation 83)
α	=	$\frac{2\pi\delta}{\lambda}$ = Wave number (4.6.1.5, Figure 66)
γ	=	Ratio of specific heats, (c_p/c_v), dimensionless
δ	=	Fin thickness, in
δ	=	Film thickness, ft (4.6.1.5, Equation 98)
$\in$	=	Porosity factor (4.6.1.3)
$\in$	=	Emissivity, dimensionless
$\in$	=	Dielectric constant, dimensionless (Table 14)
η_f	=	Efficiency, dimensionless
η_c	=	Compressor efficiency, dimensionless
η_{ct}	=	Efficiency based on Carnot cycle, dimensionless
η_t	=	Turbine efficiency, dimensionless
θ	=	Angle between incident solar rays and the normal to the surface, deg
θ_s	=	Angle between Earth-Sun line and vertical from planet to satellite, deg
θ_1	=	Slant angle measured from skin surface, deg
θ_2	=	Irradiation angle with respect to the normal to surface, deg
λ	=	Wavelength, microns
μ	=	Micron (10^{-6} m)
μin	=	Microinch (10^{-6} in)
μ	=	Viscosity, poise (4.4.2.4)
μ	=	Viscosity, lb/ft-s
ρg	=	Specific weight (density), lb/ft^3
σ	=	Surface tension, lb/ft (4.6.1.3), dynes/cm (4.6.1.1)
σ	=	Stefan-Boltzmann constant (0.173×10^{-8}) Btu/h-ft^2 -T^4
τ	=	Time, s, min, h
$\Delta\tau$	=	Time interval
φ	=	Slant angle, deg (4.6, Equation 64)
ω	=	Rotational speed, rpm (4.6.1.2)

1.3 (Continued):

Subscripts:

a	=	Air
a	=	Axial
abs	=	Absorbed
ad	=	Adiabatic
b	=	Boiling
C	=	Condenser
c	=	Cold
c	=	Compressor
c	=	Conductance
c	=	Critical flow (5.1.1)
c	=	Critical point (5.2)
cd	=	Conductivity of gas (4.2.1.3)
ct	=	Carnot
cv	=	Conductivity due to convection (4.2.1.3)
E	=	Earth or planet (4.2)
E	=	Equipment or compartment (4.4.2.3)
E	=	Source heat exchanger (4.6.1 and 4.6.3)
e	=	Earth
e	=	Evaporator
e	=	Smaller (4.6.1.6)
eff	=	Effective
ex	=	Exit
f	=	Fin
f	=	Fluid
fg	=	Evaporation (4.6.1.3)
g	=	Gas
gen	=	Generated
H	=	Plumbing hardware
Hx	=	Heat exchanger
h	=	Hot
h	=	Hydraulic
in	=	Inlet
L	=	Length
m	=	Mean
n	=	Number
o	=	Internal body surface
P	=	Pump
R	=	Reflected solar
R	=	Rejection
r	=	Radiation
ra	=	Radiation (4.2.1.3)
s	=	Solar

1.3 (Continued):

s	=	Specific speed
sc	=	Conductivity of solid conductor due to fiber content
sink	=	Heat sink
T	=	Tank (4.4.2.3)
T	=	Overall or total (4.2 and 4.4.6.1)
t	=	Tube
turb	=	Turbine
*	=	Reference area
0	=	Reference properties

Superscripts:

$\overline{x}$	=	Average x

1.4 Common Abbreviations:

%	=	Percent
abs	=	Absolute
AC	=	Alternating Current
A	=	Ampere
Al, AL	=	Aluminum
ARS J.	=	American Rocket Society Journal
ASD	=	Aeronautical Systems Division (USAF)
ASME	=	American Society of Mechanical Engineers
atm	=	Atmosphere
bp (Bp)	=	Boiling Point
Btu	=	British Thermal Unit
°C	=	Degrees Centigrade
cal	=	Calorie
cm	=	Centimeter
comp	=	Compressor
COP	=	Coefficient of Performance
cps	=	Cycles per second
ct	=	Carnot
DC	=	Direct current
deg	=	Degree
dia.	=	Diameter
ECS	=	Environmental control system
eff	=	Efficiency
Emf	=	Electromotive force
°F	=	Degrees Fahrenheit
ft	=	Feet
g	=	Gravity
gal	=	Gallon

1.4 (Continued):

g	=	Gram
gpm	=	Gallons per minute
hp	=	Horsepower
h	=	Hour
Hx	=	Heat exchanger
Hz	=	Hertz, cps
in	=	Inch
Inst.	=	Institute
J.	=	Journal
K	=	Kelvins (formerly called degrees Kelvin)
kg	=	Kilogram
kW	=	Kilowatt
lb	=	Pound
m	=	Meter
max	=	Maximum
mil	=	0.001 in
Mil.	=	Military
min	=	Minimum
min	=	Minute
MIT	=	Massachusetts Institute of Technology
mm	=	Millimeter
mol	=	Mole
mol.	=	Molecular
NACA	=	National Advisory Committee for Aeronautics
p. (pp.)	=	Page(s)
psfa	=	Pounds per square foot absolute
psi	=	Pounds per square inch
psia	=	Pounds per square inch absolute
psig	=	Pounds per square inch gage
°R	=	Degrees Rankine
rms	=	Root-mean-square
rpm	=	Revolutions per minute
SAE	=	Society of Automotive Engineers
sat	=	Saturated
s	=	Second
std (STD)	=	Standard
TN	=	Technical Note
ton (of refrigeration)	=	200 Btu/min
TR	=	Technical report
Trans	=	Transactions
USAF	=	United States Air Force
vol	=	Volume
W	=	Watt
WADC	=	Wright Air Development Center (USAF)

1.4 (Continued):

WADD	=	Wright Aeronautical Development Division (USAF)
wt	=	Weight
Δ	=	Increment
μ	=	Micron, 10^{-6} m (3.937×10^{-5} in)
Σ	=	Summation

2. ESTABLISHMENT OF DESIGN REQUIREMENTS:

Satisfactory thermal design of equipment environmental control systems (ECS) is dependent in a large measure on accurate as well as adequate knowledge of the environmental limits of the equipment. This area is of special concern to the environmental control system designer because it is obviously one of the controlling factors in the weight, size, and power requirements, and particularly in the configuration of the environmental control system. It is not only essential that complete design criteria be established but also that repeated efforts be made to reduce and simplify requirements during the course of development.

2.1 Parameters to be Studied:

In order to evolve sufficient criteria for the task of providing a satisfactory environment for equipment, the following parameters must be studied:

1. Heat input rate and required heat dissipation rate in watts or Btu/h. Where parts of equipment operate intermittently or at a varying percentage of their full load rating, this should be noted together with heat input versus time, absolute pressure, or other pertinent variables.

   It should be also noted that the heat input to the accessory package and the required heat dissipation rate are equal only in the prolonged steady-state condition. The difference between the two is ordinarily the heat that is absorbed into the equipment itself as a function of the specific heats of the various materials used in its construction.

   Where the mass of the accessory is large and the time of the accessory temperature stabilization long, the required heat dissipation rate can be much lower than the heat input rate for short-time operation. Where this factor is important, the heat dissipation rate should be stated as a function of time or other pertinent variables.

2. Maximum permissible ambient temperature conditions versus minimum average coolant supply to the equipment and versus absolute pressure and heat input rate. Ambient temperature conditions are here defined as the temperature of the ambient gas and/or the temperature of surrounding solid surfaces (wall temperatures of test chamber or enclosing compartment).

3. Temperature rise of critical equipment elements versus time and heat input in maximum ambient conditions noted in item 2.

2.1 (Continued):

4. Life of critical elements versus temperature of critical elements.

5. Approximate envelope dimensions, position and size of louvers or other openings, location and performance (versus absolute pressure) of any internal fans, location and dimensions of any special heat transfer fins, and color and type of surface finish.

6. Provisions for attachment of equipment to vehicle. For example, accessories mounted by shock mounts are effectively isolated against conduction from the vehicle structure, but accessories mounted metal to metal on structure may achieve considerable cooling or heating by direct conduction.

7. Maximum permissible temperature of outside surface of equipment versus heat input rate.

8. Temperature rise of surface of package versus time and heat input, with stated ambient temperature and coolant supply conditions.

9. Quantity of gas required for pressurization of equipment, in lb/min, versus compartment absolute pressure.

10. Minimum required flow rate and maximum permissible temperature of coolant into the package versus various stated ambient temperature conditions; items 1 to 9 versus compartment absolute pressure and heat input rate.

11. Anticipated maximum coolant exit temperatures corresponding to inflow conditions noted.

12. Pressure loss of coolant flowing through package or heat transfer surface versus coolant flow rate and density.

13. Temperature rise of critical accessory elements versus time and heat input, with no cooling and with specified quantities of coolant.

14. Location and size of coolant interfaces.

15. Layout of heat transfer surfaces in package and mean operating temperature of these surfaces.

16. Specification of type or class of package seal. MIL-S-8484 (USAF) "Seals and Seal Testing Procedure for Electronic Enclosures" may be used as a guide.

17. Positive and negative pressure differential capability of the package, along with surface deflection.

18. Humidity and contamination control requirements.

2.1 (Continued):

19. Ground support requirements; interfaces, temperature, pressure, and flow of coolant.

20. Storage environmental requirements under sea level and vacuum conditions.

3. REGULATION, SENSING, AND CONTROL OF ENVIRONMENTAL SYSTEMS:

3.1 Temperature:

3.1.1 Performance: Often, temperature control systems designed for space vehicle applications have not performed as well as expected. As a result, several major redesign efforts are required before an acceptable system is developed. This poor system performance can usually be traced to the improper choice of locations and types of sensors, controller and regulator devices, and the neglect of dynamic response analysis for prediction of system performance.

From a consideration of the analysis approach used for most designs, the heat transfer and thermodynamic analyses appear satisfactory, but the control and flow rate choices are usually based on maximum and minimum temperature and heat load considerations. Obviously, this procedure does not lead to an optimum and/or a well-controlled system, since neither consideration for the heat storage of the equipment, coolant, and components nor prediction of control system response is included.

The real importance of dynamic response analysis for space vehicle temperature control systems is not apparent unless a detailed breakdown of the system heat loads is considered. The basic heat loads can be listed as:

1. Solar, reflected, and planetary radiant heat (variable with vehicle spin, orientation, distance from Sun and orbit conditions).

2. Equipment and personnel heat load to heat exchangers and cold plates (variable with time and/or function).

As can be seen, the heat load for most vehicles must vary with time. Thus, there should be no doubt that such factors as speed of response, damping factor, phase lag and dead band, stability, control band, and prediction of temperature versus time for individual components are necessary outputs to any analysis. (Note that, in most cases, the use of dynamic response analysis methods is necessary for optimization, since the system designed without dynamic response analysis will be overdesigned to supply control for the maximum and minimum heat load conditions.)

Apparently, the main cause of neglect of dynamic response analysis is the fact that most texts on dynamic response systems are directed toward hydraulic, pneumatic, and electrical systems, with little or no mention of temperature control applications.

3.1.1 (Continued):

Another cause is the educational background requirement of three or four courses in linear and nonlinear system analysis needed for basic understanding of the block diagram Laplace transform analysis method. Also note that a block diagram Laplace transform solution becomes extremely complex or impossible when a temperature control system with fluctuating heat loads and temperature control by fluid flow modulation is used.

Another method of analysis, the differential equation method, uses the basic differential equations for temperature, heat transfer, and fluid flow in a form that can be solved by computer programs or analog networks.

3.1.2 Components: Components associated with the temperature control circuits are sensors, anticipators, amplifiers and controllers, servomechanisms, and feedback position indicators. Figures 1 through 4 illustrate the relationship of the controller circuit to some simple semipassive temperature control methods. Even with the controller circuit setup as shown in these figures, numerous controller circuit component problems exist in choice of sensors, controllers, and servomechanisms. To show some of the choices available, tables of methods of controller operation and of sensor and thermoswitch operation and accuracy are shown in Tables 1 and 2.

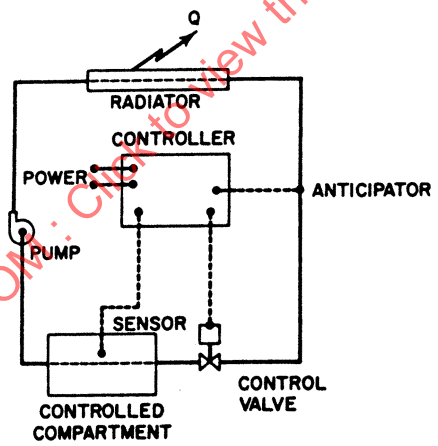

FIGURE 1 - Temperature Control by Fluid Flow Modulation

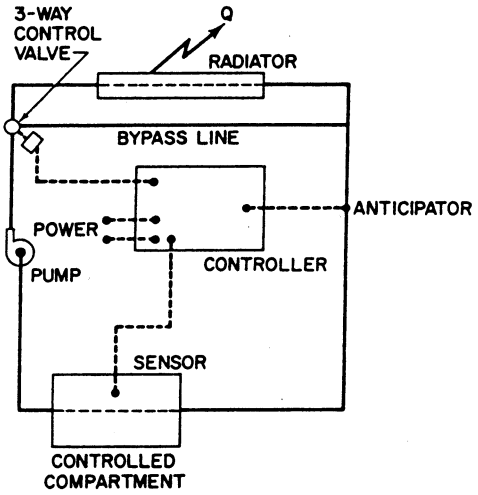

FIGURE 2 - Temperature Control by Mixing and Bypass

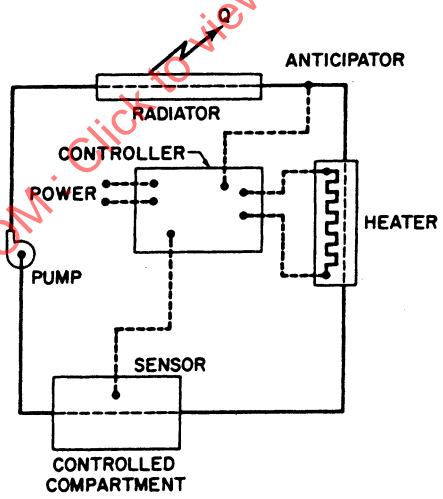

FIGURE 3 - Temperature Control by Heat Addition

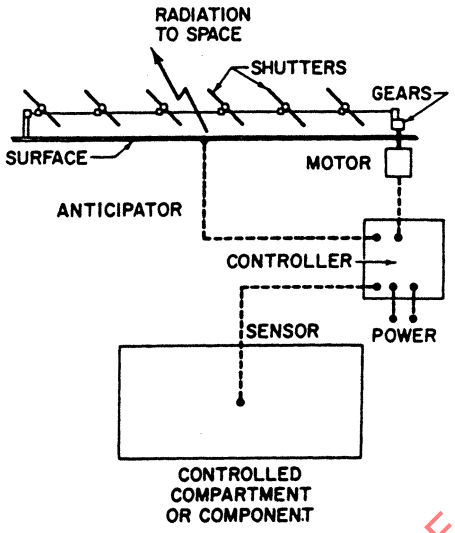

FIGURE 4 - Temperature Control by Varying Surface Emissivity and Solar Absorptivity

TABLE 1 - Types of Automatic Controllers for Temperature Control Systems

Type of Controller	Description
On-Off	Receives signals, compares, amplifies, and opens or closes a servo such as a solenoid valve
Proportional	Receives signals, compares, amplifies, and modulates servo proportional to signal
Constant Frequency, Pulse Modulated	Receives signals, compares, amplifies, and modulates pulse width of constant frequency on-off servo action
Feedback	Position indicator sends signal to controller for comparison to rate of response of servo. This allows speedup of response and increased accuracy in positioning of servo. Can be used with proportional or pulse modulated controllers.

TABLE 2 - Temperature Sensors and Thermoswitches

Type	Range, Low	Range, High	Sensi-tivity	Controller Required?	Description
Wire Resistor	-460	+5000	±0.05 °F	Yes	Resistance of wire increases with temperature
Thermistor	-200	+900	±0.05 °F	Yes	Resistance decreases with temperature
Thermocouple:					
Copper-Constantan	-460	+600	±0.05 °F	Yes	Emf at junction increases with temperature
Iron-Constantan	0	+1600	±0.1 °F		
"Chromel-Alumel" (Hoskins Corp.)	+600	+2100	±0.2 °F		
Platinum-Platinum Rhodium	+1300	+2800	±0.1%		
Mercury Thermoswitch	-80	+750	±0.1 °F	No	Length of mercury column increases with temperature, contact with points can be used for switching
Bimetallic Disk Thermoswitch	-100	+1000	±3%	No	Bimetallic disc snaps into reverse position at desired temperature and can be used for switching
Bimetallic Expansion Thermoswitch	-100	+1000	±1%	No	Differences in thermal expansion of bimetallic strip cause switching
Thermal Expansion Thermoswitch		+1800	±1%	No	Thermal expansion of material causes switching

3.1.2 (Continued):

In consideration of the controller circuit, the controller is usually the key component. These controllers can be extremely complex or nonexistent, depending on the temperature control system. For example, in a complex system with precise temperature control requirements, the controller may consist of electronic circuits to:

1. Interpret sensor and anticipator measurement signals.
2. Amplify the interpreted signal.
3. Direct a signal to the servomechanism for corrective action.
4. Alter the output signal to linearize the servo action.
5. Interpret and compare feedback signals from position indicators with the desired servo control position to speed up the rate of response.

3.1.2 (Continued):

The opposite in complexity is the thermoswitch and solenoid valve type of combination wherein the thermoswitch directly controls the valve and no controller is needed.

At any rate, in most cases a controller of some form is required. This controller is usually electronic for space applications because electronic controllers are usually lighter, more reliable, and smaller than hydraulic or pneumatic controllers. (Also, electricity is more readily available.) Much useful information on controllers for particular applications can be obtained from the electronic controller companies. Some of these companies will not only design a controller for the application, but will also analyze the dynamic response of the system.

3.2 Compartment Pressure Regulation:

Compartment pressure regulation for space vehicles is dependent on the allowable positive and negative pressure differentials established by structural requirements for ascent and reentry flight phases, respectively, and the total pressure level that must be controlled during orbit of space flight under hard vacuum conditions.

Generally, positive pressure relief is required during ascent, to reduce internal total pressure to the level that will be maintained throughout the space mission. Once the prescribed compartment total pressure level has been reached during ascent, further loss of compartment gas occurs only from leakage. Internal pressure regulation is accomplished by controlled addition of makeup gas. The method and rate of makeup gas addition depends on the allowable control tolerances and leakage rate.

During reentry and subsequent terminal flight to touchdown, negative pressure relief is required to prevent excessive crushing pressures on the structure. If inflow of hot boundary layer air cannot be tolerated, internal pressure increase to match ambient pressure increase must be accomplished by the onboard pressure regulation system. A typical compartment pressure schedule is shown in Figure 5.

A compartment pressure regulation system may consist of a supply of makeup gas stored at high pressure, a pressure regulator, a flow control valve and/or orifice, pressure sensors, and a positive and negative pressure relief valve.

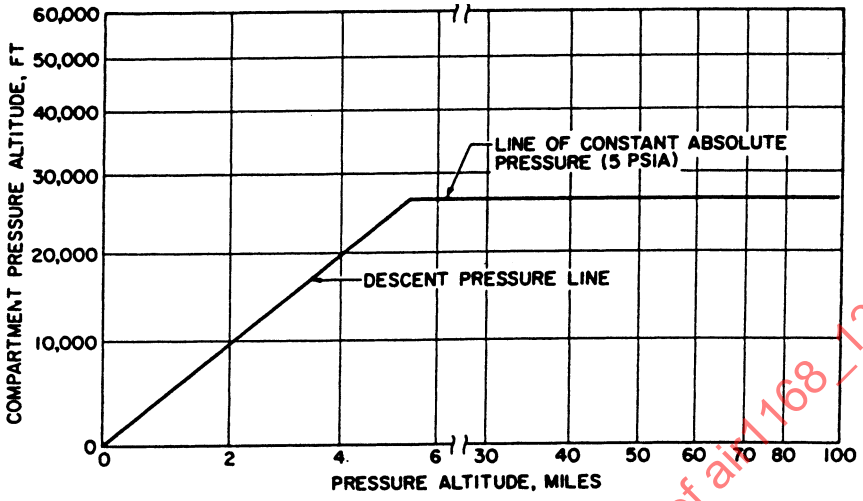

FIGURE 5 - Compartment Pressure Schedule Chart

3.2.1 High-Pressure Regulation: A high-pressure regulator is required to reduce the supply makeup gas pressure from its stored level to a constant reduced level on which to base flow control valve and/or orifice sizes and the supply flow rate. A typical regulator is a balanced poppet type valve operated pneumatically and automatically by a metal diaphragm. Single stage pressure reductions as high as 75:1 are possible.

3.2.2 Low-Pressure Regulation: Low-pressure regulation is accomplished by the controlled addition of a makeup gas quantity to maintain the required compartment total pressure level. Excess quantities of gas are relieved overboard through the compartment pressure relief valve.

Makeup gas control can be accomplished by either an on-off shutoff valve controlled by compartment total pressure sensing or by an orifice sized to provide a gas flow equal to the total leakage flow from the compartment. In the latter case, a shutoff valve will be required in series with the orifice, to prevent loss of makeup gas until pressure control is required.

The compartment pressure relief valve functions to maintain the internal-to-ambient pressure differential within allowable limits for all phases of the flight. Such a valve (Figure 6) contains an aneroid that senses compartment pressure and is adjusted to close a small pilot valve when the compartment pressure reaches the desired absolute pressure. The small pilot valve, in turn, blocks the escape of gas from the outflow valve head chamber when the pilot valve is in this position.

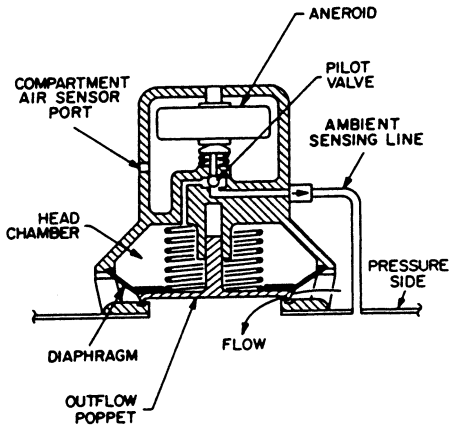

FIGURE 6 - Compartment Relief Valve

3.2.2 (Continued):

As the pressure outside the compartment drops, the cabin-to-ambient differential pressure provides a closing force on the outflow poppet, which helps prevent leakage. Regulators may be adjustable and limit the compartment pressure range within less than ±5% of the nominal setting. Leakage of a typical regulator with 0.5 psia outlet pressure and 5 psia inlet pressure may be expected to be of the order of 0.0005 lb/h.

Regulators are generally mounted inside and require a sensing line to the atmosphere. The pneumatic sensing line is provided with a check valve which causes the regulator to open automatically when atmospheric pressure exceeds compartment pressure.

For maximum reliability, it may be necessary to provide a duplicate regulator that will act in the capacity of a safety valve. This regulator would be identical to the compartment pressure regulator described above except for calibration. Obviously, the setting of the standby regulator would be at pressure somewhat higher than the primary regulator. Pressure setting of the backup unit is established by the structural criteria.

4. TEMPERATURE CONTROL:

The basic problem involved in aerospace equipment temperature control is the provision of a transfer loop from the internal heat source to various types of heat sink systems. If this loop consists of no fluids and no moving parts, it is considered "passive." The system becomes "semipassive" when moving parts or fluids are introduced in order to energize the loop and reject heat at a value less than the source temperature. If a heat pump is employed, heat is rejected at a higher temperature than the source and the system is classified as "active."

4.1 Passive Temperature Control Methods:

4.1.1 Fixed Resistance Heat Path (Insulation):

Figure 7 shows how a fixed resistance is used to control temperature.

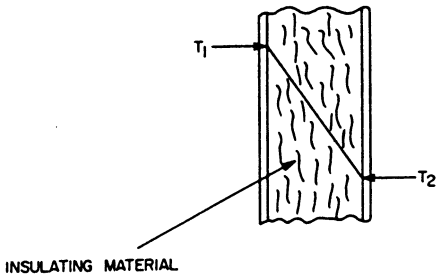

FIGURE 7 - Temperature Control by Fixed Resistance

The function of insulation in the control of temperature is to impede the transfer of heat across a space. This is often done by breaking up this space into very small volumes, thereby preventing the formation of the convection currents by which most of the heat transfer would occur. This effect is produced by the use of materials such as foams, powders, and matted hairlike or fibrous substances.

Heat transfer across a space by convection or conduction can be eliminated almost completely by producing a vacuum between the walls. However, this does not prevent radiation transfer, and the so-called superinsulations become necessary. These evacuated insulation types are laminated combinations of aluminum foil and Fiberglas paper or layers of thin metallized plastic film which provide multiple radiation barriers to reduce transfer of radiant energy.

Characteristics of the types of insulation described above include:

1. Power – No external power is required.

2. Weight – Densities vary from 3 to 15 lb/ft^3 for thermal conductivities in the range of 0.015 Btu/h-ft-°F at a mean temperature of 560 °R for unevacuated materials, to 0.005 Btu/h-ft-°F for evacuated materials at 560 °R. Laminated foil-Fiberglas insulation at an average temperature of 300 °R has a conductivity less than 5 x 10^{-5} Btu/h-ft-°F.

3. Method – Vacuum of outer space may be used to evacuate a desired region of vehicle. Insulation can be combined with self-sealing of walls.

4. Limitations – Extra weight. May prevent easy access to some structural areas.

5. General – Simple, no power requirements, nontoxic, noncorrosive; easy to apply.

4.1.2 Fixed Conductance Heat Path: This method of temperature control differs from the one previously described in that it has paths of high conductivity interposed between two areas rather than paths that are thermally isolated from each other. The purpose here is to remove heat, and this is done by joining the heat source and the heat sink by paths of high conductivity. The best conductive materials are metals, so that rods or plates of solid metal provide the necessary service.

Characteristics include:

1. Power – No power is required.

2. Weight – Depends primarily on length and cross-sectional area of path and upon density and thermal conductivity of metals used. The density of common materials varies from 114 lb/ft^3 for beryllium to 556 lb/ft^3 for copper.

3. Integration – Sections of structure, enclosures, fluid conduits, or protective shielding can all be used.

4. Limitations – The best conducting materials have the highest densities. Radiation from conductive paths may necessitate insulation.

5. General – A simple, reliable process involving easily predicted behavior of familiar materials and numerous possibilities for integration.

4.1.3 Heat Storage: Heat storage devices may be used to minimize the temperature excursion of space vehicles subjected to extremes of cooling and heating. A storage device may also be utilized as a heat sink for active systems during periods when normal rejection to space is impossible or inadequate.

These devices may become solid or liquid materials, but not, ordinarily, gases. The important properties to be considered in selecting heat storage materials are high thermal capacity and high latent heat of fusion. While gases may possess these required properties, the specific volumes of gases at practical pressures are excessive.

Thermal properties of some promising materials for heat storage are tabulated in Table 3.

TABLE 3 - Thermal Properties of Some Heat Storage Materials

Material	Melting Point, °F	Latent Heat of Fusion, Btu/lb	Heat Absorbed from 70 °F Through Fusion, Btu/lb	Chemical Symbol
Tristearin	133	82.1		$(C_{17}H_{35}COO)_3C_3H_5$
Beeswax	143	76.1		
Methyl Bromobenzoate	178	54.4		$C_8H_2O_2Br$
Catechol	220	88.9		$C_6H_4(OH)_2$
Phenacetin	279	58.8		$CH_3CONHC_6H_4OC_2H_5$
Hydroquinone	342	111.1		$C_6H_6O_2$
P-Aminobenzoic Acid	371	65.7		$C_6H_4(NH_2)COOH$
Lithium	367	59.5	270[1]	Li
Beryllium	2330	468	2032[1]	Be
Silicon	2570	776	1330[1]	Si

[1] Computed from available data.

4.1.3 (Continued):

Characteristics of these materials are as follows:

1. Power – In themselves, storage systems require no power, but circulation may be required to transport heat to storage.

2. Weight – Based on Table 3 and allowing 100% extra for containers and circulating system, the range is 4.2 to 24.3 lb/kW-h.

3. Method – Storage material may be any body, solid, or liquid that is on board and which will not be materially altered by the addition of heat.

4. Limitations – The rate of transfer may be slow and recovery more difficult than accretion. Containment of material may be difficult.

5. General – Simplicity and wide possibilities of integration make this method attractive.

4.1.4 Heat of Solution Storage System: This is a unique method for storing heat, or more accurately, the effects of heat. It depends upon the fact that the addition of water to concentrated solutions of some alkaline materials is attended by the production of considerable quantities of heat. After reaching a certain degree of dilution, no more heat is given off, so that the solution must then be reconcentrated.

Excessive heat can be used to drive off water, which is condensed and then re-used to dilute the reconcentrated solution. Some representative values are given in Table 4.

TABLE 4 - Heats of Solution of Representative Substances

Solution	Molecular Weight	Heat of Solution (18 °C, 1 atm) kg-cal/g-mol	Heat of Solution (18 °C, 1 atm) Btu/lb
$CaCl_2$	111.0	18.0	292
NaOH	40.0	10.3	463
$MgBr_2$	184.2	43.3	423
$BeBr_2$	168.5	62.6	668
$AlCl_3$	133.3	77.9	1054
$Al_2(SO_4)_3$	342.1	126.0	662

4.1.4 (Continued):

Characteristics of these substances include:

1. Power – No external power is required beyond that needed for circulation of the heat exchange medium

2. Weight – A representative weight is indicated by the heat of solution value of 249 W-h/lb of solution for 1 mol of aluminum chloride, $AlCl_3$, dissolved in 2 mols of water.

3. Method – This system can act to store heat and release it on demand, or it can be used to generate energy, and so can be integrated with either a heat sink or a heat source.

4. Limitations – Materials are usually highly corrosive. Temperatures of system operation are relatively low.

5. General – Materials are cheap and readily obtainable in pure form. The system is reliable and easily controlled. The high-temperature requirement of meltable heat storage materials is avoided.

4.1.5 Radiators: A radiator is any surface whose purpose it is to emit heat by electromagnetic radiation. Heat may be transported to the radiator by means of conduction, free or forced convection, or radiation (Figure 8). In the interior of a vehicle, heat may be removed from the face of a radiator by radiation or by the passage of convective air currents, whereas in space the only means of transmission is through radiation.

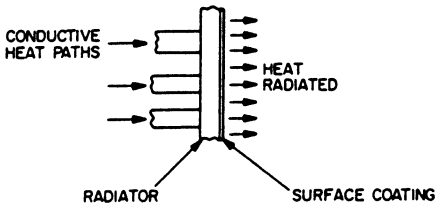

FIGURE 8 - Heat Disposal by Radiation

4.1.5 (Continued):

The interchange of radiant energy between the face of a radiator and its surroundings is in accordance with the Stephan-Boltzmann law, which states that this interchange will be a function of the emissivity and the fourth power of the absolute temperatures of the surfaces.

Emissivity is a property of the material and condition of the surface, being low for gold, silver, and aluminum, and high for black oxides of metals. Ideally, a radiator should have high thermal conductivity and low density in order to minimize weight.

Characteristics of radiators are:

1. Power – No power is required to operate the radiator, although a fluid transporting heat to the radiator would have to be moved by some mechanical means.

2. Weight – The specific weight (weight per unit of heat transfer) would be a function of the overall effectiveness of the radiator, the density of the material, and other factors, such as whether the radiator forms an integral part of the vehicle structure or surface.

3. Method – Can be integrated with vehicle outer surface or auxiliary surfaces, such as radar antennas.

4. Limitations – Ordinarily not subjected to control, although movable shutters may alter emissivity of surface. Surface properties are subject to change through meteoritic damage, high vacuum, and other space environmental factors.

5. General – Insensitive to gravity field; long lived; high reliability; no power requirements; and (ordinarily) no moving parts.

4.2 Technical Approach, Passive Methods:

Passive methods previously discussed in this section depend upon conduction, radiation, or a combination of conduction and radiation as a means for heat transfer. Since natural convection does not occur in a zero gravity environment, heat transfer by this process will not be considered here.

Figure 9 illustrates a simple passive temperature control system that depends on conduction and radiation for heat transfer.

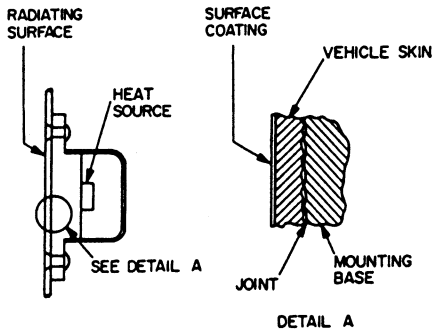

FIGURE 9 - Simple Passive Temperature Control System

4.2 (Continued):

Passive methods, because of their relative simplicity, have been the sole means for temperature control of first generation space vehicles. Although more complex control methods will be required in future vehicles, passive methods will be an integral part of the overall temperature control system.

High conductance heat paths can be achieved by utilizing high-heat conducting material and by placing the heat source close to the heat sink, such as the vehicle skin. The conduction path should be designed with a minimum number of joints.

An important consideration for the efficient design of conduction paths is the effect of joints on heat transfer. Currently (circa 1965), there is a need for more data, particularly at very low pressures, and a development of methods for analysis. Limited information currently available indicate thermal resistance of joints can be minimized by:

1. Increasing contact pressure.
2. Reducing surface roughness.
3. Maintaining surface flatness.
4. Utilizing shim materials that have lower hardness than joint materials.

Through continued development efforts, high efficient insulations have been developed. Most efficient insulations require very low interstitial pressure to minimize or eliminate gas conduction, which is the major mode of heat transfer, accounting for 50 to 90% of the total conductance. In addition, radiation heat transfer is minimized by use of powder and fibrous materials and by utilizing multilayer foils. Foil type insulations are available for vehicle thermal conductivity of 0.000025 Btu/h-ft-°F. Being nonload bearing, this type of insulation usually requires additional structure for rigidity.

4.2 (Continued):

Proper selection of surface coating for space vehicles is a very important consideration for the efficient design of a temperature control system. Vehicle skin temperature has direct influence on the interior temperature and thus affects temperature control requirements. Many surface coatings have been developed and provide a wide range of values for α_s/ϵ.

An analysis for multilayer radiation shields and the plots of equations developed indicate the marked effect of shields to reduce radiation heat transfer. As shown on Figure 19, three or four shields should be used for maximum reduction in the value of heat transfer coefficient. Increasing the number beyond four has only a small effect in reducing the heat transfer coefficient. Shielding material should have low values of emissivity, such as aluminum foil, for which $\epsilon = 0.05$.

The principal mode of heat transfer from heat source to the outer skin surface is by conduction. From the outer skin, surface heat is dissipated to space, the ultimate heat sink, by radiation. The prime requirement of this simple system is to provide an efficient heat path from the source to the sink. One very important consideration, which will be discussed, is the heat transfer across the interface of mating surfaces, illustrated in detail A of Figure 9.

In addition to discussing means for providing efficient heat transfer by conduction and by radiation, methods for providing effective heat resistance or insulation will also be considered. This is very important in providing thermal protection for space vehicles while in orbit and particularly during reentry.

4.2.1 Conduction: The subject of heat conduction has been treated extensively in many books on heat transfer, such as References 1 and 2. Therefore the discussion here is limited to selected material on the subject.

Study of heat flow through many materials has established the fact that materials differ in their ability to conduct heat. Those that are good conductors of heat are also good conductors of electricity. This includes well-known metals such as silver, copper, and aluminum. Many nonmetallic materials such as wood, liquids, and gases are poor heat conductors, and are classified as insulators. Thus, depending upon the material utilized, either high thermal conductance or high thermal resistance can be achieved.

4.2.1.1 Thermal Conductance: To obtain efficient heat transfer by conduction requires more than just the consideration of the conducting material. As indicated by the fundamental law of conduction (Fourier's equation)

$$q = \left(\frac{kA}{L}\right)\Delta T \qquad \text{(Eq.1)}$$

high heat flow rate can be achieved by obtaining large values for the term (kA/L) or the temperature difference ΔT.

4.2.1.1 (Continued):

To obtain a large temperature difference between the heat source and sink requires, for a given heat source temperature, the determination of a heat sink at the desired lower temperature. For the temperature control system illustrated in Figure 9, the intermediate heat sink is the vehicle skin, so that ΔT is dependent upon the skin temperature, which in turn is governed by the net energy exchange by radiation.

The term (kA/L) is a combination of the conducting property of the conductor and its physical dimensions. Good heat conductors, such as copper and aluminum, have specific gravity values greater than l; therefore weight is an important consideration in addition to conductivity. Increase in area A would increase heat flow rate, but it would also result in a larger conductor, and hence an increase in weight. The most significant quantity is the length L, since a smaller value would result not only in higher heat flow rate, but also a lighter-weight conductor.

For the simple system illustrated in Figure 9, the heat source should be placed as close to the thermal radiating surface as possible. The conduction path shown is composed of several solid conductors, which introduce joints; thus, joint effect on heat flow becomes an important consideration.

4.2.1.2 Joint Resistance: For efficient design of conduction paths, knowledge of joint resistance is necessary. A survey of available literature (circa 1965) indicates a lack of analysis and experimental data directly applicable to spacecraft, particularly for extremely low pressure environment. Many variables (which include contact pressure, temperature, heat flow rate, interstitial pressure, interstitial fluid, joint materials, surface finish, material hardness, and surface flatness) must be taken into consideration to provide useful data on this subject.

Some of the more important earlier work on joint resistance was published in 1949. Weills and Ryder (Reference 3) conducted tests using copper, steel, and aluminum for varying temperature and pressure. Brunot and Buckland (Reference 4) used laminated and machined joints, using steel with cement, steel, and aluminum foils sandwiched between the surfaces; only pressure was varied.

In 1953, WADC (Reference 5) reported an experimental method of measuring thermal resistance by using a Mach-Zehnder interferometer. The results of these measurements were tabulated. Fenech (Reference 6) developed an idealized model for thermal contact and compared the theoretical analysis with experimental data for Armco-iron contact surfaces of 600 rms roughness for varying pressure and temperature. Groff (Reference 7) introduced a dimensionless conductance (h_c p/kρ), which was used to correlate test data presented by other investigations.

Investigators for NACA (References 8 to 11) have presented a considerable amount of experimental data on aircraft joints at atmospheric pressure for surface finish ranging from 10 to 120 µin, rms surface roughness. Contact pressure, temperature, and heat load were the principal variables. Figure 10 presents a portion of the data given in Reference 9. The influence of surface finish and contact pressure on joint conductance is clearly indicated.

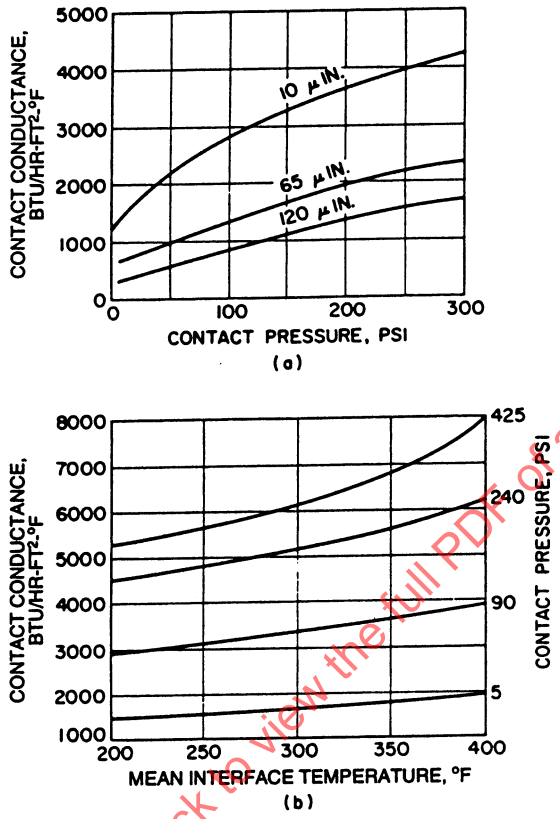

FIGURE 10 - Thermal Conductance Across Interface of Conductor Joint
(a) 75S-T6 Aluminum-to-Aluminum Joint;
(b) 75S-T6 Aluminum-to-Aluminum Joint, 10 μin rms Surface Roughness

4.2.1.2 (Continued):

Recently, Fried and Costello (Reference 12) have presented the results of experimental work for tests conducted at ambient pressures of 10^{-4} to 10^{-6} mm Hg abs and relatively low range of contact pressures (2 to 35 psi). The experimental values indicate that joint conductance is lower at vacuum conditions. Tests were also conducted utilizing various interface shim materials. The results of these tests are presented in Figure 11, indicating the marked influence of soft materials, such as lead foil, in increasing the joint conductance.

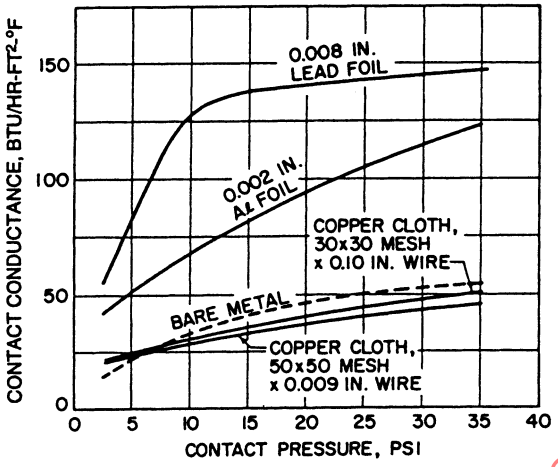

FIGURE 11 - Thermal Conductance Versus Contact Pressure for Joints With Shim Material

4.2.1.2 (Continued):

Based on the review of available reports, joint resistance can be decreased by:

1. Increasing contact pressure.
2. Reducing surface roughness.
3. Maintaining surface flatness.
4. Utilizing shim materials with lower hardness than that of the joint material.

The problem of analyzing thermal resistance of joints consists of two steps: determining the true contact area through which heat flows by solid conduction, and identifying the modes of heat transfer, other than solid conduction, and their relative importance. True contact area is difficult to establish because it is made up of many small points of contact, which depend upon the surface roughness, contact pressure, contact material hardness, and surface flatness. The amount of deformation of the contact points establishes the true or effective contact area.

Reference 12 suggests gaseous, or molecular or other conduction through the interstitial fluid or filler and radiation as possible modes of heat transfer in addition to solid conduction through the contact area. The contribution of each mode to the total heat transfer has not been established (circa 1965).

In the transfer of heat by conduction, the thermal resistance across the mounting surfaces can decrease the overall heat transfer. This decrease in heat transfer becomes particularly important when considering cold plate mounted components where the small change in heat transfer can cause the junction temperature to operate 10 °F higher or more.

4.2.1.2 (Continued):

For cold plate mounted components, a spacer with high electrical resistance and low thermal resistance is required. Two new methods of decreasing joint resistance have been used:

1. RTV rubber between component, washer, and cold plate.

2. Special washer with high dielectric and low thermal resistance.

RTV rubber has been used successfully in at least one company in the aerospace industry. For example, a newly developed washer (spacer) material, which may be classified as a breakthrough in material development, has resulted. It consists of 30% (by weight) of 0.002 in dia. glass balls bonded into a single layer solid by Epoxy 907, which constitutes the remaining 70% finished material. This is sandwiched between two layers of 0.020 in thick dead-soft aluminum (110 SO) and then bonded to it.

As an alternate, a single layer of aluminum may be used; the washer would then be bonded to the electronic element during the packaging phase. The dielectric layer thickness of 2 mils is fixed by the glass ball diameter (state-of-the art of 1965); however, the aluminum thickness is limited only by physical considerations (see Figure 12).

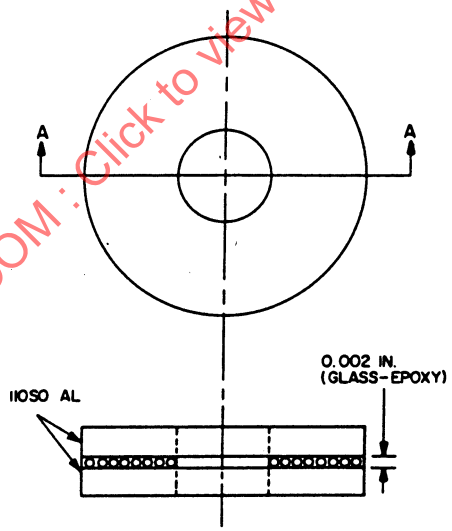

FIGURE 12 - Section A-A of an Electrical Separation Washer Using Glass Balls as Dielectric Material

Preliminary tests have been conducted on glass-epoxy and comparisons made with other materials (see Table 5) including beryllium oxide (ceramic). The latter is an excellent electrical dielectric and is also favorable for thermal conductivity. The major disadvantage of beryllium oxide, other than brittleness, is its extremely high cost.

TABLE 5 - Comparative Thermal and Electrical Resistances of Various Electrical Insulating Materials (Washers)

Resistance	Type of Washer Mica (0.002 in)	Type of Washer BeO	Type of Washer Glass-Epoxy	Type of Washer Anodized Aluminum
Thermal, °F/W	2.61	1.7	1.5	2.6
Electrical, megohms	150×10^3	0.250×10^4	150×10^3	Range $(100\text{-}750) \times 10^3$

4.2.1.2 (Continued):

Along with the above-mentioned glass-epoxy and BeO, the often discussed mica and anodized aluminum are also compared for electrical and thermal resistance. It should be emphasized that these are comparative values, due only to the nature of the preliminary tests, and are not to be used as absolute values for design purposes.

From the summary of the preliminary test data shown in Table 5, it can be seen that beryllium oxide is by far the best material, although, in addition to extremely high cost, it is quite brittle and requires a form of grease or smear gasket for maximum usefulness. Based on these test results, the glass-epoxy has great promise. As a complete sandwich (between two layers of aluminum), the dead-soft aluminum provides a smear gasket, with a good thermal bond between the aluminum and glass-epoxy joint. Used with a single sheet of aluminum, this epoxy joint is made direct to the heat source or heat sink.

More extensive tests of this nature are planned (circa 1965). This is expected to provide more data on joint resistance in general. Table 6 shows the results of a series of laboratory tests designed to indicate the magnitude of thermal resistance of the materials investigated as compared to mechanical joints with no electrical insulation.

TABLE 6 - Effect of Electrical Insulators on Thermal Resistance of Typical Component Mounting Joint (refer to Figure 13)

Run No.	Washer A		Washer B	Temperature Gradient, °F/W
1	Bare Al	(2)	Mica (0.006 in)	1.05
2	Bare Al		None	0.94
3	Mica (0.006)	(2)	Mica (0.006)	2.61
4	Anodized Al	(2)	Mica (0.006)	2.55
5	None	(2)	Mica (0.006)	1.17

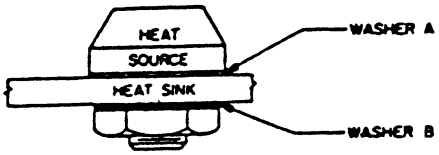

FIGURE 13 - Typical Component Mounting Joint

4.2.1.3 Thermal Resistance: There are many materials available which can be used to achieve good thermal resistance. Solids, solid particles, liquids, and gases are used in various combinations to provide the necessary insulation. The selection of the material is dependent upon, in addition to low thermal conductivity, whether structural rigidity is important. For example, insulation for cryogenic storage vessels must have not only high thermal resistance but also structural rigidity.

Solid insulating material, such as wood, stone, and plastics, are not considered here because there are other insulations that have not only much lower thermal conductivity but also lower densities. Table 7 presents a list of representative insulations that are commonly used and are readily available.

TABLE 7 - Effect of Air Removal Upon Thermal Conductivity of Various Materials at 100 °F Mean Temperature

Material	Density, lb/ft^3	Thickness in	Thermal Conductivity, k At 1 atm.	Reduced Pressure μ Hg	Thermal Conductivity At Reduced Pressure k	Percent Reduction
Air Space-Copper Surfaces		1	0.572	0.07	0.187	67.3
Corkboard	6.67	1	0.283	0.06	0.106	62.5
Corkboard	12.4	1	0.314	0.13	0.120	61.8
Cotton	0.78	1	0.288	0.07	0.072	75.0
Cotton	1.53	1	0.257	0.12	0.052	79.8
Cotton	2.62	1	0.248	0.14	0.033	86.7
Coarse Glass Wool	2.8	1	0.267	0.04	0.055	79.4
Fine Glass Wool A	0.58	1	0.2505	0.08	0.050	80.0
Fine Glass Wool A	1.94	1	0.2145	0.05	0.0195	90.0
Fine Glass Wool A	3.8	1	0.211	0.11	0.012	94.3
Fine Glass Wool B	0.78	1	0.302	0.04	0.0665	78.0
Hairfelt	11.1	3/4	0.260	0.10	0.031	88.1
Kapok	0.26	1	0.366	0.10	0.091	75.1
Kapok	0.99	1	0.2445	0.10	0.0375	84.7
Kapok	3.96	1	0.244	0.12	0.0175	92.8
Mineral Wool	7.7	1	0.258	0.05	0.037	85.7
Silica Aerogel	8.6	1	0.1715	0.07	0.0255	85.1
Special Specimen	3.1	1	0.231	0.00	0.0145	93.7
Wood Fiberboard	15.5	3/4	0.353	0.05	0.075	78.8
Wood Fiber	3.5	1	0.2715	0.08	0.052	80.8
Wood Fiber	6.9	1	0.277	0.09	0.033	88.1

Source: References 15 and 42.

4.2.1.3 (Continued):

These insulating materials are nonhomogeneous and porous so that thermal conductivity is a function of composition, density, temperature, and (particularly) pressure. For materials of this type, heat transfer is effected not by conduction alone but also by convection and radiation. Reference 13 suggests that the term "apparent thermal conductivity" should be used for fibrous insulation rather than the term "thermal conductivity" and gives the following expression for the overall thermal conductivity:

$$k'_T = \frac{(k_{cd} + k'_{cv} + k'_{ra})}{1 - f} + k_{sc} \qquad \text{(Eq.2)}$$

Table 2 of Reference 13 shows measured thermal conductivity values for various densities of fiber insulation with four gases (helium, air, carbon dioxide, and Freon 12) at atmospheric pressure, except for one test at 76 mm Hg pressure. The results indicate that at atmospheric pressure, gas conduction is by far the most important mode of heat transfer in fibrous insulation, contributing from 50 to 90% to the overall thermal conductivity. Also, at atmospheric pressure, helium gas gives the highest thermal conductivity and Freon 12 gives the lowest value.

Figure 14, which is reproduced from Figure 6 of Reference 13, shows the contribution by each of the different modes of heat transfer at atmospheric pressure, for changes in insulation density. It is readily apparent that air conduction is the major mode of heat transfer and does not vary with change in insulation density. Radiation and convection decrease rather rapidly with increase in insulation density (up to about 3 lb/ft^3) and further increase in density has less influence on these two modes of heat transfer. Solid conduction due to fiber contacts contributes very little to the heat transfer in the fibrous insulations.

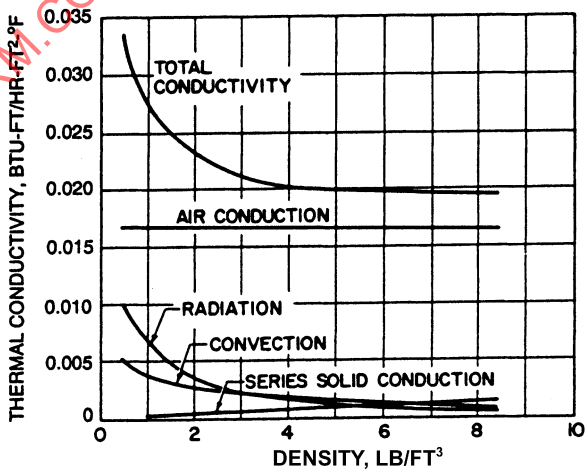

FIGURE 14 - Thermal Conductivity Versus Density.
Contribution by Various Modes of Heat Transfer (for Fibrous Type Insulation)

4.2.1.3 (Continued):

The predominant mode of heat transfer (gas conduction) can be minimized or eliminated by evacuating the gas from the insulation. The marked effect of low pressure on decreasing the thermal conductivity is clearly indicated in Table 7. The variation of thermal conductivity with pressure for powdered insulation is given in Figure 15.

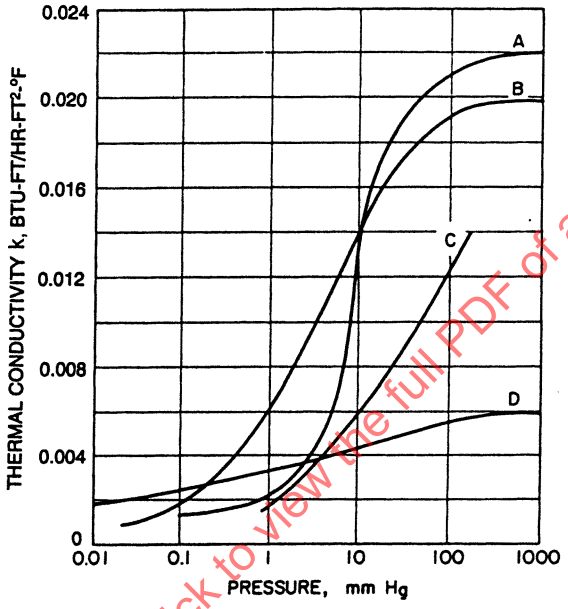

FIGURE 15 - Variation of Thermal Conductivity k With Pressure for Various Powdered Insulations of Temperatures Between 138 and 540 °R; T_{av} = 339 °R; A = Diatomaceous Earth; B = Perlite; C = Lampblack; D = Santocell (Reference 15)

When gas conduction is eliminated by lowering the insulation pressure, radiation becomes the predominant mode of heat transfer. This mode of heat transfer can be minimized by the use of powdered or solid particle insulation, by fibrous materials, or by multiple layers of highly reflective surfaces. This latter method is discussed more fully in the part on radiation.

Highly efficient insulating materials with lower thermal conductivities than those listed in Table 7 have been developed through improvements in cryogenic insulation. Table 6 of Reference 14 lists a number of such materials. As indicated in Reference 14, the best forms of insulation are the laminated types of insulation, which have mean thermal conductivities on the order of 0.000025 Btu/h-ft-°F. However, they are not load bearing, so that an application such as insulating a cryogenic storage vessel requires additional structural members, which introduce the additional problem of heat leaks. Evacuated powders and fibers have been used extensively, particularly in small vessels. The thermal conductivities of these materials are approximately ten times as high as those of laminated materials.

4.2.1.3 (Continued):

Christensen, Reference 15, draws the following conclusions with regard to some of the commonly used insulation materials.

1. Cellular foams are not the best insulation for space environments because the totally enclosed interstices cannot be evacuated by the vacuum of space.

2. Fiberglas mats may be the best conventional insulation for space application because they are vibration- and pressure-resistant and have conductivities as low as 0.001 Btu-ft/h-ft^2-°F at low temperatures.

3. Fiberglas mats and powders must be used at the relatively high densities of 5 lb/ft^3 and more in order to reduce radiation transfer through the insulation.

4. Powders, while having the best thermal properties as insulators, have the disadvantages of being nonload bearing or vibration resistant, and are susceptible to effects of moisture.

These insulating materials are applicable primarily for extremely low temperatures and are not suitable for specific application such as for reentry bodies. The insulation requirements during reentry are low thermal conductivity at high temperatures for short duration. This insulation problem is discussed in Reference 19.

4.2.2 Radiation: Radiation is a very important means of heat transfer for temperature control of equipment. Surface temperatures, disposal of waste or excess heat, highly efficient insulation, all are dependent upon radiation or the control of radiation. Knowledge of thermal radiation and means for its control are vital for the design of temperature control systems. Reference 16 gives a comprehensive treatment on radiation heat transfer analysis. Reference 17 gives a detailed analysis for the design of efficient radiating surfaces. A more general discussion of thermal radiation is presented in many books on heat transfer, such as References 1, 2, and 18.

The selection of surface coatings for space vehicles is one of the important tasks to provide proper temperature control. Surface coatings must have appropriate values of solar absorptivity and emissivity, to keep the vehicle and equipment surface temperatures within required ranges. Table 8 illustrates the variety of materials and finishes found on the internal or external surfaces of Explorer VII (Reference 20).

TABLE 8 - Absorptance and Emittance of Materials Found in Explorer VII Satellite Vehicle

Material	Short Wave Absorptance, Solar Radiation	Long Wave Emittance
Sandblasted Al	0.42	0.21
Polished Al	0.31	0.07
Sandblasted Mg	0.63	0.54
Rokide A	0.15	0.77
Gray TiO_2 Paint	0.87	0.87
White TiO_2 Paint	0.19	0.94
Solar Cells	0.80	0.40
Sauereisen	0.34	0.88
Fused Silica	0.06	0.84
Gold Foil	0.21	0.07

Source: Reference 20.

4.2.2.1 Equipment Surface Radiation: Consider a piece of heat generating equipment. It may be electronic or electromechanical. A fluid moving (hydraulic or pneumatic) equipment item is ruled out because it would fall in the semipassive class. If the equipment is considered to be uniform in temperature at any time, it can be treated thermally as a unit.

The parameters of interest in steady-state cooling of the equipment are:

1. Heat generated in the equipment, Q_{gen}. (In the steady-state condition, this is also the heat to be dissipated.)
2. Effective radiating surface area A.
3. Allowable equipment surface temperature T.

If transients are being looked at, the thermal capacity C is also of interest.

For an object cooled only by radiation, the heat balance is

$$C\left(\frac{dT}{d\tau}\right) = Q_{gen} - Q_{net} \qquad \text{(Eq.3)}$$

where:

Q_{gen} = Rate of heat generation in equipment, watts
Q_{net} = Rate of net heat loss by radiation from equipment, watts

4.2.2.1 (Continued):

If the equipment is reasonably small compared with an enclosing spherical satellite, the following equation can be used to a good approximation, provided the satellite inner surface is at a uniform temperature:

$$Q_{net} = \sigma A \in T^4 \qquad \text{(Eq.4)}$$

If the satellite inner surface is nonuniform in temperature, the same equation may apply, with T^4 replaced by $\overline{T}^4$, an effective radiation temperature, provided the equipment is near the center of the satellite or is (essentially) flat and wall mounted. In either case, the simple term T^4 can describe the heat sink temperature; further, this temperature can be obtained from a gross vehicle heat balance of the type:

$$\frac{\pi}{4} D^2 \in_T \sigma \overline{T}^4 = \alpha_s S \frac{\pi D^2}{4} + \sum Q_{gen} \qquad \text{(Eq.5)}$$

Equation 5 can be rearranged as

$$\left(\frac{\in_T}{\alpha_s + r} \right) \sigma \overline{T}^4 = S \qquad \text{(Eq.6)}$$

where:

$$r = \sum Q_{gen} \Big/ \left[\left(\pi D^2 / 4 \right) S \right] \qquad \text{(Eq.7)}$$

Referring to Figure 16, ω is defined as

$$\omega = \frac{\in_T}{\alpha_s + r} \qquad \text{(Eq.8)}$$

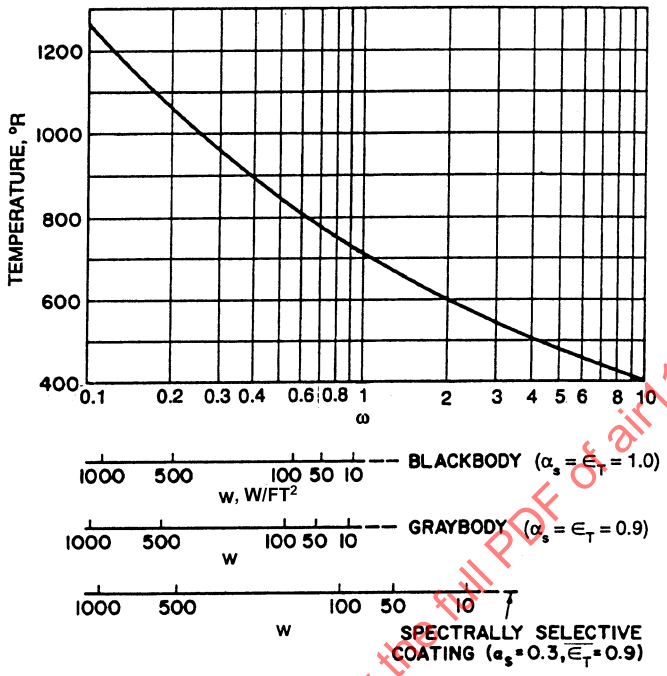

FIGURE 16 - Thermal Balance Solution for Flat Plate Normal to Sun's Rays at Top of Atmosphere

4.2.2.1 (Continued):

If w in Figure 16 is defined as

$$w = \frac{\sum Q_{gen}}{\pi D^2 / 4} \text{ W/ft}^2 \qquad \text{(Eq.9)}$$

then Figure 16 can be used to give the sink temperature:

$$T_{sink} = \left(\overline{T}^4\right)^{1/4} \qquad \text{(Eq.10)}$$

T_{sink} will vary from 400 to 600 °R for most Sun-illuminated satellites. T_{sink} = 400 °R corresponds to ϵ_T/α_s = 10 and w = 0 W/ft^2. T_{sink} = 600 °R corresponds to ϵ_T = 0.9, α_s = 0.3, and w = 20 W/ft^2.

Also in Figure 16,

$$r = \frac{w}{S} \qquad \text{(Eq.11)}$$

4.2.2.1 (Continued):

where w is the thermal input to the plate in W/ft^2 in addition to solar radiation S, the value of which is

$$S = 130 \text{ W/ft}^2 \quad \text{(Eq.12)}$$

Higher vehicle surface thermal loadings than these are possible, of course, for equipment compatible with the resulting temperature level. At w = 50 W/ft^2, ϵ_T = 0.9, and α_s = 0.3, T_{sink} = 650 °R. These thermal loadings are per unit disc area of the spherical satellite; they should be divided by 4 to get the equivalent loading per unit of satellite surface area.

Figure 17 is a generalized plot of the basic radiation equation:

$$\frac{Q}{A} = \sigma\left(T^4 - T_{sink}^4\right) \quad \text{(Eq.13)}$$

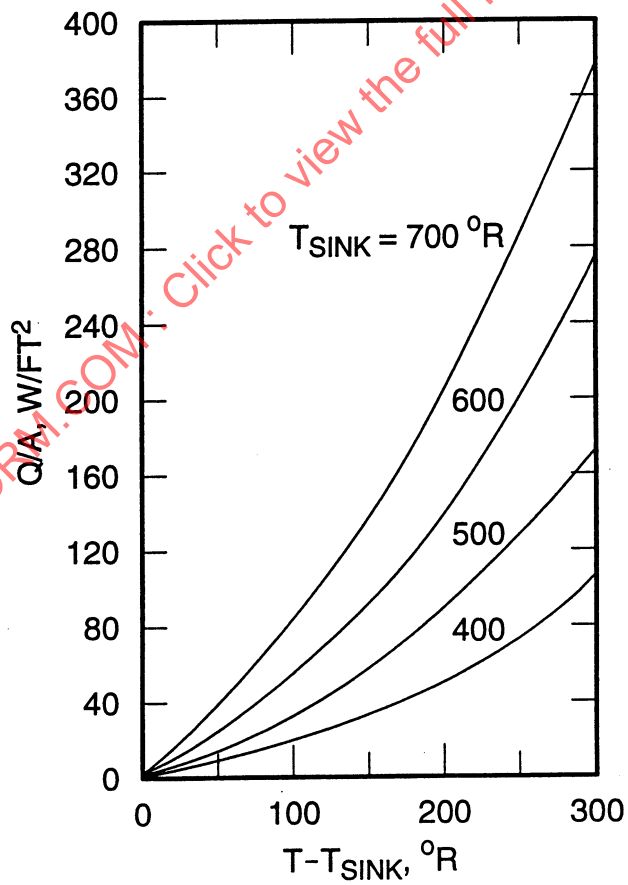

FIGURE 17 - Solution of Radiation Equation (Equation 13)

4.2.2.1 (Continued):

It may be used to show temperature levels associated with cooling by radiation alone, even under favorable conditions.

At reasonable sink temperatures, in the range of 600 °R, it takes a temperature rise of 110 °R to dissipate 60 W/ft^2 from equipment. The loading of 60 W/ft^2 is a rather light thermal loading, typical of electronic elements in a power limited installation. The conclusion is that radiation cooling is satisfactory for items of low to moderate thermal loading. For high thermal loadings, additional cooling means are desirable, to avoid excessive temperature rise. The exception to this would be single components of high thermal output, designed to be radiation cooled at fairly high temperature rises.

4.2.2.2 Thermal Radiation Shield: The heat transfer equations derived here are for a vehicle whose surface is shielded by n layers of protecting materials. It is assumed that a vacuum exists in the space between the body and the shield, as well as between the individual layers, and that no heat flows by conductivity between the elements under consideration. One further assumption is that the layers are flat, parallel, and infinitely large, so that the configuration factor is equal to 1.

Each of the several layers is assumed to have an emissivity ϵ except for the outside surface of the last layer (the most external one), which has an emissivity ϵ_m. The rate at which radiant energy leaves the body, whose temperature is T_0 and emissivity is ϵ_0, can be analyzed by use of Figure 18.

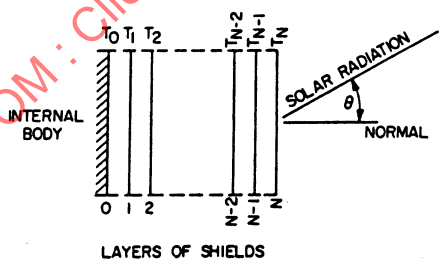

FIGURE 18 - Multilayer Shielding

Heat transfer between surface 0 and layer 1 is

$$q_{0,1} = \frac{1}{(1/\epsilon_0)+(1/\epsilon)-1}\sigma\left(T_0^4 - T_1^4\right) = \frac{\epsilon_0\epsilon}{\epsilon+\epsilon_0-\epsilon_0\epsilon}\sigma\left(T_0^4 - T_1^4\right) \quad \text{(Eq.14)}$$

4.2.2.2 (Continued):

and the heat transfer between layers 1 and 2 is

$$q_{1,2} = \frac{1}{(1/\epsilon)+(1/\epsilon)-1}\sigma\left(T_1^4 - T_2^4\right) = \frac{\epsilon}{2-\epsilon}\sigma\left(T_1^4 - T_2^4\right) \quad \text{(Eq.15)}$$

Similarly, it follows that heat transfer between layers n – 1 and n is

$$q_{n-1,n} = \frac{\epsilon}{2-\epsilon}\sigma\left(T_{n-1}^4 - T_n^4\right) \quad \text{(Eq.16)}$$

The heat transfer equation between the nth layer and the environment is

$$q_n = \epsilon_n \sigma T_n^4 - S\alpha_s \cos\theta \quad \text{(Eq.17)}$$

For steady-state condition, heat flow rate is the same through all the layers; thus, by equating Equations 15 and 16, the following relation is obtained:

$$T_1^4 - T_2^4 = T_{n-1}^4 - T_n^4 \quad \text{(Eq.18)}$$

Equation 18 is typical for any of the layers and shows the change in the value of the fourth power of the temperatures between succeeding layers. For n layers, there will be n – 1 changes in value between the first and the nth layer, or

$$T_1^4 - T_n^4 = \left(T_{n-1}^4 - T_n^4\right)(n-1) \quad \text{(Eq.19)}$$

Now, equating Equations 14 and 16,

$$\frac{\epsilon_0 \epsilon}{\epsilon + \epsilon_0 - \epsilon_0 \epsilon}\sigma\left(T_0^4 - T_1^4\right) = \frac{\epsilon}{2-\epsilon}\sigma\left(T_{n-1}^4 - T_n^4\right) \quad \text{(Eq.20)}$$

It follows that

$$T_0^4 = T_1^4 + \frac{\epsilon + \epsilon_0 - \epsilon_0 \epsilon}{\epsilon_0 (2-\epsilon)}\left(T_{n-1}^4 - T_n^4\right) \quad \text{(Eq.21)}$$

Also, equating Equations 16 and 17 and simplifying,

$$T_{n-1}^4 - T_n^4 = \frac{\epsilon_n (2-\epsilon)}{\epsilon} T_n^4 - \frac{2-\epsilon}{\epsilon\sigma} S\alpha_s \cos\theta \quad \text{(Eq.22)}$$

4.2.2.2 (Continued):

Combining Equations 19, 20, and 22,

$$T_0^4 = T_n^4 + \left[\frac{\epsilon_n (2-\epsilon)}{\epsilon} T_n^4 - \frac{2-\epsilon}{\epsilon\sigma} S\alpha_s \cos\theta\right]\left[\frac{\epsilon + \epsilon_0 - \epsilon_0\epsilon}{\epsilon_0 (2-\epsilon)} + (n-1)\right] \quad \text{(Eq.23)}$$

which may be expressed simply as

$$T_0^4 = T_n^4 + \left(C_a T_n^4 - C_c\right) C_b \quad \text{(Eq.24)}$$

where:

$$C_a = \frac{\epsilon_n (2-\epsilon)}{\epsilon} \quad \text{(Eq.25)}$$

$$C_b = \frac{\epsilon + \epsilon_0 - \epsilon_0\epsilon}{\epsilon_0 (2-\epsilon)} + (n-1) \quad \text{(Eq.26)}$$

$$C_c = \frac{2-\epsilon}{\epsilon\sigma} S\alpha_s \cos\theta \quad \text{(Eq.27)}$$

Finally,

$$T_n^4 = \frac{T_0^4 + C_b C_c}{C_a C_b + 1} \quad \text{(Eq.28)}$$

Substituting Equations 28 and 17, the general equation for the amount of heat radiated through a cover consisting of n layers as a function to T_0 and angle θ is obtained as

$$q_n = \epsilon_n \sigma \frac{T_0^4 + C_b C_c}{C_a C_b + 1} - S\alpha_s \cos\theta \quad \text{(Eq.29)}$$

When in free space, if a side of the vehicle is not exposed to the Sun, $\theta = 90°$, $\cos\theta = 0$ and $C_c = 0$ (see Equation 27), therefore

$$q_n = \frac{\epsilon_n \sigma T_0^4}{C_a C_b + 1} \quad \text{(Eq.30)}$$

4.2.2.2 (Continued):

Further, in the particular case where $\epsilon_n = \epsilon$, Equation 30 reduces to

$$q_n = K_{\epsilon,\epsilon_0}\sigma T_0^4 \qquad \text{(Eq.31)}$$

where:

$$K_{\epsilon,\epsilon_0} = \frac{\epsilon\,\epsilon_0}{\epsilon + \epsilon_0\,(1-\epsilon)} + \epsilon_0\left[2(n-1) - (n-1)\epsilon\right] \qquad \text{(Eq.32)}$$

If $\epsilon_0 = \epsilon$, Equation 32 reduces to

$$K_{\epsilon,\epsilon_0} = \frac{\epsilon}{1+n(2-\epsilon)} \qquad \text{(Eq.33)}$$

The heat transfer coefficient K_{ϵ,ϵ_0} versus n, the number of shields, is plotted in Figure 19 for the case in which an enclosed body is in free space receiving no solar energy. The figure indicates a rapid decrease in the value of heat transfer coefficient as the number of shields increases from zero to 2. As n increases beyond 3, the reduction in the value for K_{ϵ,ϵ_0} becomes negligible.

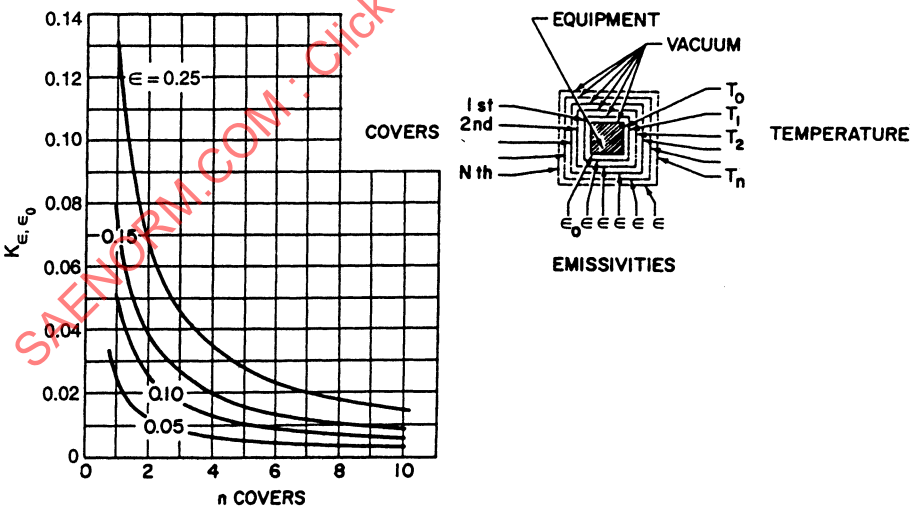

FIGURE 19 - Multishield Heat Transfer Coefficient (Box in Free Space and No Solar Heat);
$Q = K_{\epsilon,\epsilon_0}\sigma T_0^4$ Btu/h-ft^2
A value of $\epsilon_0 = 1.0$ Was Used, Since Only Small Deviations
Result From Using Values as Low as 0.5

4.2.2.2 (Continued):

Also indicated by Figure 19 is that the coefficient K_{ϵ,ϵ_0} is reduced by decreasing the value for emissivity. By using three or four shields of low emissivity material, such as aluminum foil (ϵ = 0.05), very low values for the heat transfer coefficient can be obtained.

Figures 20 and 21 show plots of Equation 29 for n = 3 and n = 4, for the case where the body is exposed to solar radiation for which the incident angle varies from 0 to 90 deg. Curves are plotted for several values of body temperature from 400 to 800 °R. For a given Sun angle θ, the heat transfer rate increases almost exponentially with increase in body temperature. Comparison of Figures 20 and 21 indicates the reduction of heat transfer rate by increasing the number of shields from three to four, which is as expected.

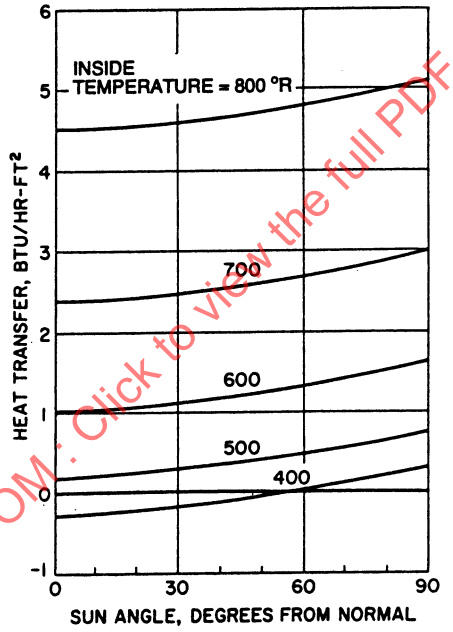

FIGURE 20 - Heat Transfer in Space Using Three Shields
Assumed Conditions: S = 430 Btu/h-ft^2; ϵ_0 = 0.80; ϵ = 0.05; ϵ_n = 0.95; α_s = 0.18

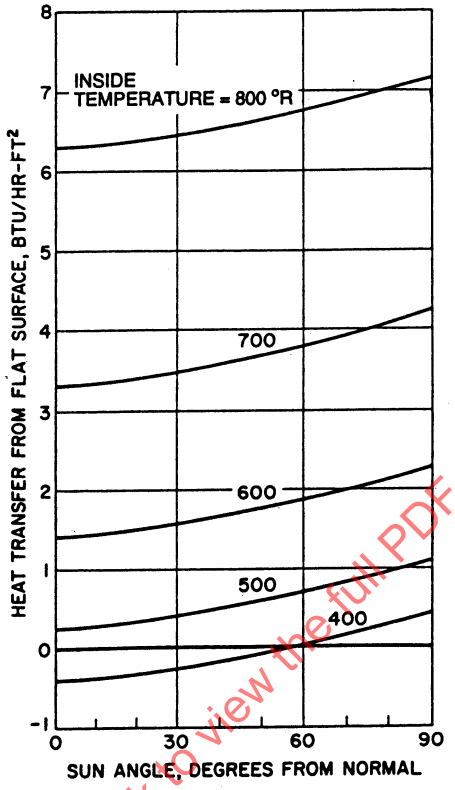

FIGURE 21 - Heat Transfer in Space Using Four Shields
Same Assumed Conditions as for Figure 20

4.2.2.2 (Continued):

The preceding analysis is limited for the case of infinite flat plates, but it does illustrate the effectiveness of using multilayer shielding. For surfaces of finite size, the interchange factor between the layers must be computed, since the geometric form factor is not equal to 1. This can be readily accomplished by utilizing the radiosity analog method, described in References 16 and 21.

4.3 Semipassive Temperature Control Methods:

4.3.1 Variable Insulation: The ability to vary the effectiveness of insulation with time can be one method of controlling temperature. For example, a satellite of low internal power generating ability may require a change in the insulating ability of its shell, as it moves from sunlight into shadow and back into sunlight again.

4.3.1 (Continued):

One type of variable insulation alters its overall conductivity by admitting small amounts of gas into the otherwise evacuated space. A thermal switch, sensing the temperature of the equipment to be controlled, actuates a valve that admits gas into the insulating space. The insulation may be vented to space and returned to a vacuum condition when the gas admission valve is closed.

The very small quantities of gas required for large changes in conductivity make this system feasible for satellites of even moderate duration. Its use in cases where gases would normally be discharged overboard in any event is particularly attractive.

The system may be arranged so that the section of the vehicle facing the Sun is a poor conductor, while that facing away is a good conductor, or vice versa. It can also accommodate a wide range of heat loads and component temperature requirements. A variation in insulating ability can be made to compensate for the deterioration of radiation properties of outer surfaces, which may occur during protracted operation in a space environment.

Characteristics of variable insulation systems are:

1. Power – Only that necessary to actuate valves.

2. Weight – The weight of the system would be made up of weights of the valves, switches, ducts, and extra gas.

3. Method – The gas used could be that ordinarily ejected overboard in normal operation.

4. Limitations – Reliability is dependent upon that of switches and valves. Malfunction could cause complete evacuation of vehicle. Extended missions may require large quantities of gas.

5. General – A system of relative simplicity, designable upon well-established principles and readily determined data.

4.3.2 Thermal Switch: The operation of a thermal switch (Figure 22) involves the opening and closing of a thermal conductive circuit in response to a temperature change. Any device that will break contact will perform satisfactorily, but the contact must be positive, to ensure good thermal conduction. A bellows filled with a temperature-sensitive fluid has given good performance. The fluid may operate on volume variation produced by a phase change or simply by temperature expansion. Simple bimetallic devices can also be used, but the thermal contact resistance is usually high.

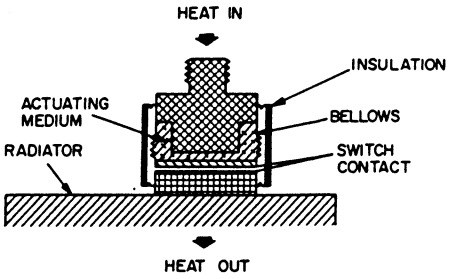

FIGURE 22 - Thermal Switch for Control of Conductivity

4.3.2 (Continued):

Characteristics of this type of switch include:

1. Power – No external power is required for actuation.

2. Weight – Weight of a bellows type of thermal switch filled with liquid metal that depends on fusion phase change ranges from 5 to 20 lb/ft^2.

3. Method – While integral with structure, no possibility of any function other than electrical conductance appear obvious.

4. Limitations – Bellows may fatigue or leak. Actuating medium may be toxic. Contact surfaces must be precise and remain unchanged in properties.

5. General – No external power or control requirements increase reliability. Temperature operating range is 20 to 2000 °F. The heat conducting rate depends on the material, cross-sectional area, and type of gap (air or vacuum) when open circuited. Typical thermal resistance values are 0.5 to 10 °F-h-ft^2/Btu for open circuit and 0.001 to 0.01 °F-h-ft^2/Btu for closed circuit.

4.3.3 Radiator With Shutters: A radiator with a shutter will allow close temperature control if the proper surface coatings are used (see Figure 23). When the shutters are closed, the surface will be a poor emitter; when open, the surface will be a good emitter. By varying the degree of opening, any value between the open and closed emittance can be obtained.

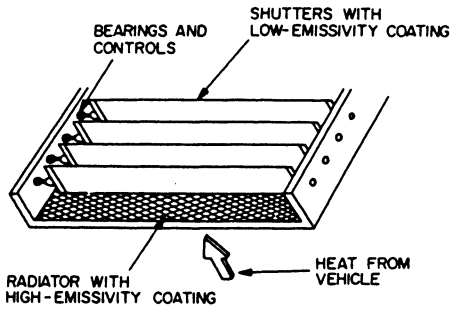

FIGURE 23 - Shutter for Controlling Emissivity

4.3.3 (Continued):

The shutter opening can be varied by a bimetallic element controlled by the surface temperature. The shutter can be louvered or rotary, but the rotary, or pinwheel, type does not allow as wide control as does the louvered shutter. Typical values of thermal emissivities are 0.01 to 0.05 for the closed shutter condition and 0.92 to 0.93 for the open shutter condition. Flexure type bearings eliminate zero gravity effects and high-vacuum lubrication problems.

Characteristics of the shuttered radiator are:

1. Power – No power requirements unless the shutters are actuated mechanically or electromagnetically.

2. Weight – The weight of the shutter and controls, exclusive of the radiator, should be in the range 0.1 to 0.3 lb/ft^2.

3. Method – Functional integration is difficult to achieve.

4. Limitations – Operation of bearings and controls in vacuum is subject to some uncertainty and to meteoritic damage.

5. General – Emissivity is controllable over a wide range, probably 20 to 1. Operative in the same temperature range as plain radiators. Insensitive to gravity field.

4.3.4 Forced Convection Loop: This system (see Figure 24) consists of a pump or fan, a circulating heat transfer fluid, a radiator, and the necessary ducting. The heat is transported from or to the vehicle interior by circulating the working fluid, after increasing its sensible or latent heat. The working fluid may be contained in a duct or may occupy an enclosed space such as a cabin. Air, helium, nitrogen, ethylene glycol, water, or ammonia can be used as the circulating fluid.

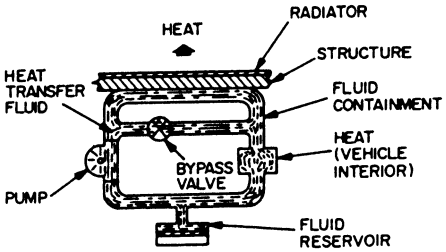

FIGURE 24 - Forced Convection Loop

4.3.4 (Continued):

Characteristics of the system are:

1. Power – The power required depends on the fluid, circulation rate, and length and type of ducting. Using ethylene glycol, a pump-motor efficiency of 40%, a total system pressure drop of 100 psi, and a radiator temperature drop of 20 °F, the pump power is approximately 0.025 kW per kW of heat rejected.

2. Weight – The weight depends on the arrangement. Based on the example in item 1, a weight of 3 to 10 lb/kW is reasonable.

3. Method – The air circulation loop can be integral with the cabin air distribution system; fluid loops can serve as attitude control devices; ducts may be formed by structure; the radiator may be integral with structure.

4. Limitations – Heat transfer rate is subject to difference in internal and external temperatures. Fluid leakage must be prevented. Gravity field affects heat transfer rate in mixed phase, but not in single phase forced flow.

5. General – Relatively simple control and good stability characteristics. Relatively low power requirements.

4.3.5 Expendable Heat Sink: The heat sink (see Figure 25) consists of an expendable material such as water, liquid oxygen, nitrogen, hydrogen, or any substance that can store energy in some manner, with or without a change of phase. The heat can be brought to the heat sink material by a passive, semiactive, or active heat transport system, or the heat sink can be brought to the heat source.

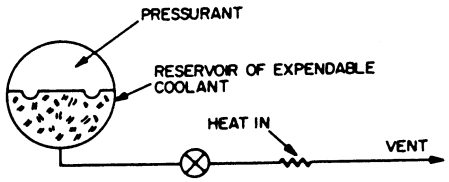

FIGURE 25 - Expendable Heat Sink System

4.3.5 (Continued):

Characteristics of the heat sink are:

1. Power – The power required would be that to operate an active or semipassive heat transport system and to actuate a vent valve.

2. Weight – The weight depends on the expendable fluid. For example, water can absorb around 1100 Btu/lb; hydrogen, oxygen, and nitrogen (from liquid to 70 °F), 1100, 175, and 183 Btu/lb, respectively.

3. Integration – Expendable material may be chemical fuel fed to a secondary power system, breathing and/or cabin pressurization gases, or attitude control propellant. The fluid may be contained within structural members.

4. Limitations – The heat capacity of a practicable amount of fluid may be insufficient for the mission. The system may be heavier, initially, than an equivalent radiator.

5. General – Temperature range of operation is 40 to 620 °R; pressure range is 1 to 500 atm. Simple controls. Largely insensitive to outside environment.

4.3.6 Transpiration Wall Insulation: A scheme has been proposed for the thermal protection of cabin occupants during reentry. This scheme, known as transpiration wall insulation, consists of placing perforated sheets over all otherwise exposed interior surfaces of the hot skin. Cooling air is admitted into the cabin compartment and then flows out through the perforated sheet and into the space between the perforated sheet and the basic structure. The net effect is that the perforated sheet is maintained at essentially the air compartment inlet temperature, thereby shielding the occupants from the high radiation heat of the basic structure.

The air, after passing through the perforated sheet, will gain heat from the skin, but this heat cannot be transmitted back to the occupants, owing to the air continuously flowing through the perforations and the shielding effect of the perforated sheet. The incoming air, therefore, should absorb only the heat generated by the occupants and the equipment inside the compartment. Consequently, the air circulation rate would be only a small fraction of the rate that would be required if the transpiration wall were not used.

4.3.6 (Continued):

These perforated sheets need not cover the entire inner surface and may be removed for access to the basic vehicle skin for any needed repairs during space flight.

Characteristics of the system include:

1. Power – The only additional power requirement would be that necessary to overcome the resistance to the passage of air through the perforations.

2. Integration – The high-temperature air downstream of the transpiration wall could be used as an efficient energy source for a cryogenic power system.

3. Limitations – Hole sizes must be selected so that radiant energy does not enter through openings that are too large, and so that the openings are not too small to permit the free flow of air. The side facing the outer skin should be thermally reflective.

4. General – A relatively simple solution to a difficult problem of prime importance. Can be adapted, together with convection loop and radiator, or expendable heat sink, to space cabin cooling.

4.3.7 Vacuum Cooling Cycle: The vacuum cooling cycle (see Figure 26) is similar to an expendable heat sink system, but has the advantage that the coolant is recovered for subsequent reuse. The name derives from the use of a vacuum for producing a pressure differential and for recovery.

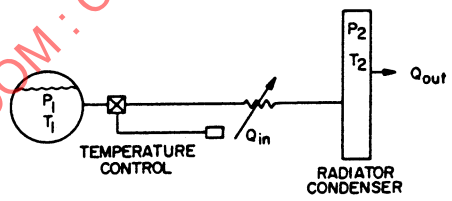

FIGURE 26 - Vacuum Cooling System

Low temperature, easily obtainable in space, is used to condense the coolant. As illustrated, the coolant flows from storage, picks up heat and vaporizes, and then goes to the radiator-condenser, where it is reduced to its liquid or solid phase. The operation of the system may be made continuous by using a small pump for recirculation, or may be made intermittent by the use of a dual system with necessary valving and plumbing to permit the cyclic operation of two separate systems.

4.3.7 (Continued):

Characteristics of the system are:

1. Power – There may be none or a very small amount.

2. Weight – This system would use, as a coolant, only such liquids that were aboard for other purposes, so that assignable weight would be that of the plumbing and radiator.

3. Integration – Coolant or fuel intended for reentry could be used, and the radiator integrated with the outer surface or a radar antenna.

4. Limitations – Generally restricted to low heat dissipation requirements.

5. General – Spot cooling may be the principal application. Elimination of circulating fluids appears attractive.

4.3.8 Silica Gel Cooling Process: This process (see Figure 27) is similar to the vacuum cooling cycle described above; the difference is that a vacuum is maintained by adsorbing the coolant in a silica gel bed.

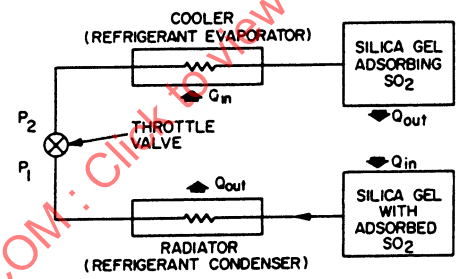

FIGURE 27 - Silica Gel Cooling System

The refrigerant is desiccated as a vapor from a quantity of silica gel where it was previously adsorbed. This vapor is then condensed, after which the liquid pressure is reduced by passing it through a throttling valve. The cold liquid is next evaporated, providing refrigeration by picking up the heat that is to be disposed of, and the vapor is then adsorbed by a second quantity of cooled silica gel.

After the adsorbed vapor has been completely driven off the hot silica gel and adsorbed by the cold lot, the roles of the two lots are reversed. By proper valving, this reversible process can be followed and refrigeration continued.

4.3.8 (Continued):

Characteristics of the cooling process are:

1. Power – Low, possibly involved only with heating of one lot of silica gel and cooling of the other.

2. Weight – Estimated to be comparable to a vacuum cooling system of same capacity.

3. Integration – Heating and cooling of silica gel could be done in a compartment forming part of structure, heating accomplished on one side and cooling on other side of the vehicle. Condensation could be accomplished by the cold of outer space.

4. Limitations – Generally restricted to low heat dissipation requirements.

5. General – No circulation pumps are required. By using naturally available heat sources and sinks, the power requirement for regeneration may be reduced. Operating pressures are relatively low and leakage is preventable. A variety of coolants are available; sulfur dioxide is commonly used. Operation can be intermittent.

4.4 Technical Approach, Semi-Passive Methods:

Semipassive methods previously discussed can be classified in a number of different ways. The one used here is the mode of heat transfer; that is, by systems involving variations in conduction, in convection, or in radiation. It should be noted that the use of some methods to be discussed (namely, differential metallic expansion or fluid expansion) can also be used to operate switches, relays, or other means to reduce or halt the heat producing activity of some component. This type of operation is not considered here.

The wide range of available semipassive temperature control methods gives a choice of control through variation in surface coating or variation in the internal heat transfer rate. The variable coating and variable conduction type control will usually be restricted to equipment with small heat loads, whereas the forced convection fluid loops and expendable methods adapt better to equipment with high heat loads, since cold plate or direct forced convection cooling is available for removing heat from high dissipating components.

The semipassive methods are usually limited only by the requirement that the heat sink (heat exchanger, vehicle skin, or radiator) must be at a lower temperature than the equipment. However, the expendable, vacuum, and silica gel methods do not even have this restriction.

At the present time (circa 1965), semipassive methods of variable surfaces and fluid loops have been used on some space vehicles. These methods have proved to be reliable and fairly light. However, some coatings have deteriorated and fluid loops have an inherent danger of leakage. Much research is needed in improving coating and fluid loop reliabilities.

4.4 (Continued):

Since extensive research in surface coatings is already underway, recommendation is made that some research be directed toward fluid components and loops. If the probability of leakage is decreased, toxicity, corrosiveness, and dielectric strength become negligible considerations in most fluid loops. As a result, basic coolant considerations of weight, volume, and surface area can be used as the only criteria needed for optimization. Increase in the efficiencies and operating life of fans and pumps is also desirable.

4.4.1 Variable Conduction Methods:

4.4.1.1 Differential Metallic Expansion: The simplest type of thermal switch is one made up of welded parallel strips of two metals having different coefficients of thermal expansion. Changes in temperature cause expansions or contractions of the strips, but the differences in coefficient cause a bending or warping that can be used to make or break a thermal conductive path. This is illustrated in Figure 28. A number of bimetallic elements and applications are illustrated in Reference 22.

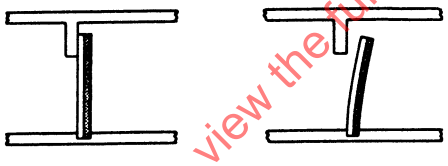

FIGURE 28 - Differential Metallic Expansion Device for Controlling a Thermal Path

While simple in operation, this switch can be made quite sensitive to temperature changes, the make or break being controlled to within a degree or less of temperature. The rate of heat transfer may be less easy to regulate, being subject to the degree of finish and contamination on the surfaces and the forces between surfaces.

4.4.1.2 Fluid Expansion: The use of fluid expansion or contraction to regulate heat flow can take many forms. For example, a variation of the differential strip switch just described would be one in which contact was made or broken between the elements by temperature-induced fluid pressure. A thermal switch actuated by fluid volumetric change is illustrated in Figure 29.

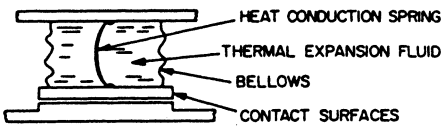

FIGURE 29 - Thermal Switch for On-Off Conductivity Control

4.4.1.2 (Continued):

The thermal switch of Figure 29 is characterized by on-off operation. Figure 30 illustrates a method of temperature control employing a variable resistance heat path. This device also employs a bellows containing a temperature-sensitive fluid, but this material is not required to conduct heat. Heat transfer takes place across surfaces of soft materials, the contacting area being variable and related to the amount of heat to be conducted.

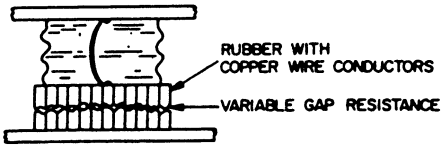

FIGURE 30 - Thermal Switch for Variable Conductivity Control

These soft materials may be rubber, cork, or any other material that deflects easily. Thermal conductivity of such materials is usually low, but may be improved by impregnating with metal fibers, ribbons, springs, chips, or other flexible paths (Reference 23).

4.4.1.3 Variable Gas Conduction: The difference in conductivities of insulating materials before and after degassing was discussed in 4.2.1.3 and shown in Table 7 for some materials. By regulating the amount of gas within the insulation, it is possible to produce conductivities to meet specific requirements.

Table 9 shows variation with pressure for several insulating materials. Figure 15 graphs the pattern of change for typical powdered insulators. Generally, the behavior of reduced, pressured insulation is a very slow increase in conductivity with pressure increase, followed by a rapid rise, and finally stabilizing in a region of little change in conductivity.

TABLE 9 - Variation of Thermal Conductivity at 100°F of Various Insulating Materials with Interstitial Pressure

Insulating Material	Thickness, in	Density, lb/ft^3	Pressure, μ Hg	Thermal Conductivity, Btu-in/h-ft^2-°F
Air Space Between Copper Surfaces	1	--	1 atm	0.572
			0.10	0.245
			0.07	0.187
			0.0	0.145[1]
Corkboard	1	6.67	1 atm	0.283
			0.08	0.121
			0.06	0.106
Cotton	1	0.78	1 atm	0.288
			0.11	0.0805
			0.07	0.072
Fine Glass Wool	1	0.78	1 atm	0.302
			0.05	0.0695
			0.04	0.0665
Mineral Wool	1	7.7	1 atm	0.258
			9.0	0.059
			3.0	0.0425
			0.02	0.037

[1] Calculated.
Source: Reference 15, p. 20

4.4.2 Variable Convection Methods: The methods examined here are of two principal classes: those using expendable coolants and those having closed loops in which the coolant is recovered for re-use. The environment assumed for all systems is that of zero gravity, so that a fan, blower, pump, or some other device is necessary to force convection.

4.4.2.1 Expendable Coolant Convection Method: Expendable coolant methods are those in which a coolant absorbs heat, usually with one or two changes of phase, and is then vented overboard. Such systems are practicable only for missions of short duration because of the relatively large weight and volume requirements of the coolant for the amount of cooling done.

Two classes are recognized: those having separate coolant storage and heat exchange components; and those in which storage and heat exchange are combined in one component. These are illustrated in Figures 31 and 32, respectively. It can be seen that in the integral system, no pressurant is required.

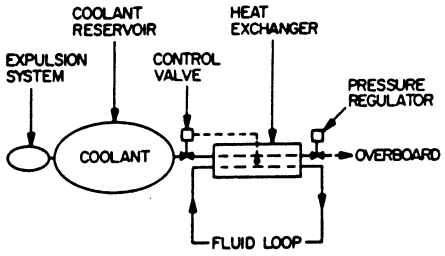

FIGURE 31 - Separate Expendable Coolant Storage

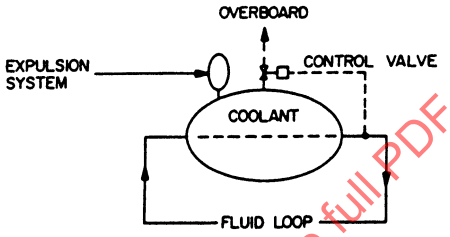

FIGURE 32 - Integral Expendable Coolant Storage

4.4.2.1 (Continued):

A comparative analysis of these two types of systems (Reference 24) led to the conclusion that the separate storage arrangement had decided advantages of weight and volume, while the reliability of the integrated system was only very slightly higher. The greater weight and volume of the latter resulted from two necessities:

1. Keeping an adequate portion of the heat transfer surfaces wet during the mission, with acceleration possible in any direction, and at the end of a mission, when the liquid level would be low because of coolant losses.

2. Preventing carryover of the liquid coolant through the vent.

By providing heat transfer surfaces, storage volume, and quantity of coolant in excess of the minimum requirement, and by packing the coolant space of the exchanger with Fiberglas wicking to disperse the liquid, a sufficient area of the exchanger was kept wet to ensure good heat transfer rates. The Fiberglas wicking and the location of the vent entrance at the geographical center of the exchanger prevented the carry-over of unvaporized coolant. Although simple and reliable, these provisions add considerably to the weight and space requirements of the integrated system.

4.4.2.1 (Continued):

One of the problems in expendable methods is the expulsion of the coolant from the tank. This becomes a major problem in space, where gravity cannot be used as an aid to expulsion. Usually some form of bladder with a pressurized gas such as helium or nitrogen is used. The gas is kept in a high-pressure tank and bled into the coolant tank to force the coolant out. The bladder is used to prevent mixing of gas and coolant. Control of the coolant tank pressure is maintained by a pressure regulator between the gas pressurant tank and the coolant tank. Another method of expulsion is to spin the tank so that the liquid is forced out by centrifugal force.

4.4.2.2 Selection of Expendable Fluids: Analyses of expendable fluid cooling methods will almost always show the best fluids to be water and ammonia. While water has most of the advantages, ammonia has a lower freezing point and can therefore be used at lower temperature. In addition, ammonia vapor can be used for certain pressurization applications where steam would condense.

Table 10 lists a number of materials that could be used as expendable coolants and the important properties that would have to be considered in making a selection. Note that the relative temperature level between the coolant boiling temperature and the equipment operating temperature is also important in choice of coolant.

TABLE 10 - Properties of Some Substances Suitable as Expendable Coolants

Substance	Liquid Density, lb/ft^3	Bp, °F	Heat of Vapori-zation Btu/lb	Specific Heat, Btu/lb-°F at Bp	Specific Heat, Btu/lb-°F at 200 °F	Specific Heat, Btu/lb-°F at 450 °F	Specific Heat, Btu/lb-°F at 1500 °F	Total Heat Absorption Btu/lb Bp to 200 °F	Total Heat Absorption Btu/lb Bp to 450 °F	Total Heat Absorption Btu/lb Bp to 1500 °F	Total Heat Absorption Btu/ft^3 Bp to 200 °F	Total Heat Absorption Btu/ft^3 Bp to 450 °F	Rank on the Basis of: Vol.	Rank on the Basis of: Wt.
H_2	4.37	-423	194	3.42	3.45	3.47	3.62	2335	3200	6966	10,200	13,980	18	1
H_2O	62.4	212	970	0.45	0.45	0.47	0.52	970[2]	1131	1671	60,500[2]	70,500	1	2
He	7.62	-452	11	1.24	1.24	1.24	1.24	821	1132	2437	6,250	8,620	20	3
NH_3	40.6	-28	589	0.48	0.53	0.59	0.81	703	844	1572	28,550	34,250	3	4
HF	62.0	67	650	0.34	0.34	0.35	0.38	695	782	1165	43,000	48,500	2	5
CH_4	25.9	-258	248	0.50	0.58	0.71	1.09	495	675	1638	12,800	17,500	11	6
CH_3OH	48.1	148	472	0.39	0.39	0.46	--	492	600	--	23,650	28,850	4	7
CH_3CH_2OH	48.1	173	367	0.41	0.41	0.45	--	377	486	--	18,100	23,350	7	8
--	53.1	148	596	0.41	0.41	0.46	--	369[2]	733	--	19,600[2]	38,900	6	9
C_2H_6	34.1	-127	210	0.33	0.50	0.63	1.00	345	486	1290	11,750	16,600	14	10
C_2H_4	35.3	-155	208	0.33	0.45	0.55	0.83	345	474	1168	12,200	16,700	12	11
[1]CO_2	62.0	-110	252	0.20	0.22	0.24	0.30	317	377	656	19,650	23,400	5	12
CO	49.3	-313	91	0.25	0.25	0.26	0.29	219	283	577	10,790	13,950	17	13
N_2	50.2	-320	86	0.25	0.25	0.25	0.28	216	279	569	10,820	14,000	16	14
--	57.4	-318	87	0.24	0.24	0.25	0.28	211	276	556	12,140	15,850	13	15
O_2	71.2	-297	92	0.22	0.22	0.23	0.26	201	260	525	14,330	18,540	9	16
Ne	75.2	-411	37	0.25	0.25	0.25	0.25	187	249	507	14,080	18,700	10	17
NO	62.4	-129	161	0.21	0.23	0.25	0.31	164	226	514	10,020	14,100	19	18
A	88.0	-302	68	0.13	0.13	0.13	0.13	130	161	292	11,450	14,190	15	19
Kr	162.3	-241	47	0.13	0.13	0.13	0.13	103	135	268	16,750	21,910	8	20

Note: All values at 14.7 psia except as noted.
[1] Solid carbon dioxide assumed cubed and occupying 65% of total volume. Sublimes without evaporation.
[2] Boiling assumed at 11.5 psia and 200 °F.
Source: Reference 26, pp. 17 to 18.

4.4.2.2 (Continued):

A relationship that may be of assistance in the selection of a suitable expendable liquid is known as Trouton's rule. This rule states that the molal latent heat divided by the normal absolute temperature of evaporation is equal to a constant. However, this ratio actually varies considerably, as seen in Table 11, but averages about 21.

TABLE 11 - Liquid Properties and Trouton's Rule

Substance	Boiling Temp., K	Critical Temp., K	T_b/T_c	Latent Heat of Vaporization L_e, cal/mol	L_e/T_b
He	4.2	5.2	0.81	22	5.2
H	20.3	33.2	0.61	216	10.6
O	90.2	154.3	0.58	1610	16.9
NH_3	239.7	405.5	0.59	5560	23.2
CCl_4	350	556	0.63	7140	20.4
CH_3CH_2OH	351	516	0.68	9450	26.9
C_6H_6	353	562	0.63	7500	21.2
H_2O	373	647	0.58	9700	26.0

Source: Reference 25, p. 145.

The polar or associated liquids, such as water and ethyl alcohol, have higher values than the nonassociated liquids. This results from the heat of vaporization of these substances, and while it is true that their boiling points are also relatively high, the difference in temperatures is not so great as the difference in latent heat. Attention should therefore be directed toward liquids having high values of the latent heat of vaporization temperature ratio for expendable coolants.

Figures 33 and 34 show for a number of possible liquids the value of latent heat at various boiling temperatures. It appears that water has more ability to absorb heat than any other liquid in the temperature range covered. The vapor pressures of these liquids are shown in Figures 35 and 36.

A method of comparing expendable coolants that is more complex than Trouton's rule is the weight comparison technique developed in 4.4.2.4.

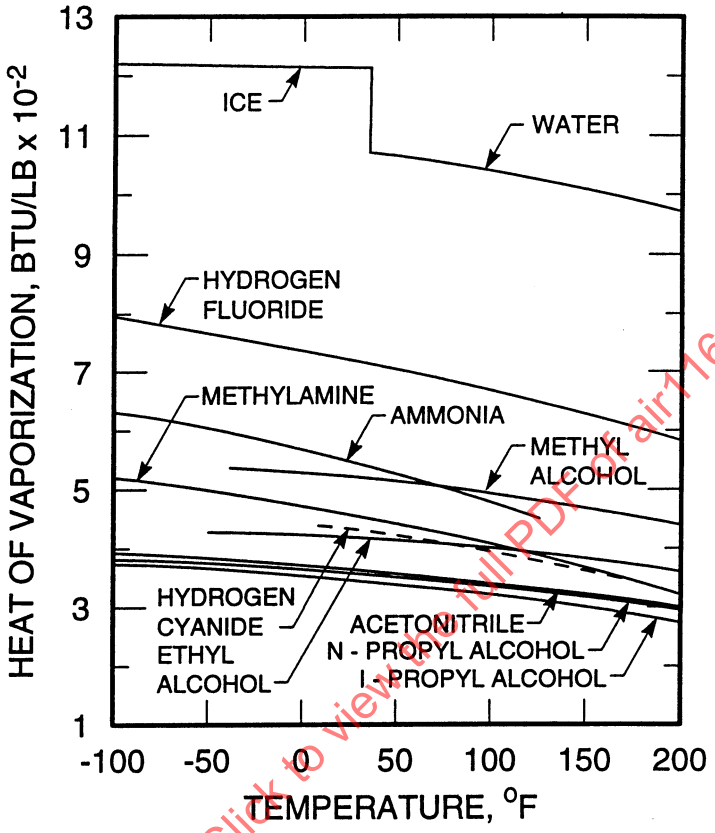

FIGURE 33 - High Latent Heat Liquids

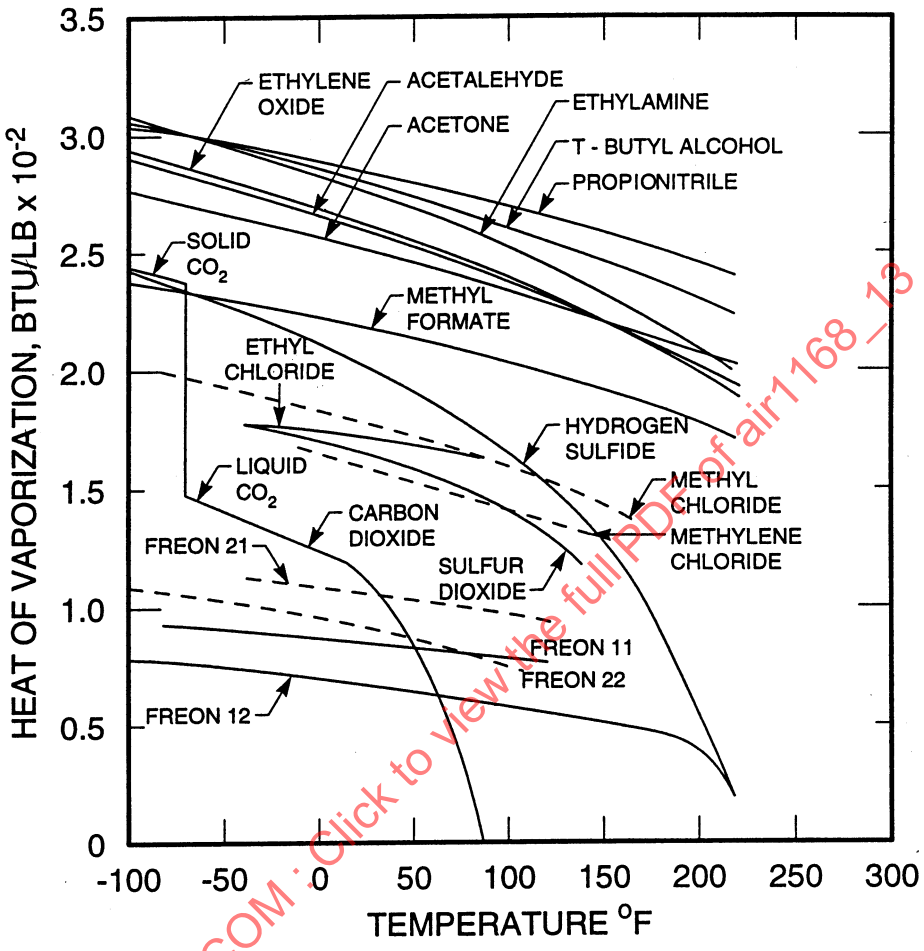

FIGURE 34 - Moderately High Latent Heat Liquids

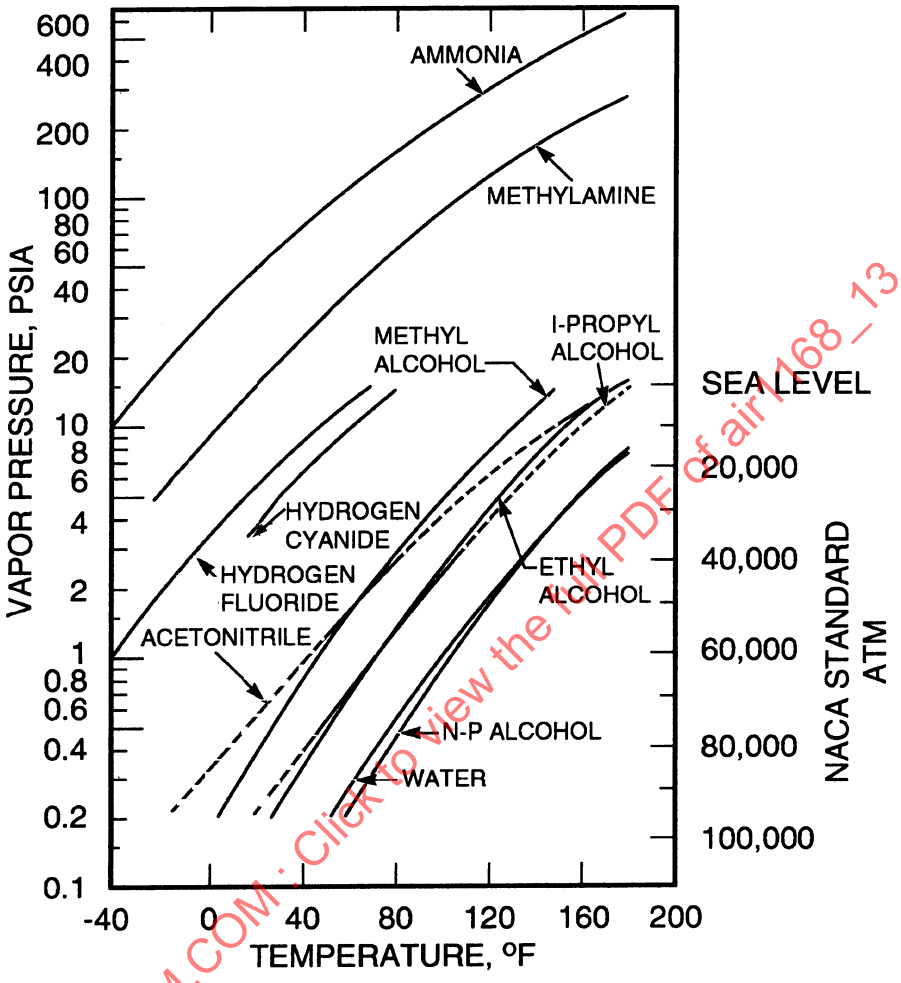

FIGURE 35 - Vapor Pressure of Liquids With High Latent Heats;
for Dashed Lines, Data Computed Using Clausius-Clapeyron Equation

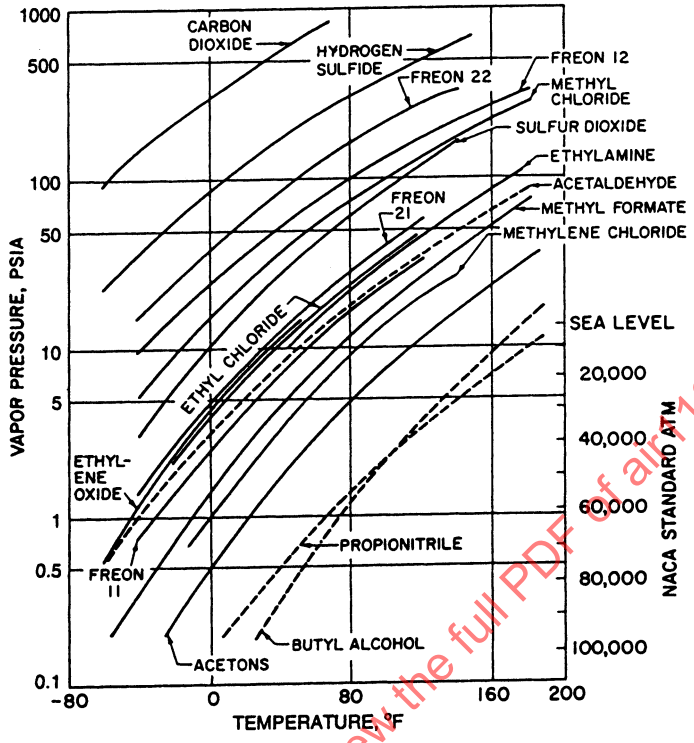

FIGURE 36 - Vapor Pressures of Liquids With Moderately High Latent Heats; for Dashed Lines, Data Computed Using Clausius-Clapeyron Equation

4.4.2.3 Evaluation of Expendable Coolant Liquids: Several comparisons, including Trouton's rule, L_e/T_b, have been used to choose a coolant fluid. However, most comparisons do not seem to carry through to an ultimate goal of showing which coolant requires the least total weight for a given heat load q, equipment temperature T_E, and time interval $\Delta\tau$.

Using Figure 37 and Table 12, a useful coolant comparison can be made for given values of q, T_E, and $\Delta\tau$.

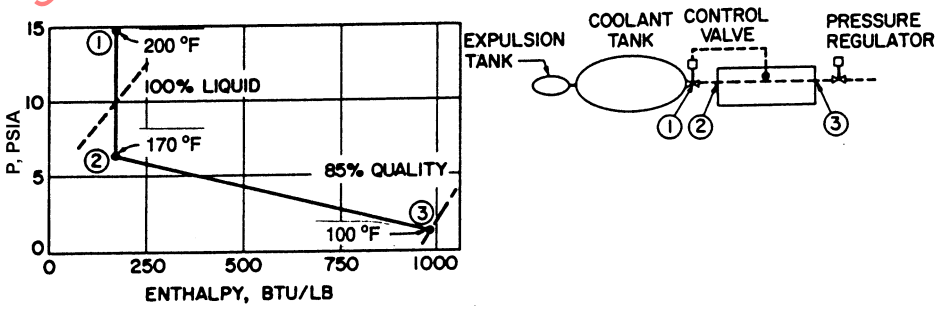

FIGURE 37 - Expendable Water Method (see Table 12)

TABLE 12 - Comparison of Water Method to Ammonia Method (see Figure 37)

	Weight, lb H_2O	Weight, lb NH_3	Volume, in^3 H_2O	Volume, in^3 NH_3
Tank	2	14.6	55.5	278
Heat Exchanger	5.2	1.0		
Fluid	4.2	10.4		
Total[1]	11.4	26	55.5	278

[1] Does not include tubing, valves, cold plates.

4.4.2.3 (Continued):

For the system in Figure 37,

$$L = 978 - 168 = 810 \text{ Btu/lb} \qquad \text{(Eq.34)}$$

$$w = \frac{(1000)(3.41)}{810} = 4.2 \text{ lb/h}$$

The weight of the tank can be considered as a function of coolant pressure, density, the heat load, and latent heat of vaporization. The thickness of the tank varies directly with the pressure so that $W_T \propto P_T$. Since the volume of the tank varies directly with the inverse of density of the stored coolant, a spherical container with volume (4/3) πr^3 and surface area 4 πr^2 yields $V_T \propto (1/g\rho_T)$, $A_T \propto W_T$, $A_T \propto (V_T)^{2/3}$, or $W_T \propto [1/(g\rho_T)]^{2/3}$. Finally, consideration of the latent heat of vaporization of the fluid determines the amount required, which also influences the tank weight as a volume change:

$$W_T \propto \sqrt{w\Delta\tau} = \sqrt{\frac{q\Delta\tau}{L_e}} \qquad \text{(Eq.35)}$$

Combining these terms,

$$W_T \propto P_T \sqrt{\frac{q\Delta\tau}{L_e g \rho_T}} \qquad \text{(Eq.36)}$$

or the weight of the tank can be expressed as

$$W_T = K_1 P_T \sqrt{\frac{q\Delta\tau}{L_e g \rho_T}} \qquad \text{(Eq.37)}$$

where K is a constant.

4.4.2.3 (Continued):

The weight of the heat exchanger can be considered as an inverse of the film coefficient of the coolant and the temperature difference between this compartment and the coolant:

$$W_{Hx} \propto \frac{1}{h(T_E - T_b)} \quad \text{(Eq.38)}$$

or

$$W_{Hx} = \frac{K_2}{h(T_E - T_b)} \quad \text{(Eq.39)}$$

where K_2 is a constant.

The weight flow of the coolant can be considered as

$$w = \frac{q}{L_e} = \frac{\Delta m}{\Delta \tau} \quad \text{(Eq.40)}$$

or the fluid weight as

$$W_f = \Delta m = \frac{q\Delta\tau}{L_e} \quad \text{(Eq.41)}$$

Of course the coolant flow path may include other weight considerations such as tubing, fittings, pressure regulators, and valves, but the weight of these components is usually not a direct function of the coolant. Therefore this weight can be neglected or considered as a constant $W_H = K_3$.

Combining the weight, described in the previous paragraphs, the total weight becomes

$$\begin{aligned} W &= W_T + W_f + W_{Hx} + W_H \\ &= K_1 P_T \sqrt{\frac{q\Delta\tau}{L_e g \rho_T}} + \frac{K_2}{h(T_E - T_b)} + \frac{q\Delta\tau}{L_e} + K_3 \end{aligned} \quad \text{(Eq.42)}$$

Equation 42 can be simplified for comparison purposes by nondimensionalizing the terms in the equation. Such nondimensionalizing could be based on a known coolant and flow system so that K_1, K_2, K_3 can be estimated. The nondimensionalized equation would appear as

$$\frac{W}{W_0} = K' \left(\frac{P_T}{P_{T,0}}\right)\left(\frac{L_{e,0} g \rho_{0,T}}{L_e g \rho_T}\right)^{1/2} + K_2' \frac{h_0(T_E - T_{b,0})}{h(T_E - T_b)} + K_4' \left(\frac{L_{e,0}}{L_e}\right) + K_3' \quad \text{(Eq.43)}$$

4.4.2.3 (Continued):

where 0 is a known coolant and K'_1, K'_2, K'_3 and W'_0 are known values:

$$K'_1 = \frac{W_{T,0}}{W_0}, \quad K'_2 = \frac{W_{Hx,0}}{W_0} \qquad \text{(Eq.44)}$$

$$K'_3 = \frac{W_{H,0}}{W_0}, \quad K'_4 = \frac{W_{f,0}}{W_0} \qquad \text{(Eq.45)}$$

This equation can be reduced even more if the boiling film coefficient of the liquids is held constant by varying the heat exchanger or cold plate flow area. Then $h/h_o = 1$ and Equation 43 becomes

$$\frac{W}{W_0} = K'_1\left(\frac{P_T}{P_{T,0}}\right)\left(\frac{L_{e,0}g\rho_{T,0}}{L_e g\rho_T}\right)^{1/2} + K'_2\left(\frac{T_E - T_{b,0}}{T_E - T_b}\right) + K'_3 + K'_4\left(\frac{L_{e,0}}{L_e}\right) \qquad \text{(Eq.46)}$$

Equation 46 can be used to compare coolants for use in an open-loop coolant method with known compartment heat load q and temperature T_E. Tank weights and volumes and coolant method parameters, estimated in Reference 26, are presented in Figures 38, 39, and 40 for use in comparisons.

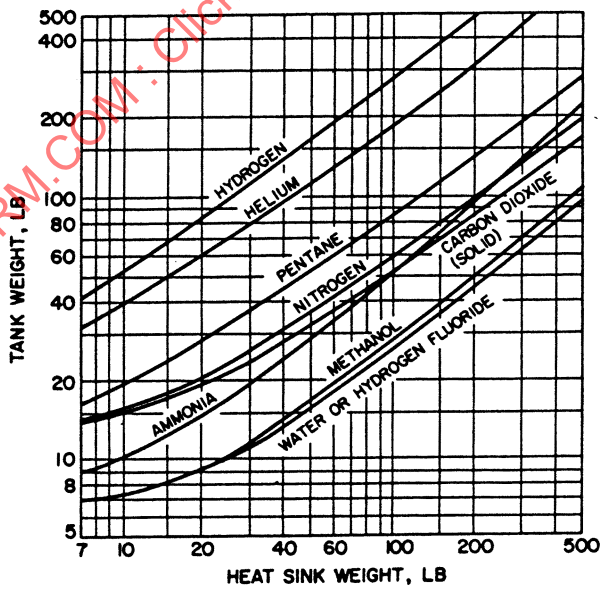

FIGURE 38 - Liquid Heat Sink Storage Weight; Includes Tank, Insulation Where Applicable, Supports and Fill, Vent, and Safety Valving

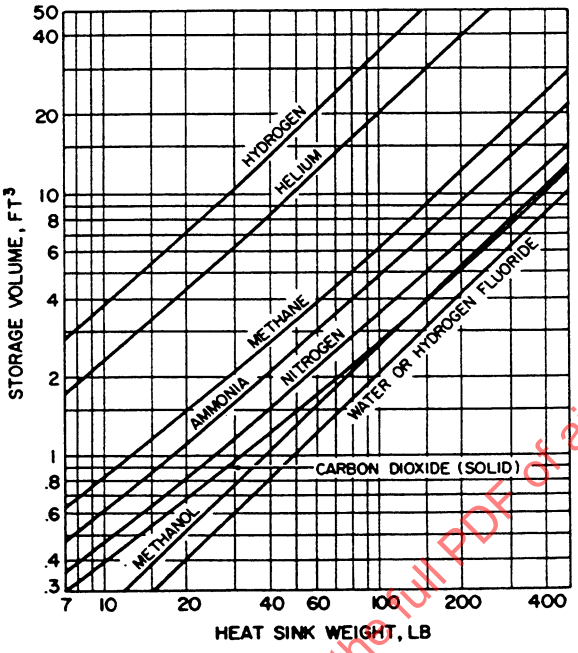

FIGURE 39 - Liquid Heat Sink Storage Volume (Reference 26)

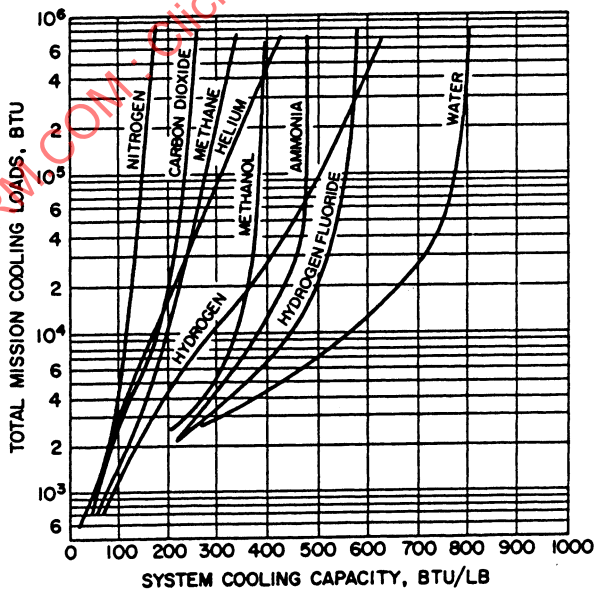

FIGURE 40 - Capacity of Expendable Heat Sinks (200 °F Equipment Surface Temperature) (Reference 26)

4.4.2.4 Comparison of Coolants for a Simple Open-Loop Expendable Coolant Method: Consider the sketch in Figure 31. If the weight of the coolant lines, fittings, and pressure regulators is neglected, then $K_3' = 0$, and the weight of the method is dependent on the heat exchanger, coolant, and tank. For a known ammonia method of this form, with Q = 1000 W and t_E = 130 °F, the equation constants can be evaluated. Figure 37 shows a possible expendable water method and Table 12 gives the data for comparison with ammonia.

Referring to Figure 40, the following conditions apply:

1. System weight includes coolant, tank, and a volume allowance of 1.5 lb of structure per ft^3 of storage.

2. Coolant heated from stored liquid to 200 °F vapor.

3. Tank weight and volume same as for Figures 38 and 39. All assumptions for these figures apply to Figure 40.

4. No ground standby time is assumed.

The properties of the ammonia method are as follows:

$C_{p,0}$ = 1.07 Btu/lb-°F
k_0 = 0.29 Btu/h-ft-°F
$g\rho_0$ = 42.6 lb/ft^3
μ_0 = 0.0024 poise
$L_{e,0}$ = 300 Btu/lb (15 to 85% quality), 14.7 psia
t_0 = -28 °F
$P_{T,0}$ = 130 psia (70 °F sat NH_3 liquid)

and the weights are as follows:

$W_{Hx,0}$ = 1.5 lb
$W_{f,0}$ = 10.4 lb
$W_{T,0}$ = 14.6 lb
W_0 = 26.5 lb

4.4.2.4 (Continued):

Evaluating K' constants:

$$K_1' = \left(\frac{W_{T,0}}{W_0}\right) = \frac{14.6}{26.5} = 0.551$$

$$K_2' = \left(\frac{W_{Hx,0}}{W_0}\right) = \frac{15}{26.5} = 0.057 \qquad \text{(Eq.47)}$$

$$K_4' = \left(\frac{W_{f,0}}{W_0}\right) = \frac{10.4}{26.5} = 0.392$$

Use of these values in Equation 43 gives the ratios of W/W_0 for coolant fluids, shown in Table 13.

TABLE 13 - Weight Comparison of Expendable Coolants ($\dot{Q}$ = 1000 W, t_E = 130 °F, $\Delta\tau$ = 1 h)

Coolant	Tank Pressure[1] P_T, psia	Vapor Pressure P_L, psia	Boiling Temp. T_L, °F	Usable Latent Heat[2] L_e, Btu/lb	Weight Ratio $\frac{W}{W_0}$	Volume Ratio $\frac{V}{V_0} = \frac{L_{e,o}\rho_o}{L_e}$	
Water	14.7	1.0	100	810	0.5	0.3	
Ammonia	130	14.7	-28	330	1.0	1.0	
Ethanol	14.7	--	100	200	1.0+	1.5	
Freon 21	80	14.7	48	80	2.2	2.1	
Nitrogen	14.7	14.7	-322	70	2.0	4.0	Stored at -322 °F
CO_2 Solid	14.7	14.7	-110	246	0.9	0.6	Stored at -110 °F

[1] Tank pressure at 70 °F except for nitrogen and CO_2 (solid).
[2] Useful latent heat of vaporization to 85% quality for high film coefficients except nitrogen and CO_2 (solid).

4.4.3 Closed Cycle Convection Methods: There are a number of different closed cycle methods, all having in common the conservation of the coolant for repeated use in heat transportation. In the open cycle or expendable coolant systems, the disposal of the coolant served the purpose of removing the unwanted heat from the vehicle. Since radiation is the only means by which heat may be rejected in space without this loss of the coolant, all closed systems have a radiator as a necessary component. Aside from these two common characteristics, closed cycle systems may differ from each other quite widely. A number of methods of the closed cycle type are described in the following paragraphs.

4.4.3.1 Forced Convection: The basic convection loop accomplishes transfer of heat from a heat sink to a heat transport fluid, transporting the fluid to a radiator, and a return of the cooled fluid to a reservoir or to the heat exchanger. Such a method is illustrated in Figure 41. The degree of complexity can be changed by the addition or removal of controls for regulating the temperature of the heat sink. The transport fluid may be water, air, ammonia, or any other suitable liquid or gas.

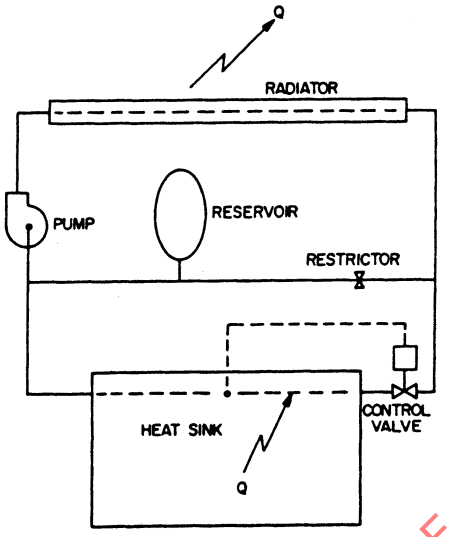

FIGURE 41 - Forced Convection Loop Temperature Control Method

4.4.3.1 (Continued):

The weight, volume, and power requirements of a forced convection loop depend upon the heat load, temperature range, fluid, and ducting. One analysis has been made for a system employing ethylene glycol, a pump-motor efficiency of 40%, a fluid pressure drop of 100 psi, and a temperature change of 20 °F of the fluid in passing through the radiator. The power requirement was found to be 0.025 kW per kW of heat rejected, and the weight to be 3 to 10 lb/kW (Reference 27, p. 22).

4.4.3.2 Comparison of Liquid Coolants for Closed Loop Semipassive Control Methods: The semipassive closed loop liquid cooling method consists of a flow control valve, a space radiator exchanger, a pump, and a compartment heat exchanger (see Figure 41).

Ideally, the comparison of various liquids for this method would include detailed design of the complete loop for each coolant. However, such a comparison is time consuming and costly. Therefore, the use of parameters for comparison purposes is advisable. Several parameters that appear to affect the weight and effectiveness of the loop are the pump power and the forced convection film coefficient parameters.

The pump power parameter P has been derived in Reference 14. This parameter is

$$P = \frac{\mu}{\left(\rho g c_p\right)^2} \text{ (laminar flow)} \qquad \text{(Eq.48)}$$

4.4.3.2 (Continued):

and

$$P = \frac{\mu^{0.2}}{(\rho g)^2 c_p^{2.8}} \text{ (turbulent flow)} \qquad \text{(Eq.49)}$$

For comparison purposes μ, ρg, and c_p are used as ratios relative to turbulent water at 80 °F.

Referring to Table 14, these ratios may be expressed as

$$\frac{\mu / (\rho g c_p)^2}{\mu_0 / (\rho_0 g c_{p,0})^2} \text{ (laminar flow)} \qquad \text{(Eq.50)}$$

and

$$\frac{\mu^{0.2} / (g\rho)^2 c_p^{2.8}}{\mu_0^{0.2} / (g\rho_0)^2 c_{p,0}^{2.8}} \text{ (turbulent flow)} \qquad \text{(Eq.51)}$$

The final coefficient parameter H is based on McAdams' equation (Reference 18) with D = 1 ft and u = 1 ft/h, where fluid properties are evaluated at the average fluid bulk temperature. Note that $c_p\mu/k$ = Prandtl number is raised to the 0.4 power for use with the bulk fluid temperature properties, whereas the more accurate Colburn "j factor" has $c_p\mu/k$ raised to the 1/3 power. However, the Colburn equation as shown in Reference 1, p. 169, is based on fluid properties at the average film temperature. Since, for evaluation purposes, it is felt that the bulk temperature of a liquid is more likely to be known than the average film temperature, the bulk temperature has been used. In the gas comparison, the difference is less noticeable, so that the more accurate Colburn equation is used:

$$H = 0.023k\left(\frac{\rho g}{\mu}\right)^{0.8}\left(\frac{c_p\mu}{k}\right)^{0.4} \qquad \text{(Eq.52)}$$

These two parameters, as well as other comparison information such as freezing and boiling temperature, toxicity, flammability, corrosiveness, and dielectric strength, are presented for some liquids in Table 14. A curve, Figure 42, shows the comparison of H and P for various coolants at different temperatures.

TABLE 14 - Comparison of Liquids for Semipassive Closed Loop Cooling

Fluid and Temperatures	Properties: Conductivity, k	Viscosity, μ	Density, ρg	Specific Heat, c_p	Pump Power Ratio to Turbulent Water: Laminar	Turbulent	Film Coefficient Parameter H, Equation 52	Temperatures, °F: Freeze	Boil	Flash	$\in$	Corrosive	Toxic
Water	Btu-ft/hr-ft²-°F	lb/ft-hr	lb/ft³	Btu/lb-°F	—	—	—	+32	212	No	—	Inert	No
50 °F	0.33	3.17	62.4	1.0	1.1	1.3	0.20						
80 °F	0.367	2.0	62.4	1.0	0.7	1.0	0.275						
200 °F	0.406	0.738	60.1	1.01	0.3	0.9	0.41						
Anhydrous Ammonia	—	—	—	—	—	—	—	−108	−28	Ignition 1204	—	Corrosive to Cu and Al alloys	Yes
0 °F	0.290	0.52	41.2	1.08	0.4	2.4	0.29						
80°F	—	0.232	37.0	1.13	0.2	1.3							
28.3% Ammonia-Water	—	—	—	—	—	—	—	−85	80	Ignition 1204 (NH_3)	—	Corrosive to Cu and Al alloys	Yes
40 °F	0.26	3.95	57.0	0.95	1.9	1.6	0.15						
80 °F	—	2.18	56.2	1.0	0.8	1.2							
57% Methanol-Water	—	—	—	—	—	—	—	−44	180	Closed Cup 54 (Methanol)	—	—	Yes
40 °F	0.234	5.82	58.7	0.83	4.8	4.5	0.12						
80 °F	0.234	3.35	56.0	0.82	1.9	2.1	0.14						
200 °F	0.234	0.80	52.2	0.87	0.5	1.8	0.17						
60% Ethylene Glycol-Water	—	—	—	—	—	—	—	−51	220	Closed cup 232 (ethylene glycol)	—	—	No
0 °F	0.226	82.2	68.8	0.643	82.3	6.0	0.04						
40 °F	—	20.3	67.2	0.688	18.4	3.9	0.075						
80 °F	0.224	14.8	67.2	0.75	5.6	2.5	0.082						
200 °F	0.208	2.2	67.2	0.808	1.1	1.7	0.312						
(CCl_3F) Freon 11	—	—	—	—	—	—	—	−168	+75	No	2.28	Inert	Yes above 750 °F
0 °F	0.072	1.64	98.3	0.207	5.4	32.6	0.082						
86 °F	0.0609	0.94	91.4	0.209	2.3	32.2	0.087						
200 °F	0.046	0.64	80.7	0.225	2.7	31.0	0.080						
FC-75 (3M Co.)	—	—	—	—	—	—	—	−100	224	No	1.86	Inert	Yes above 750 °F
0 °F	0.092	9.05	116.5	0.221	26.5	25.7	0.06						
80 °F	0.0813	3.99	109.0	0.245	7.6	19.2	0.071						
200 °F	0.0705	1.1	95.5	0.278	2.1	13.4	0.104						
Coolanol 45 (Monsanto)	—	—	—	—	—	—	—	−100	630	No	2.65 1 kc (77 °F)	Inert	Yes above 759 °F
0 °F	0.087	260	57.1	0.40	—	40.8	0.0044						
80 °F	0.082	38.5	55.8	0.45	78.5	21.0	0.0216						
200 °F	—	8.0	52.2	0.512	15.2	12.2							
Dowtherm A (Diphenyl-Diphenyl oxide)	—	—	—	—	—	—	—	—	—	No	—	—	—
80 °F	—	6.15	62.4	0.40	15.0	16.0							
200 °F	—	2.92	62.4	—	—	6.1							
400 °F	—	1.01	56.8	—	—	—							
Air[1]	—	—	—	—	—	—	—	—	—	No	—	Inert	No
70 °F	0.0148	0.044	0.070	0.24	2.97×10^5	4.25×10^7	7.31×15^4						

[1]Incompressible; for comparison purposes only.

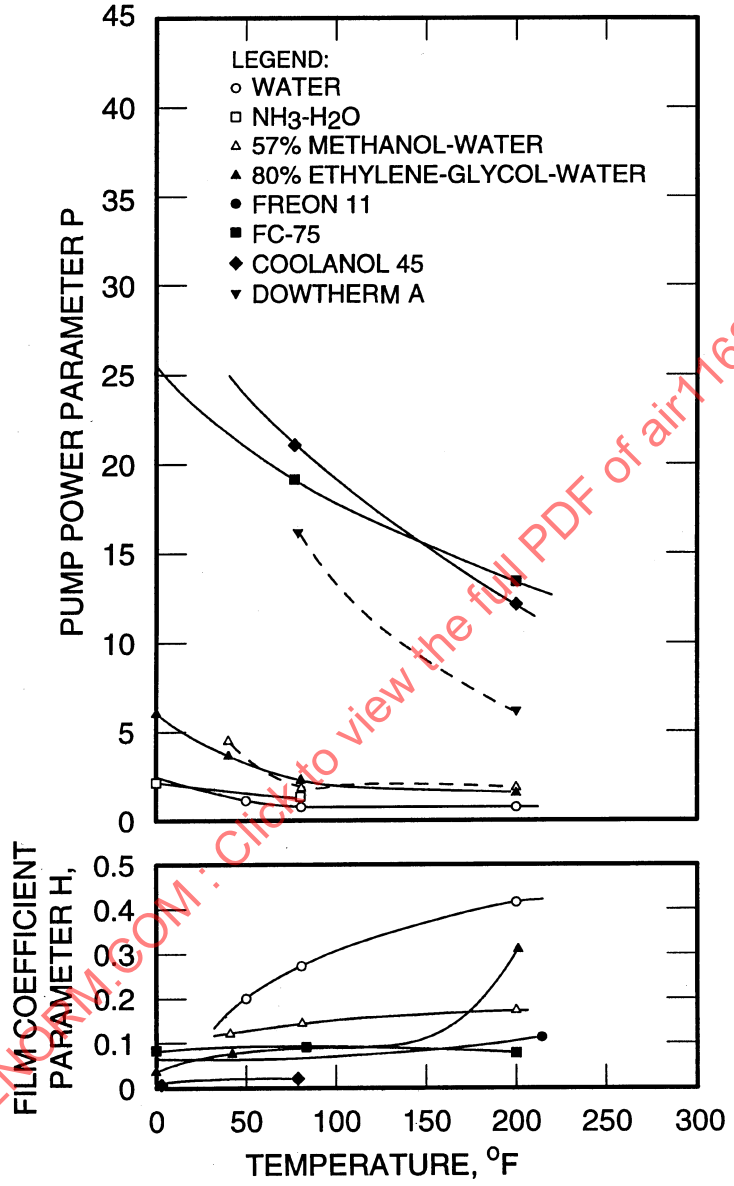

FIGURE 42 - Turbulent Flow Liquid Coolant Parameters

4.4.3.3 Comparison of Gaseous Coolants for Closed Loop Semipassive Control Methods: From Figure 43, the fan power, volume flow, pressure drop, heat transfer film coefficient, and dielectric constant can be seen to be parameters for comparison of gaseous coolants. In addition, if a sensitive component such as a stabilized inertial platform is part of the equipment, the wind force becomes a parameter.

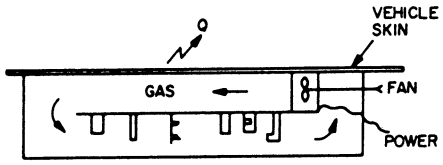

FIGURE 43 - Typical Closed Cycle Gaseous Coolant Loop

For purposes of comparison of different gases the following assumptions were made:

1. The heat load to be removed by the gas is the same for all gases.
2. The maximum temperature rise in the gas is set (ΔT_{gas} = Const).
3. The flow of the gases is turbulent.
4. All parameters will be computed as ratios relative to air at 70 °F.

The following seven parameters were derived, using these assumptions (g = gas, a = air)

1. Weight Flow Rate:

$$\frac{w_g}{w_a} = \frac{c_{p,a}}{c_{p,g}} \qquad \text{(Eq.53)}$$

2. Volume Flow:

$$\frac{u_g}{u_a} = \frac{w_g(\rho_a g)}{w_a(\rho_g g)} \qquad \text{(Eq.54)}$$

3. Film Coefficient (for turbulent flow in ducts or tubes: Reference 1, p. 169):

$$h = 0.023 \frac{k}{D_h} \left(\frac{D_h u \rho g}{\mu} \right)^{0.8} \left(\frac{c_p \mu}{k} \right)^{0.33} \qquad \text{(Eq.55)}$$

4.4.3.3 (Continued):

where properties are evaluated at the arithmetic mean boundary film temperature:

$$\frac{h_g}{h_a} = \frac{k_g}{k_a}\left(\frac{u_g \rho_g \mu_a}{u_a \rho_a \mu_g}\right)^{0.8}\left(\frac{c_{p,g}\mu_g k_a}{c_{p,a}\mu_a k_g}\right)^{0.33}$$

$$= \left(\frac{k_g}{k_a}\right)^{0.67}\left(\frac{\mu_a}{\mu_g}\right)^{0.47}\left(\frac{c_{p,a}}{c_{p,g}}\right)^{0.47} \qquad \text{(Eq.56)}$$

4. Pressure Drop:

$$\Delta P = \frac{f L u^2 \rho g}{2 g D_h} \qquad \text{(Eq.57)}$$

where:

$$f = 0.184\left(\frac{\mu}{u \rho g D_{h,g}}\right)^{0.2} \qquad \left(\text{for } N_{Re} = \frac{u \rho g D_{h,g}}{\mu} > 2100\right) \qquad \text{(Eq.58)}$$

or

$$\frac{\Delta P_g}{\Delta P_a} = \left(\frac{u_g}{u_a}\right)^{18}\left(\frac{\rho_g g}{\rho_a g}\right)^{0.8}\left(\frac{\mu_g}{\mu_a}\right)^{0.2}$$

$$= \left(\frac{c_{p,a}}{c_{p,g}}\right)^{18}\left(\frac{\mu_g}{\mu_a}\right)^{0.2}\left(\frac{\rho_a g}{\rho_g g}\right) \qquad \text{(Eq.59)}$$

5. Power Requirement ($hp \propto \Delta PW/\rho_g g$)

$$\frac{hp_g}{hp_a} = \frac{\Delta P_g}{\Delta P_a}\frac{W_g}{W_a}\frac{\rho_a g}{\rho_g g}$$

$$= \left(\frac{\mu_g}{\mu_a}\right)^{0.2}\left(\frac{g \rho_a}{g \rho_g}\right)^{2}\left(\frac{c_{p,a}}{c_{p,g}}\right)^{2.8} \qquad \text{(Eq.60)}$$

4.4.3.3 (Continued):

6. Wind Force on Platform ($F \propto \rho g S(u^2/2g)$):

$$\frac{F_g}{F_a} = \frac{g\rho_g}{g\rho_a}\left(\frac{u_g}{u_a}\right)^2$$

$$= \frac{g\rho_g}{g\rho_a}\left(\frac{g\rho_a}{g\rho_g}\right)^2\left(\frac{c_{p,a}}{c_{p,g}}\right)^2 \qquad \text{(Eq.61)}$$

$$= \frac{g\rho_a}{g\rho_g}\left(\frac{c_{p,a}}{c_{p,g}}\right)^2$$

7. Dielectric Ratio:

$$\frac{\epsilon_g}{\epsilon_a} \qquad \text{(Eq.62)}$$

These seven ratios have been used for comparison of various gases, and the results are presented in Table 15.

TABLE 15 - Comparison of Gases for Semipassive Closed Loop Cooling

Gas and Molecular Weight	Thermal Properties[1]				Parameters[2]								
	Density, ρg	Conductivity, k	Specific Heat, c_p	Viscosity, μ	Weight Flow Rate, w	Volume Flow, v	Heat Transfer Film Coefficient, h	Pressure Drop, ΔP	Fan Power, hp	Wind Force, F	ϵ	Flammable	Toxic
Air, 28.96	0.0765	0.0148	0.24	0.044	1.0	.10	1.0	1.0	1.0	1.0	1.0	No	No
He, 4.00	0.0096	0.092	1.24	0.046	0.192	1.40	1.52	0.376	0.93	0.268	0.13	No	No
SF_6, 146.066	0.372	0.00822	0.18	0.037	1.33	0.250	0.84	0.322	0.11	0.354	2.0	No	No
N, 28.02	0.072	0.0138	0.248	0.0424	0.97	1.0	1.0	1.04	0.88	1.03	1.0	No	No
H, 2.016	0.0050	0.101	3.44	0.022	0.07	0.98	1.44	0.104	0.097		0.07	Explosive	No
CO_2, 44.00	0.107	0.0096	0.21	0.0344	1.14	0.68	1.05	0.655	0.59	0.708		No	No
Ar, 39.90	0.097	0.010	0.124	0.0533	1.94	1.40	0.62	2.47	3.45	2.71		No	No
SO_2, 64.07	0.173	0.0057	0.154	0.0293	1.56	0.63	1.03	0.827	0.52	0.98		No	Yes, can form H_2SO_4

[1]At 14.7 psia, 70 °F
[2]At constant heat load and gas temperature.

Reference 28 shows a comparison of gases for use as artificial atmospheres in space vehicles. This section of the manual compares blower power requirements and heat transfer coefficients for these atmospheres. These ratios along with ratios for constant heat load are shown in Table 16.

TABLE 16 - Comparison of Artificial Atmospheres

Gas	Pressure,[1] psia	Thermal Properties[1]							Ratio of Blower Power to Air			Ratio of Heat Transfer Coefficient to Air		
		Gas Constant °R	Specific Heat c_p	Specific Heat c_v	c_p/c_v γ	Density ρg	Viscosity μ	Conductivity, k	Constant Q	Constant[1] Vol. Flow	Constant Mass Flow	Constant Q	Constant Vol. Flow	Constant Mass Flow
Air	14.7	53.3	0.240	0.172	1.40	0.0735	0.0446	0.0152	1.00	1.00	1.00	1.00	1.00	1.00
O_2-N_2	11.0	52.6	0.238	0.170	1.40	0.0559	0.0456	0.0153	1.78	0.95	1.74	1.00	0.77	0.98
O_2-He	6.5	75.2	0.302	0.205	1.47	0.0234	0.0503	0.0177	5.30	0.82	1.10	0.94	0.40	1.14
O_2-He	11.0	109.4	0.405	0.264	1.53	0.0274	0.0510	0.0208	1.70	0.90	8.00	0.91	0.57	1.34
O_2	5.0	48.2	0.220	0.157	1.39	0.0276	0.0500	0.0155	9.28	0.88	7.86	1.00	0.37	0.91
O_2	11.0	48.2	0.220	0.157	1.39	0.0608	1.0500	0.0155	1.92	0.89	1.62	1.00	0.80	0.91
O_2-Ne	11.0	63.7	0.234	0.152	1.54	0.0460	0.0605	0.0210	2.51	0.92	3.27	0.69	0.66	1.01

[1]From Reference 28.

4.4.3.3 (Continued):

The forced convection loop usually represents a relatively simple method with good reliability, easy control, good stability, and relatively low power requirements. Size and weight may impose excessive penalties, while leakage is probably the greatest danger of failure.

Most of the lightweight fans (and pumps) available for space or airborne use have small bearings and high rpm to keep weight and volume low. As a result, the life expectancy of these fans is seldom in excess of 500 h. More reliable fans for long life (such as 1 year continuous duty) must be developed. Otherwise, the alternative is to add more fans for redundancy.

4.4.4 Vacuum Cooling Method: The vacuum cooling system is similar to an expendable coolant method, but has the advantage that the coolant is recovered for subsequent re-use. The coolant picks up heat from the heat sink, is vaporized, and then flows to a radiator-condenser where it is reliquefied or solidified. The reduction in volume of the fluid brought about by the change of phase creates the vacuum that gives the method its name. The low temperature necessary for condensation is easily obtained in space.

The vacuum cooling method may operate with liquids that are aboard for other purposes, such as coolants or fuels to be used during reentry. The power required may be a very small amount or none at all. A schematic diagram is shown in Figure 44a.

If the coolant is liquefied in the condenser, it can be returned to the reservoir simply by pumping. When the coolant is solidified, it must first be liquefied. This can be done by having the radiator act as a collector of solar energy, as illustrated in Figure 44b. The operation of this arrangement depends upon the orientation of radiator and absorber to deep space and Sun, but by the manipulation of valves, the functions of the two loops become interchangeable.

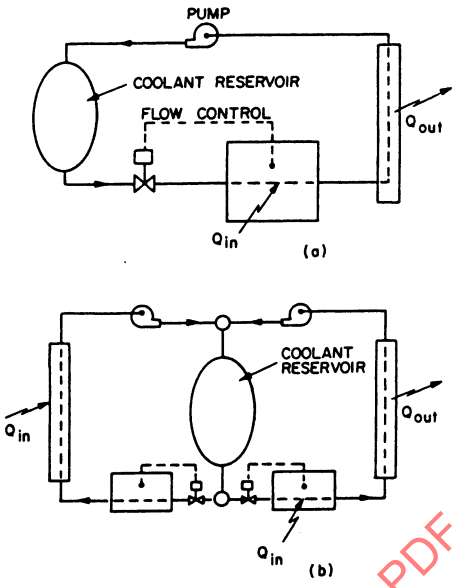

FIGURE 44 - Vacuum Cooling Method; (a) Basic Method; (b) Two Loop Method

4.4.5 Silica Gel Cooling Method: The silica gel cooling method is a type of vacuum method in which the vacuum is maintained by adsorbing the coolant in a silica gel bed. The refrigerant comes from another silica gel bed where it had been adsorbed previously.

The cycle commences with driving off the adsorbed refrigerant from a silica gel bed by the application of heat. A typical refrigerant would be sulfur dioxide, SO_2. The vapor is then condensed in a radiator and the liquid passed through a throttle valve, where the pressure is reduced. It next goes through an evaporator, where it is vaporized by heat picked up from the heat sink. The vapor is then adsorbed by the silica gel bed.

After all refrigerant has been driven off the first bed and adsorbed by the second, the roles of the two beds are reversed. By the use of appropriate interconnections, the same path through the radiator, throttle valve, and evaporator can be followed, with either bed as the source of refrigerant. A schematic diagram is shown in Figure 45.

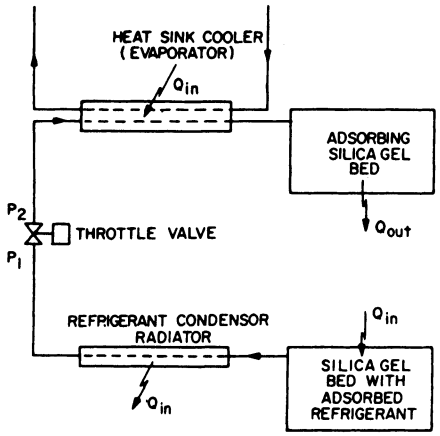

FIGURE 45 - Silica Gel Cooling Method

4.4.6 Variable Radiation Methods: One means of controlling the surface temperature of a space vehicle for the condition of varying internal heat load and varying solar radiation incident on the surface is to change the emissivity or reflectivity of the surface. Several methods for varying the emissivity are discussed in the following paragraphs. These methods are characterized by a movable element whose position or attitude is varied in order to change the emissivity or reflectivity of the outer surface of the vehicle.

4.4.6.1 Venetian Blind Shutter Type Method: This type of controller is shown in Figure 46. With the shutter open, the exposed area presents a surface of one emissivity, while the outside surfaces of the "slats" in the closed position can be made to have a different emissive and/or reflective character. By varying the degree of opening, any value between the open and closed emittance can be obtained.

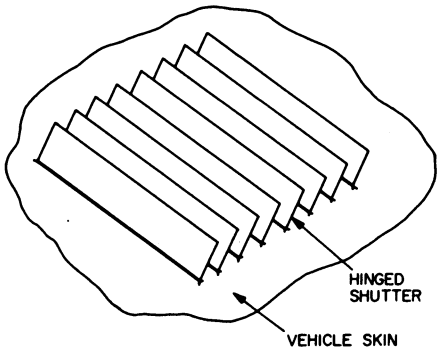

FIGURE 46 - Venetian Blind Shutter, Hinged Type

4.4.6.1 (Continued):

One way of mounting the slats is illustrated in Figure 46, in which the slats are mounted to the vehicle surface by hinges. This method permits some heat to be transmitted by conduction so that the slats serve as "radiating fins."

Another way of mounting would be to pivot the slats along their longitudinal axis; thus, no contact would be made with the radiating surface. The slats can be positioned by a single mechanism actuated by volumetric or pressure changes in a temperature sensing bulb, by photoelectric cell, or by bimetallic thermostatic elements.

The following discussion is a presentation of a way in which the required values for emissivity of the vehicle surface and both sides of the slats may be determined for a given heat load and vehicle surface temperature. It will not be a complete discussion of the slat design.

To make a rapid estimate for the required values for emissivity, the following equations may be used:

$$\sigma \epsilon_{eff} F A T_{slat}^4 - \sum \alpha A G - Q = 0 \qquad \text{(Eq.63)}$$

$$\epsilon_{eff} = \epsilon_{slat} \cos\varphi + \epsilon_{skin} \left(1 - \cos\varphi\right) \qquad \text{(Eq.64)}$$

Equations 63 and 64 illustrate the complexity involved in determining required values for emissivity, since there may be many combinations of values for ϵ and the slat angle φ. Further complexity is introduced for an orbiting vehicle because the solar radiation incident on the various surfaces varies with the vehicle orientation with respect to the various radiating bodies, such as the Sun and the Earth.

The above equations are not sufficient to determine accurately the required values for emissivity, since the radiation interchange between the various surfaces are not considered and the equations are limited to steady-state conditions only. A method that does not have these restrictions is presented in the following paragraphs. This method utilizes the radiosity analog and thermal analog networks described in Reference 16. See Figure 47. The use of networks greatly facilitates the visualization and accounting for the various modes of heat transfer and helps to establish the necessary relationships for the analysis of the problem through the use of digital computers.

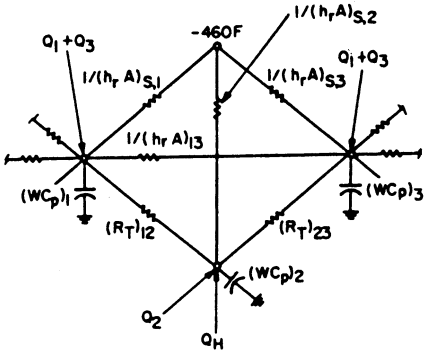

FIGURE 47 - Thermal Analog Network for Venetian Blind Shutter

4.4.6.1 (Continued):

For illustrative purpose, the case in which the slats are perpendicular to the vehicle surface will be considered, and this is shown in Figure 48. The incident angle of the solar radiation is shown to be less than 90 deg, so that a shadow is cast on side 2 and a portion of side 3 (Figure 48a).

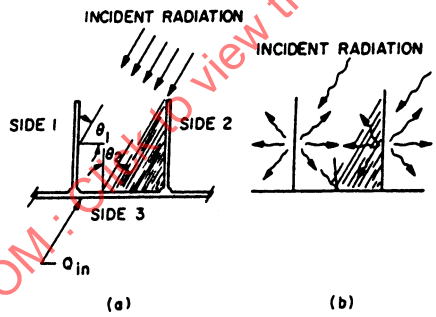

FIGURE 48 - Cross Section Through Shutter Arrangement

As shown in Figure 48b two sources add thermal energy, the heat load added to side 2 and the solar radiation incident to the three sides. The heat load Q is assumed to be applied directly to side 2 for the purposes of this discussion and requires no further elaboration.

Solar radiation requires careful consideration because of the interreflection of the three sides. Only part of the solar radiation impinging directly on a side is absorbed and the remaining energy is reflected to the other sides, which in turn reflects back again the energy not absorbed. This is illustrated in Figure 48b.

The most convenient way to determine the amount of solar radiation absorbed by the three sides is to use the radiosity method described in References 16 and 21, and the radiosity analog network illustrated in Figure 49a. A single node for each side is used for illustrative purposes. For a more refined analysis, more nodes would be introduced.

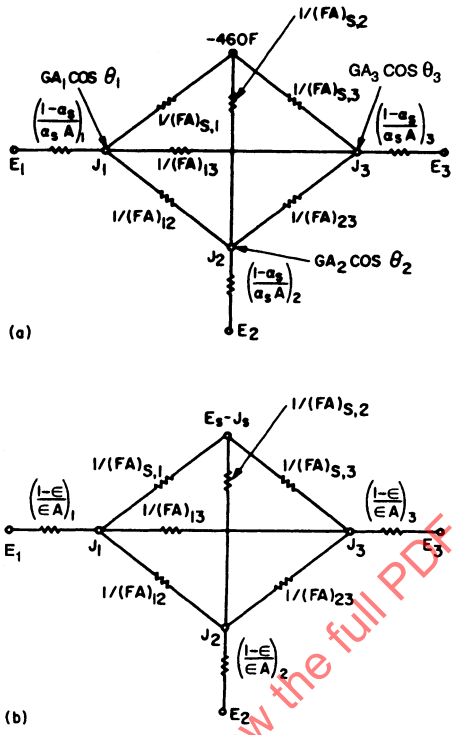

FIGURE 49 - Radiosity Analog Network for Venetian Blind Shutter

4.4.6.1 (Continued):

The radiosity method is limited to diffuse emission and reflection, so it is assumed that the surfaces considered here are of the diffuse form. One further assumption is that the surfaces are similar to "gray bodies" ($\in = \alpha$), with the exception that the value for solar absorptivity α_s is different from infrared absorptivity or emissivity.

The configuration factor F for the three sides can be readily determined by using the string method discussed in Reference 18, if it is assumed that the "slats" are infinitely long.

By applying Kirchoff's laws for electrical networks, three equations are written for heat flow into the radiosity nodes. The surface temperatures or potential (E_1, E_2, and E_3) are set to zero and the radiosities (J_1, J_2, and J_3) are determined from the following three equations:

$$GA_1\cos\theta_1+(FA)_{s,1}J_1+(FA)_{13}(J_1-J_3)+(FA)_{12}(J_1-J_2)+\left(\frac{\alpha_s A}{1-\alpha_s}\right)_1 J_1=0 \qquad \text{(Eq.65)}$$

$$GA_2\cos\theta_2+(FA)_{s,2}J_2+(FA)_{12}(J_2-J_1)+(FA)_{23}(J_2-J_3)+\left(\frac{\alpha_s A}{1-\alpha_s}\right)_2 J_2=0 \qquad \text{(Eq.66)}$$

4.4.6.1 (Continued):

$$GA_3\cos\theta_3+(FA)_{s,3}J_3+(FA)_{13}(J_3-J_1)+(FA)_{23}(J_3-J_2)+\left(\frac{\alpha_s A}{1-\alpha_s}\right)_3 J_3=0 \qquad \text{(Eq.67)}$$

The values for J_1, J_2, and J_3 are then substituted into the following equation to determine the amount of solar radiation absorbed by each of the surfaces:

$$Q_{abs}=\left(\frac{\alpha_s A}{1-\alpha_s}\right)J \qquad \text{(Eq.68)}$$

Since the incident radiation G on each side varies with vehicle orbit position, which is time dependent, it is possible to obtain the variation of Q_{abs} with respect to time, as illustrated in Figure 50.

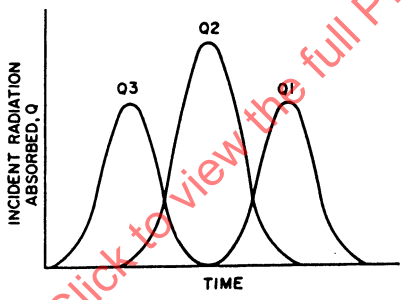

FIGURE 50 - Incident Radiation Absorbed

Radiation heat transfer involves proper accounting of all interreflections between the slat surfaces and the skin. This can be readily accomplished by utilizing the radiosity analog network similar to the one illustrated in Figure 49b. Since no energy is reflected from space, the potential E_s is equal to radiosity J_s. Also, the emissivity is different from the one used in determining the solar energy absorbed, Figure 49a, since the emitted radiation is assumed to be in the infrared band, which has a longer wavelength.

Again, three network equations are written from which radiosities J_1, J_2, and J_3 are determined. These values are then used to determine the interchange factor f, between the various surfaces and space.

$$\left(\frac{\in A}{1-\in}\right)_1(E_1-J_1)+(FA)_{s,1}(E_s-J_1)+(FA)_{13}(J_3-J_1)+(FA)_{12}(J_2-J_1)=0 \qquad \text{(Eq.69)}$$

4.4.6.1 (Continued):

$$\left(\frac{\epsilon A}{1-\epsilon}\right)_2 (E_2 - J_2) + (FA)_{s,2}(E_s - J_2) + (FA)_{12}(J_1 - J_2) + (FA)_{23}(J_3 - J_2) = 0 \quad \text{(Eq.70)}$$

$$\left(\frac{\epsilon A}{1-\epsilon}\right)_3 (E_3 - J_3) + (FA)_{s,3}(E_s - J_3) + (FA)_{13}(J_1 - J_3) + (FA)_{23}(J_2 - J_3) = 0 \quad \text{(Eq.71)}$$

To determine the interchange factor between space and sides 1, 2, and 3, let $E_s = J_3 = 1$ and $E_1 = E_2 = E_3 = 0$, and solve for J_1, J_2, and J_3. Since

$$(fA)_{s,1}(E_s - E_1) = \left(\frac{\epsilon A}{1-\epsilon}\right)_1 (J_1 - E_1) \quad \text{(Eq.72)}$$

then

$$(fA)_{s,1} = \left(\frac{\epsilon A}{1-\epsilon}\right)_1 J_1 \quad \text{(Eq.73)}$$

Similarly,

$$(fA)_{s,2} = \left(\frac{\epsilon A}{1-\epsilon}\right)_2 J_2 \quad \text{(Eq.74)}$$

$$(fA)_{s,3} = \left(\frac{\epsilon A}{1-\epsilon}\right)_3 J_3 \quad \text{(Eq.75)}$$

To determine the interchange factor between side 1 and sides 2 and 3, let $E_1 = 1$ and $E_s = E_2 = E_3 = 0$; again solve for J_1, J_2, and J_3. Since

$$(fA)_{12}(E_1 - E_2) = \left(\frac{\epsilon A}{1-\epsilon}\right)_2 (J_2 - E_2) \quad \text{(Eq.76)}$$

then

$$(fA)_{12} = \left(\frac{\epsilon A}{1-\epsilon}\right)_2 J_2 \quad \text{(Eq.77)}$$

4.4.6.1 (Continued):

Similarly,

$$(fA)_{13} = \left(\frac{\epsilon A}{1-\epsilon}\right)_3 J_3 \qquad \text{(Eq.78)}$$

Also,

$$(fA)_{23} = (fA)_{12} \qquad \text{(Eq.79)}$$

The above procedure is repeated to determine the remaining interchange factors. These factors are then used in the following equation to determine the radiation thermal resistance between the three surfaces and space:

$$R_R = \frac{1}{h_r A} = \frac{1}{\sigma (fA)_{mn} \left(T_m^2 + T_n^2\right)(T_m + T_n)} \qquad \text{(Eq.80)}$$

The values for thermal resistance and solar radiation absorbed are then utilized in the thermal analog network to compute the temperature of the three surfaces. A typical network is shown in Figure 47. In this network, R_T represents the combined conduction resistance and radiation resistance between sides 1 and 2 and sides 2 and 3:

$$R_T = \frac{1}{(1/R_c)+(1/R_R)} = \frac{1}{(kA/L)+h_r A} \qquad \text{(Eq.81)}$$

The above procedure will require several iterations to establish the desired emissivities for the specified heat load and surface temperatures.

4.4.6.2 Rotating Mask Method: A temperature control method employing rotating masks was used on the Atlas Able-4 Lunar Satellite (Reference 29). This is illustrated in Figure 51a. The spirally wound bimetallic strip senses the internal payload temperature, and these temperature changes cause the rotation of the mask through differential expansion or contraction. On the surface of the vehicle were alternating 45 deg segments of materials with ratios of high and low absorptivity to emissivity. The rotation of the mask covered one and uncovered the other as required. Fifty of these units were used on the surface of the spherical satellite, placed as uniformly as possible to reduce the influence of varying Sun angle. About 20% of the satellite surface was so controlled.

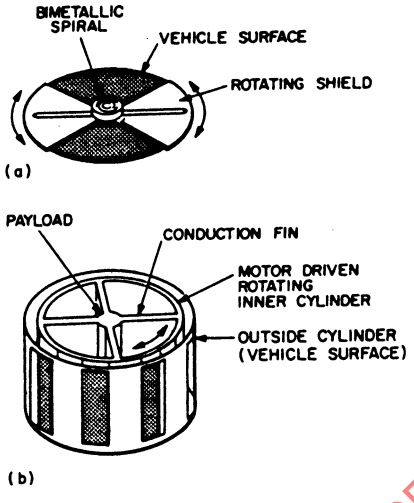

FIGURE 51 - Translating and Rotating Mask Temperature Control Units

4.4.6.2 (Continued):

Advantages claimed for this method include the fact that there is, essentially, only one moving part. This adds to simplicity and reliability and helps to keep the weight relatively low. Sensitivity to vibration is reduced because the unit is balanced about its pivot point. The large number of individual units contributes to the reliability of the whole system, since the failure of a single unit will affect the degree of temperature control far less than would a similar failure in some other systems.

4.4.6.3 Translating Mask Method: The translating type mask operates in very much the same fashion as the rotary mask. The essential difference is that the mask does not pivot about a central point but moves laterally to cover and uncover surfaces of differing thermal characteristics. Figure 51b shows the form of one translational mask method.

Four pairs of ribs are seen to radiate from the life cell to a narrow cylindrical band. This band has an outer surface of polished aluminum partially covered by alternating strips of aluminum oxide paint. An outer concentric band has openings in it of approximately the same size as the alternating polished aluminum and painted strips. A battery powered motor moves the outer band to expose the required proportion of each surface in response to signals from a thermostat in the life cell. The heat generated in the life cell is conducted to the inner band through the radial ribs.

It is interesting to observe some of the reasons that favored the choice of this method. The proponents note that:

4.4.6.3 (Continued):

"Since the shields represent added weight, it is desirable to place them where they would have the maximum effect in raising the moment of inertia about the spin axis, i.e., at the periphery of the central plane. To prevent large axial temperature gradients in the life cell, heat generated in it is best removed from near its middle, rather than from its ends. Placement of the shields at the largest diameter of the satellite would assure the least possible variation of incident radiation, since the controllable surface can then not be shaded by other parts of the satellite, but can at worst only be turned at right angles to the incoming radiation."

The purpose in quoting these statements here is to emphasize that some methods have certain advantages not possessed by other methods. For example, the rotating mask method would be of no help in stabilizing spin, but could prevent large axial temperature gradients and would have far less variation of incident radiation than would the method described here.

4.4.6.4 Mercury Film Temperature Control Method: A temperature control method has been suggested that would utilize the fluid and reflective properties of liquid mercury in a manner illustrated by Figure 52. In operation, the temperature sensing bulb, containing mercury, would be located in the region where temperature is to be controlled.

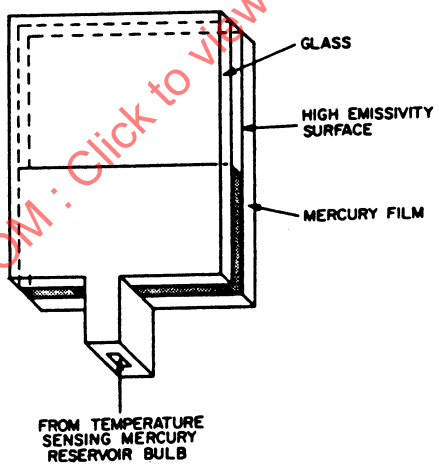

FIGURE 52 - Mercury Film Temperature Control Method

Increased or decreased temperature would cause a volumetric expansion or contraction of mercury with a consequent rise or fall of a continuous thin film in the space between a glass or quartz "window" and a suitable backing. This backing could be of high absorptivity or high emissivity material, the choice depending upon a requirement to bring solar heat into the vehicle or to reject internal heat from it.

At the present time (circa 1966), this system is undergoing analysis and shows some promise for satisfactory operation. The arrangement has simplicity and reliability.

4.4.6.4 (Continued):

Other variants of this principle involve the use of pressure changes to actuate bellows or pistons to move the mercury. The use of a photoelectric cell to signal the start of a pump also suggests itself. In each case, the object is to cover more or less of a critical area with a reflective shield, capable of adjustment to any position within a range and free, in the shield itself, of moving mechanical parts.

4.4.6.5 Particle Cloud Shield: In this method the evacuated space between the window and the backing plate would contain a cloud of particles sufficiently dense to be opaque to solar radiation. In an evacuated space in zero gravity, the distribution of particles could be expected to form a cloud of uniform density. The window would be cleared to permit the passage of thermal energy into or heat out of the vehicle by the formation of an electric field.

The electric field would be formed by applying an electric current to electrodes at the outside edges of the system, with the particles then collecting at these electrodes. To make the window opaque, the current would be shut off and the brief actuation of a vibrating device would then send the particles out in a random distribution.

The particle cloud shield operates in a manner similar to that of electrostatic precipitators used to remove fly ash from flue gas. No development work has been done on this concept.

4.5 Active Temperature Control:

4.5.1 Vapor Cycle Refrigeration: The ideal refrigeration cycle is the reverse Carnot cycle shown in Figure 53. The vapor refrigeration cycle (Figure 54) approaches this ideal more closely than other cycles. The arrangement of the components making up the physical plant are shown in Figure 55.

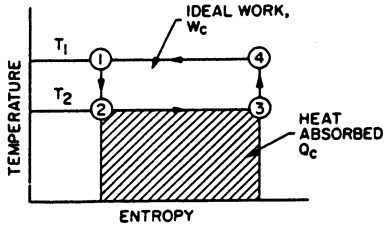

FIGURE 53 - Temperature-Entropy Diagram for Reverse Carnot Refrigeration Cycle

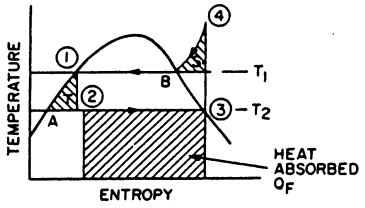

FIGURE 54 - Temperature-Entropy Diagram for a Vapor Refrigeration Cycle

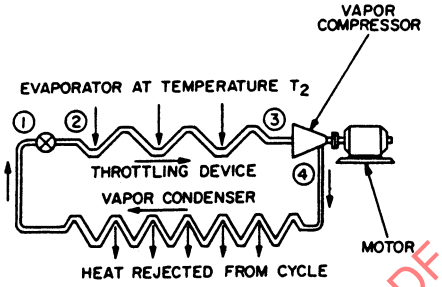

FIGURE 55 - Vapor Refrigeration Cycle

4.5.1 (Continued):

In the Carnot cycle, a fluid is expanded isentropically from a relatively high temperature, T_1, as shown by state 1, to a lower temperature at state 2. In this process, some work must be extracted from the fluid to reduce its temperature. The fluid then absorbs heat from the air conditioned or refrigerated compartment while going from state 2 to state 3 at constant temperature T_2. Next, the fluid is compressed isentropically to the high temperature, T_1, of state 4. At this temperature, heat is dissipated from the fluid in a radiator, thereby returning the fluid to its original condition at state 1.

The operation of the common refrigeration cycle is similar to the ideal. Liquid enters the throttling device at a relatively high temperature and pressure, and expands to a lower temperature and pressure at constant enthalpy, but not at constant entropy. At the cold temperature, T_2, the fluid (a mixture of liquid and vapor) flows thorough the evaporator, where heat from the refrigerated or air conditioned space is absorbed by the evaporating fluid.

To simplify the analysis, it is usually assumed that saturated vapor enters the compressor. Both the temperature and pressure of the fluid are increased in the compressor. The vapor condenser dissipates the heat energy either to space or to the environment. Condensation of the vapor takes place in this process, and by the time the fluid returns to the original condition at state 1, it has completely reverted to the liquid phase.

The required work for the cycle shown in Figure 54 is represented by the area 1a234b1, and the heat absorbed is represented by the area Q_f. An increase in work is caused by heating of the fluid (by compression) to a value higher than the maximum temperature of the ideal Carnot cycle; this work increase is represented by area S.

4.5.1 (Continued):

An additional amount of work results from the irreversible throttling from point 1 to point 2; this work increase is represented by area T. The heat equivalent of the work represented by area T remains in the fluid and thereby reduces the amount of heat that may be absorbed by the evaporating fluid. Expansion of the fluid through a power generating device, such as a hydraulic motor, could reclaim much of this lost energy; however, this complication is rarely justified in a practical situation.

The characteristics of the vapor cycle system include:

1. Power – An average value of power requirements for most vapors is 1 hp/ton of refrigeration or 0.21 kW/kW. For carbon dioxide, the figures are 1.83 hp/ton and 0.39 kW/kW. The operating temperatures assumed are 5 °F for evaporation and 86 °F for condensation.

2. Integration – Because of the nature of its function and the materials involved, integration is limited to interchanges of heat.

3. Limitations – Leakage of refrigerants could be dangerous to the crew or cabin equipment. Power requirements are relatively high.

4. General – Vapor cycle refrigeration is a well-tried method of temperature control. The materials, components, and skills necessary to design and construct a space cabin refrigerator are readily obtainable.

4.5.2 Gas Cycle Refrigeration: Gas cycle refrigeration deviates considerably from the ideal Carnot cycle because the absorption and rejection of heat take place at continuously varying temperatures. The gas, usually air, picks up heat at essentially constant pressure, as shown by process A-B in Figure 56. It is then compressed isentropically from B to C, followed by a cooling process (C-D) in which heat is rejected at constant pressure. Expansion through a turbine or air motor from D to A returns the gas to its original state.

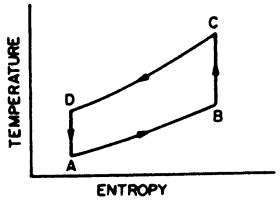

FIGURE 56 - Temperature-Entropy Diagram for a Gas Refrigeration Cycle

4.5.2 (Continued):

Characteristics of the system are:

1. Power – The power requirement for an air cycle system comparable with the vapor cycles evaluated in 4.5.1 is 2.82 hp/ton of refrigeration, or 0.6 kW/kW.

2. Integration – The manned cabin may be used as part of the plumbing, thereby eliminating a separate heat exchanger and cabin air circulation system.

3. Limitations – Gas cycle refrigeration requires much larger and heavier equipment than do vapor systems of the same capacity, especially compressors and radiators.

4. General – The chief advantage of the air cycle system is that the refrigerant is not toxic and can be replenished, within limits, from the cabin atmosphere. Because condensation does not take place, zero gravity presents no special problems.

4.5.3 Absorption Cycle Refrigeration: The absorption refrigeration cycle is similar to the vapor cycle except that the compressor is replaced by an absorption process. Following the schematic diagram of Figure 57, the vapor is seen to leave the evaporator and enter the absorber. Here it is dissolved in an absorbing agent at relatively low temperature and pressure. The solution is then pumped into the generator at higher pressure, and the refrigerant is distilled off by the application of heat.

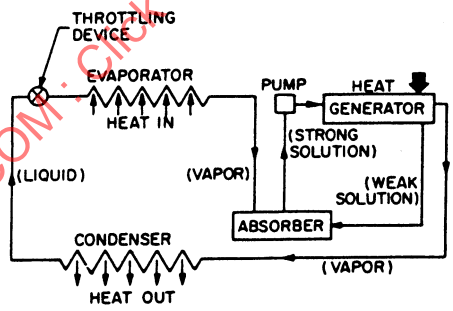

FIGURE 57 - Absorption Refrigeration Cycle

The refrigerant, now in vapor form, passes to the condenser, while the solvent, with most of the refrigerant removed, returns to the absorber. A variation of this system uses an inert gas to raise the total pressure in the evaporator and absorber to nearly the level of the condenser so that the liquid can be cycled by thermal action only, and no pump is needed.

4.5.3 (Continued):

Characteristics of this system are:

1. Power – The actual power requirements of an absorption system are very low, being only those required to operate the pump. However, heat applied to the generator must be considered when making comparisons between systems. The total heat and power requirements of an absorption system will be 10 to 20% greater than for an equivalent compression system.

2. Integration – The absorption system can use heat rejected from other systems, thereby reducing the requirement for generated power. The temperature, however, must be sufficiently high to distill the refrigerant, which, in the case of an ammonia-water system, is 220 °F.

3. Limitations – Some difficulty could be expected in zero gravity in separation of the vapor and the circulating solvent.

4. General – The possibility of using solar power or waste heat for the greater part of the energy requirements of this system makes it worthy of study.

4.5.4 Vortex Tube: By expanding gas through a vortex tube, sometimes referred to as a Ranque or a Hilsch tube, a portion of the gas will be cooled. A vortex tube is shown schematically in Figure 58.

The gas enters the tube through a nozzle, which discharges the gas tangentially and thus sets up a whirling motion within the tube. The portion of gas removed from the central core of the tube is colder than the portion removed from the periphery. For maximum temperature depression, only about 20% of the gas can be removed in the cooled state. However, a larger refrigerating effect (that is, the product of temperature drop and weight flow) can be obtained by extracting a larger percentage of the flow.

The temperature drop in the cooled portion is generally less than 50% of the isentropic temperature drop for the same overall pressure ratio. As the overall pressure ratio is increased, lower percentages of the isentropic temperature drop are obtained.

The performance of a vortex tube is poor as compared to expanding the gas through a turbine or a piston engine. Consequently, a vortex tube can rarely be justified as a separate entity. However, as part of an integrated system, it may have merit. Assuming that a blower and a gas distribution system are already required in a vehicle, little or no additional penalty may be accrued by the addition of a vortex tube. The vortex tube can serve as a flow divider while additionally delivering cooler gas to critical components. Also, the absence of moving parts makes a vortex tube attractive from a reliability point of view.

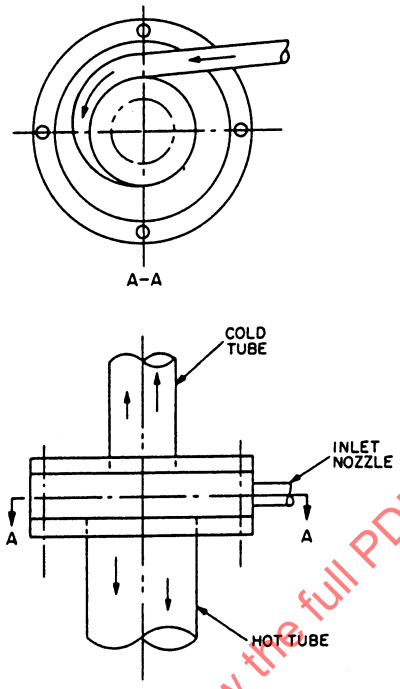

FIGURE 58 - The Vortex Tube

4.5.5 Peltier Cooling: Because of the Peltier effect, heat is generated or absorbed whenever a direct current flows through a junction between two unlike materials. This effect is most pronounced when certain types of semi-conductors, such as bismuth telluride, are used in the circuit. A practical device based on this principle usually has a configuration similar to that shown in Figure 59. The passage of a direct current produces a temperature differential (T_h – T_c) between the junctions.

The device is used for cooling by placing the colder of the two junctions next to the heat source, which is the body or space to be refrigerated. A Peltier cooler is a heat pump; consequently, the heat removed from the source is pumped from the cold to the hot junction, along with the heat to which the electric power degenerates.

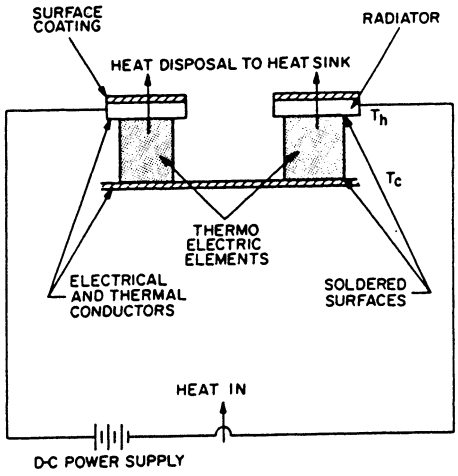

FIGURE 59 - Peltier Heat Pump

4.5.5 (Continued):

Thermal insulation must be provided between element arms to prevent the backflow of heat in those areas. Electrical insulation must be placed in appropriate areas to prevent electrical shorting. Connecting a number of elements electrically in series and thermally in parallel produces a simple and compact cooler that finds its best application where relatively low cooling loads and small temperature differentials are involved.

Characteristics of the Peltier heat pump are:

1. Temperature Differential – The maximum temperature differential that can be produced between the junction is

$$\left(T_h - T_c\right)_{max} = \frac{1}{2} Z_0 T_c^2 \qquad \text{(Eq.82)}$$

where Z_0 is the combined figure of merit of the two types of materials used. Realistic values for Z_0 are 0.0025 to 0.0030/K.

2. Performance – The maximum coefficient of performance (cooling load per unit power input, $\in_0$) that can be obtained is

$$\in_0 = \left[\frac{T_c}{T_h - T_c}\right] \frac{\sqrt{1 + Z_0 \frac{T_h + T_c}{2}} - \frac{T_h}{T_c}}{\sqrt{1 + Z_0 \frac{T_h + T_c}{2}} + 1} \qquad \text{(Eq.83)}$$

4.5.5 (Continued):

3. Weight – A representative range of heat flow density is 1000 to 5000 Btu/h-lb of cooler, excluding heat transfer surfaces or radiator. With normal cold and hot plates, these values will be decreased by a factor of 3 to 5.

4. Integration – Elements may be soldered directly to vehicle structure. In some cases, the cooler may be revised to act as a heater.

5. Limitations – The system is not suitable for high-capacity refrigeration or for transport of heat over long distances. Adequate removal of heat from the hot junction is sometimes a problem. External power is required.

6. General – No moving parts result in no noise or vibration, simplicity, long life, and high reliability. No fluids or consumable refrigerants are required; therefore it is insensitive to gravity field. Temperature ranges from 0 °R to about 1500 °R. Operation in vacuum is best for insulation and prevents oxidation. Peltier cooling is best applied where accurate control and/or spot cooling is required.

4.6 Technical Approach, Active Temperature Control Methods:

Active temperature control methods have been defined as methods that require a heat pump, removing heat from a source or evaporator to a sink or radiator-condenser at a higher temperature. The cycles discussed in this section include vapor cycles, gas cycles, and thermoelectric cycles. Modified gas cycles that incorporate a vortex tube are also included.

The zero gravity effects of the space environment create major problems in the design and operation of the vapor cycles. Consequently, detailed discussion of methods of design for evaporators and radiator-condensers for operation in zero gravity is included. Note that although the term "heat pump" is used here, most of these cycles are refrigeration cycles and cannot be reversed as in the usual "heat pump" sense because the evaporators and condensers are completely different in design, owing to the zero gravity requirements. The usual "heat pump" is less efficient than a refrigeration cycle, since dual purpose condensers and evaporators are required and these result in lower condensation and evaporation efficiencies.

Zero gravity effects are not a problem in gas and thermoelectric cycles. However, all refrigeration cycles have one drawback in common – a high power requirement. That the power requirements are evident in the COP relationship is shown by

$$\text{COP} = \frac{\text{Cooling power}}{\text{Input power}} \qquad \text{(Eq.84)}$$

Unfortunately, increasing the efficiency of the compressor or system does not drastically change the COP relationship, since the COP is more a function of the thermodynamics of the cycle. Thus, power penalties in weight, surface area, and volume must always be considered in comparisons of active methods to passive and semipassive methods.

4.6.1 Vapor Cycle Methods: For several reasons, vapor cycle methods should be considered for certain space applications. These methods have high performance characteristics, are able to provide refrigeration for large heat loads at the required location, and can operate over a wide range of altitudes from ground to outer space.

The extensive development of vapor cycle systems for aircraft and missiles provides a wealth of data and experience for space applications. The use of the vapor cycle in space, however, introduces special problems involving the operation of components in a weightless environment. In addition, the continued exposure of refrigerants to space radiation may create new problems not considered in the past.

As an element of the active thermal control system for space vehicles, the vapor cycle system finds its application in meeting a requirement for large cooling capacity. Two general conclusions concerning its use are:

1. With present (circa 1965) state-of-the-art, the components of the vapor cycle can be made to operate in a zero gravity environment by introducing some modifications to present designs for ground application. Within a condenser temperature range of 150 to 250 °F, a simple vapor cycle using Freon 11 appears most promising for space application.

   The evaporator of this zero g vapor cycle would be of conventional design, using a heat transfer surface such as the plate-fin or vortex type. The condenser would be of the radiator type using a tapered tube design.

2. Other components of the cycle are common to that of high-speed aircraft environmental control systems. This present-day approach is characterized by a specific weight on the order of 35 lb/ton of cooling capacity.

4.6.1.1 Conventional Evaporators: The evaporator in a vapor cycle refrigeration system is the heat exchanger in which heat is transferred from the source to the refrigerant. In conventional evaporators operating on Earth, the heat transfer regime is a mixture of two basic boiling mechanisms, one a transfer due to forced convection and the other a contribution due to pool boiling. Boiling takes place by the formation of bubbles around nuclei of unknown nature. These vapor bubbles grow and collapse at a rate controlled by the liquid temperature, pressure, and surface tension.

For effective transfer, these bubbles must be continuously removed from the heat transfer area, which thus remains wet. Removal of a bubble takes place when it collapses upon contact with a subcooled liquid or under the influence of the inertia of the surrounding liquid. In a zero gravity environment, there are no body forces.

A still liquid without inertia does not contribute toward the removal of these bubbles. The coefficients of boiling heat transfer would therefore be several orders of magnitude lower than those usually accepted. Forced convection would then remedy and help maintain the heat transfer coefficients at a higher level by contributing to the removal of the vapor bubbles.

4.6.1.1 (Continued):

It appears that a conventional evaporator can be used for zero g applications if the amount of forced convection is increased. This will occur at the expense of a higher pressure drop or a reduction in Δt across the heat transfer surface.

If conventional designs are to be applied effectively to space equipment, the parameters characterizing these processes must be maintained close to the values known to yield satisfactory operation on Earth, since boiling heat transfer is a mixture of dynamic and thermal processes. For dynamic similarity, dimensionless Bonde and Weber numbers must be introduced, along with the usual Reynolds number.

The following example illustrates the evaluation of these numbers for a typical Earth application design, given these conditions:

1. For Freon 11, $\rho g = 91.4$ lb/ft^3 (or 1.413 g/cm^3)
2. Surface tension $\sigma = 19$ dynes/cm (Note: 1 dyne = 1 g - cm/s^2)
3. Hydraulic diameter $D_h = 0.1$ in = 0.00833 ft (or 0.254 cm)
4. Acceleration of gravity on Earth, $g_0 = 986$ cm/s^2
5. Local gravity field, $g = kg_0$

   where k = 1 for Earth gravity conditions.
6. Flow of fluid in evaporator, V = 1 ft/s (or 30.48 cm/s)
7. Bonde number,

$$N_{Bo} = \frac{D_h^2 \rho g k g_0}{\sigma} = 4.7k \qquad \text{(Eq.85)}$$

8. Weber number,

$$N_{We} = \frac{\rho g V^2 D_h}{\sigma} = 17.55 \qquad \text{(Eq.86)}$$

For a Bonde number smaller than 1, the gravity field has a preponderant effect on capillary forces. For the preceding conditions, this takes place in an environment with $g = (1/4.9)\, g_0$. To maintain this similarity in flow gravity operation, the evaporator requires a larger D_h and thus becomes heavier and more voluminous. As zero gravity approaches, there is increasing difficulty in keeping the Bonde number at the same magnitude as in conventional design. An investigation must be made into this deviation to determine a rational design approach.

4.6.1.1 (Continued):

Inertia force will be preponderant in comparison to capillary force if the Weber number is larger than 1. From the above example, a velocity of 1 ft/s still yields a good Weber number. Thus it appears that this number can be easily maintained in designing for zero gravity.

Since the thermal process is generally correlated in terms of the previous physical parameters, the heat transfer parameters possibly can be maintained within a range of practical values. Pending further investigation of the problem of zero g boiling, these arguments are presented to support a design approach based on the conventional technique for evaporation design (References 30 and 31).

The volumes and weights of some lightweight evaporators using the plate-fin, tube-fin construction are presented in Figures 60, 61, and 62. The success of the conventional approach is presently supported by the operation of the plate-fin evaporators used on the Project Mercury environmental system, as shown in Figure 63. The heat transfer surface on this unit is made from offset finned packages. The offset fins act as turbulators, creating a flow field that aids vapor bubble entrainment.

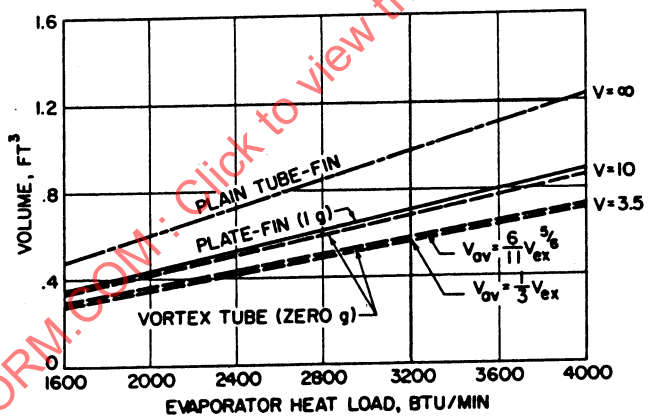

FIGURE 60 - Comparison of Volumes of Freon 11 Plate-Fin, Vortex Tube, and Plain Fin-Tube Evaporators

All Evaporators Finned on Air Side; t_E = 40 °F; Air Side Δt = 25 °F, ΔP_{air} = 0.3 psia (Reference 31)

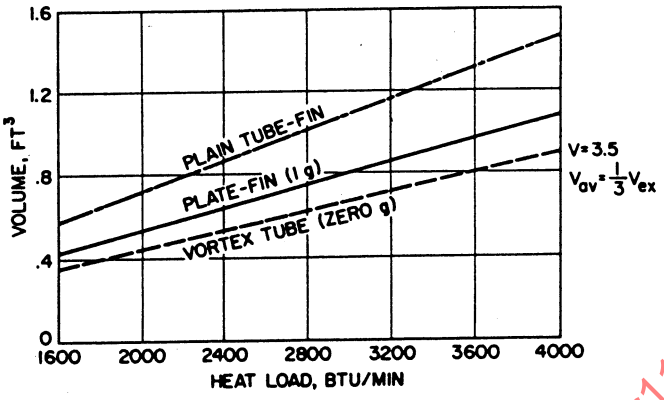

FIGURE 61 - Comparison of Volumes of Freon 11 Plate-Fin, Vortex Tube, and Plain Fin-Tube Evaporators
Same Conditions as for Figure 60 Except That ΔP_{air} = 0.1 psia

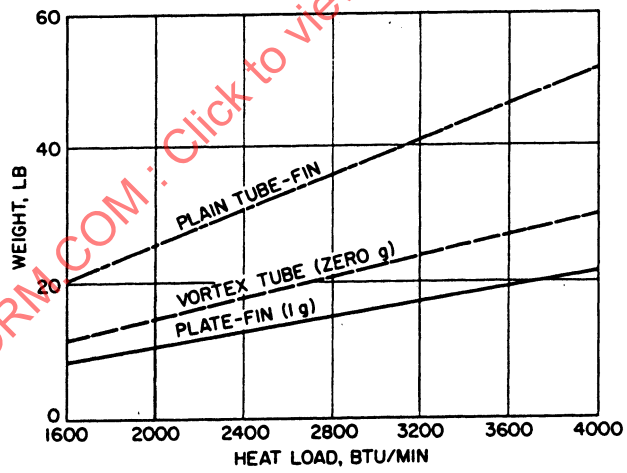

FIGURE 62 - Comparison of Weights of Freon 11 Plate-Fin, Vortex Tube, and Plain Fin-Tube Evaporators; t_E = 40 °F, Δt_{air} = 25 °F, ΔP_{air} = 0.3 psia

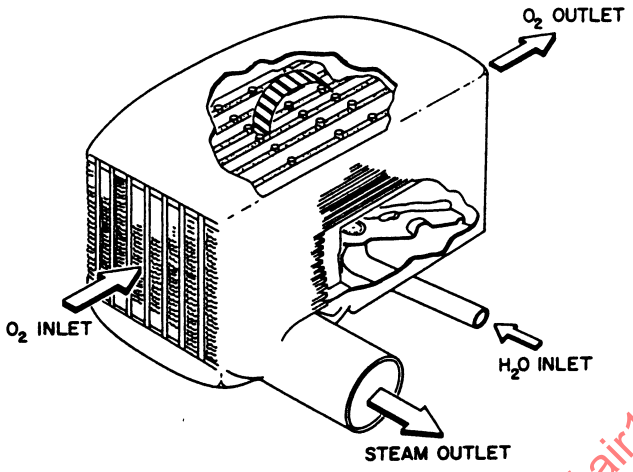

FIGURE 63 - Environmental Control System Evaporator for Zero Gravity Operation

4.6.1.2 Vortex Evaporators: Vortex evaporators have been considered for space applications, to take advantage of the artificial gravity field induced by rotating the fluid in stationary passages. Physically, the evaporators consist of tubes with twisted tapes inserted internally. The boiling refrigerant flows inside these tubes in a helicoidal path. The rotational motion imparts an artificial gravity field g' in which

$$g' = \omega^2 r \qquad \text{(Eq.87)}$$

where the radius of rotation r is expressed in inches.

From Reference 5, the rotational speed can be calculated by assuming that the flow follows the twist Y of the blade with a mean axial velocity V_a; thus,

$$\omega = \frac{30\,V_a}{YD\left[1-(\pi/2Y)^2\right]^{1/2}} \qquad \text{(Eq.88)}$$

where the rotational speed ω is given in rpm and the expansion factor Y is expressed by the number of diameters advanced per 180 deg twist.

Preliminary evaluation of the merits of vortex evaporators has been made with a simple modification of the Roshenow correlation for boiling heat transfer:

$$h = K\left(\frac{\omega^2 r}{g_0}\right)^{0.1}\left(\frac{Q}{A}\right)^{2/3} \qquad \text{(Eq.89)}$$

where K is a grouping of physical properties of this fluid (Reference 32).

4.6.1.2 (Continued):

Evaluation of the pressure drop due to the two-phase flow on the vortex side of the evaporator can be made from data in Reference 36 and application of the Lockhart-Martinelli theory.

The results of the calculations of vortex evaporators carried out by Reference 31 are shown in Figures 60, 61, and 62. It appears that the vortex evaporator does offer an advantage in weight and volume, accompanied by a reasonable pressure drop. These comparisons have been made with a 1 g evaporator. If due consideration were given to the reasoning of 4.6.1.1, calling for a relatively higher forced evaporation, the conventional evaporator would not hold the more favorable position in the competitive picture.

Although these preliminary calculations have been made with data of reasonable reliability, further investigation is still needed to ensure the definite advantage of the vortex evaporator for zero g application.

4.6.1.3 Evaporators Using Capillary Material: Capillary material has been proposed in space evaporator design to provide a liquid feed to all surfaces. Reference 31 describes a typical design using capillary material in an ice-water evaporator in which a wick (Liquid Lock) fills the boiling side of the heat-exchanger.

A capillary evaporator for use in space applications must present some free passages through which the boiling bubble can escape. Such an approach is shown in Figure 64, where a cross-flow evaporator is presented. Air flows in one side through the plate face surfaces. Fibrous material fed from water storage lines the other side of the heat transfer surface. The surface tension properties of the fibrous material move and distribute the water along the heat transfer surface. When evaporation takes place, the vapor escapes through the perforated spacer fin.

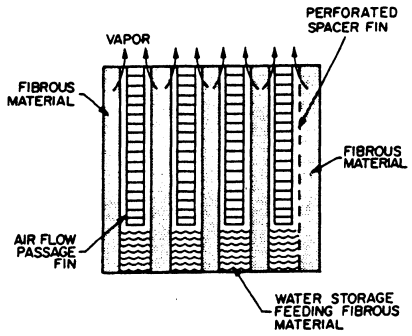

FIGURE 64 - Proposed Design of an Evaporator Using Wick Material

Capillary material may take less forced convection power than other designs and also provide a fluid storage reservoir. Heat transfer data on these materials, particularly in zero g operation, are still scarce. Pending further experimentation, Reference 31 suggests using the correlation due to Gilmour:

4.6.1.3 (Continued):

$$\frac{h}{c_p G'}\left(\frac{c_p \mu}{k}\right)^{0.6}\left(\frac{\rho g L \sigma}{P^2}\right)^{0.21} = 0.072\left(\frac{D_e G'}{\mu}\right)^{-0.77} \quad \text{(Eq.90)}$$

where:

$$G' = \frac{q}{A \in h_{fg}} \quad \text{(Eq.91)}$$

and

$$\frac{q}{A} = \text{Heat flow, Btu/h-ft}^2 \quad \text{(Eq.92)}$$

$$D_e = \text{Dimension parameter}$$

$$\in = 1 - \frac{\rho g_{wick}}{\rho g_{fiber}} \quad \text{(Eq.93)}$$

A preliminary investigation of these materials, reported in Reference 31, shows that material stability is the major problem. Unless the material is properly selected or the additional forced convection is kept within a limiting value, the behavior of the material alters after a period of operation. Table 17 presents the physical characteristics of some wick material reported to be promising (Reference 31).

TABLE 17 - Physical Properties and Absorption Characteristics of Wick Materials

Sample Number and Material	Width, in	Height, in	Thick-ness, in	Volume, in^3	Weight, lb	Density, lb/ft^3	Maximum Rise, in[1]	Time, min[1]	Volume Ratio, V_w/V_d	Weight Ratio, W_w/W_d	Density Ratio, P_w/P_d	Maximum Water Absorption lb/lb	Maximum Water Absorption lb/ft^3
1. Refrasil Batt	--	--	--	--	--	--	1.5	35	0.675	11.78	17.4	10.77	26.6
Dry Condition	4.0	5.0	1.0	20.0	0.0287	2.47							
Wet Condition	4.125	5.25	0.625	13.5	0.337	43.2							
2. Refrasil Bulk	--	--	--	--	--	--	6.25	31	1.00	3.87	3.87	2.87	40.9
Dry Condition	Dia.												
	Length	1.875	--	24.8	0.205	14.2							
Wet Condition	Length	1.875	--	24.8	0.793	55.1							
3. DuPont Cellu-lose Sponge	--	--	--	--	--	--	3.5	60	1.35	10.10	7.51	9.09	31.9
Dry Condition	1.613	5.0	0.75	5.98	0.0121	3.54							
Wet Condition	1.75	5.25	0.875	8.04	0.122	26.3							
4. American Felt Co. No. 7546	--	--	--	--	--	--	4.375	6600	1.03	3.68	3.58	2.68	53.4
Dry Condition	Dia.	0.28											
	Length	11.33	--	0.717	0.0084	20.2							
Wet Condition	Dia.	0.28	--										
	Length	11.94	--	0.737	0.038	72.3							
5. American Felt Co. Co. 17/3, No. 7545	--	--	--	--	--	--	5.25	1440	1.00	3.49	3.49	2.49	42.0
Dry Condition	2.813	6.125	0.813	14.01	0.137	16.9							
Wet Condition	2.813	6.125	0.813	14.01	0.477	58.8							

[1] Maximum height to which water rose in the dry specimen against gravity and the time to reach this height.

4.6.1.4 Condenser-Radiator: In some instances, the refrigerant of the vapor cycle rejects heat directly to the outer space without an intermediate heat transfer loop. This rejection takes place in a condenser-radiator. For simple analysis, the heat rejected per unit of cooling load is calculated as

$$\frac{Q_R}{Q_c} = 1 + \frac{1}{h_{ct}(COP)_{ct}} \quad \text{(Eq.94)}$$

where:

$$(COP)_{ct} = \text{Carnot coefficient of performance of vapor cycle} \quad \text{(Eq.95)}$$

$$= \frac{T_1}{T_1 - T_2}$$

in which

T_1 = Condenser temperature

T_2 = Evaporator temperature

$$Q_R = \left[1 + \frac{1}{\eta_{ct}} \frac{1}{(COP)_{ct}}\right] Q_c \quad \text{(Eq.96)}$$

$$= A \sigma \in T_1^4$$

and

$$\frac{A}{Q_c} = \frac{\sigma \in T_1^4}{1 + \left[1/\eta_{ct}(COP)_{ct}\right]} \quad \text{(Eq.97)}$$

Equation 97 is plotted on Figure 65 to offer a rapid estimate of the required radiator area. It is calculated for an evaporator temperature of 40 °F (T_2) and an assumed emissivity of the radiator surface of 1.

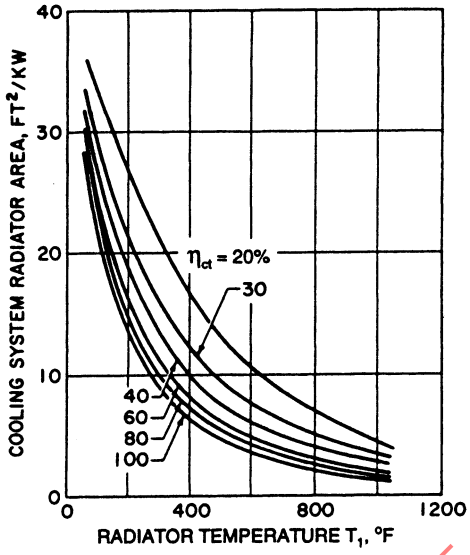

FIGURE 65 - Radiator Area Versus Radiator Temperature for Cooling System; Evaporator Temperature = 40 °F

4.6.1.5 Conventional Condensers: Design with Tapered Tubes: In applying conventional techniques to the design of condensers required to operate in weightless environments, the main problems are:

1. Maintaining a reasonably stable flow at the interface of the condensing film and the vapor.

2. Coalescing and collecting the condensed refrigerant.

With wetting refrigerants, such as Freon, a thin layer of condensate tends to form on the condenser. Nonwetting fluids such as mercury appear in the form of condensate droplets. If the vapor velocity is sufficiently high, the interface between vapor and liquid becomes unstable.

Any small perturbation will be amplified and thus tend to destroy the continuity of the interface. A "sluggy" flow takes place with an increase in pressure drop and with the resulting possibility of completely clogging the condensing side of the condenser. The decrease in condensing heat transfer coefficient may have a negligible adverse effect, since the controlling coefficient is generally on the cooling side, that is, the radiating of intermediate heat transfer loop sides.

Three factors contribute to the stability of the interface:

1. Viscosity – Higher viscosity results in an increase in the damping of all the disturbances. For Freon type refrigerants the viscosity is relatively small; thus, in laminar flow, stabilizing with viscosity effect is less feasible.

4.6.1.5 (Continued):

2. Turbulence – A condensate film with a turbulent flow regime will have good damping characteristics. As Freons have low kinematic viscosity, the condensate film will soon reach the transition Reynolds number and benefit from the subsequent turbulence.

3. Gravity Field and Surface Tension – The stabilizing effects due to gravity and surface tensions have been extensively examined. In a zero g field, condenser operation is closely related to surface tension effect. Stability then consists of maintaining the velocity of the vapor phase below the critical value.

Theoretical investigations of the hydrodynamic stability of thin films of condensate, reported in Reference 32, show that if the Reynolds number and Weber number of the condensate are kept within the range shown in Figure 66, stability will exist for a wide range of small disturbances. The use of this relationship is illustrated as follows: condensing Freon 11 = 250 °F, tube diameter = 0.2 in, and condensate thickness = 0.001 in. The corresponding Reynolds and Weber numbers are tabulated for typical vapor velocities, V, in Table 18. From Figure 66:

$$N_{Re} = \frac{\rho g V \delta}{\mu} \qquad \text{(Eq.98)}$$

$$N_{We} = \frac{\rho g V^2 \delta}{\sigma g}$$

Table 18 in conjunction with Figure 66 shows that for a velocity of 1 ft/s, an absolute stability exists. For velocity of the order of 50 ft/s or higher there is a possibility of instability. The tolerable degree of instability for a satisfactory condensing process has not been determined. Therefore the theoretical analyses can at best serve as a guide to the designer.

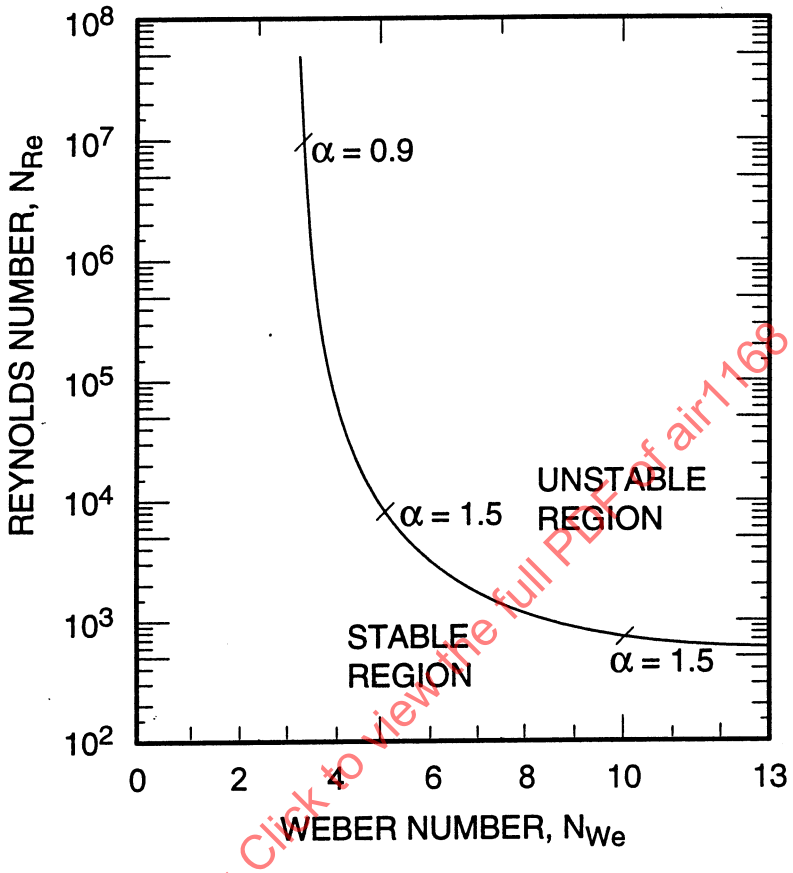

FIGURE 66 - Domains for Two Phase Flow Stability; α = Wave Number = $2\pi\delta/\lambda$ (Reference 32)

TABLE 18 - Typical Vapor Velocities N_{Re} and N_{We}

V, ft/s	N_{Re}	N_{We}
1	1.374	0.15
10	13.74	15.0
50	68.7	395.0
100	137.4	

4.6.1.6 Coalescing and Collecting the Condensed Refrigerant: This will also be a problem in zero g environment. Although sponge materials have been suggested, the most practical solution currently (circa 1965) seems to be in a tapered tube configuration.

In Figure 67 the surface forces acting on the fluid (pressure and surface tension) will cause a slug of a wetting liquid to migrate toward the larger end and a nonwetting liquid toward the smaller end. Under forced condensation in a tapered tube, a slug will be drawn into the header of the condenser in one direction or the other. Besides this, the taper helps to maintain the vapor velocity constant, thereby avoiding the usual deceleration of flow found in a constant diameter tube. Because of potential advantages of the condenser-radiator with tapered tubes, a detailed treatment of the subject is warranted.

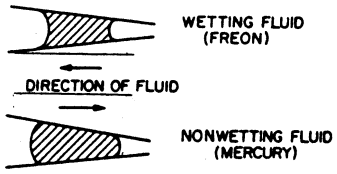

FIGURE 67 - Influence of Surface Tension on Tapered Tubes

1. Heat Transfer Coefficient on the Condensate Side – For space design, it is generally assumed that the controlling thermal resistance is on the radiating side; the film condensation coefficient h_c is much higher than the radiating coefficient h_r. In the design of ground equipment, the film condensation coefficient is given by well-known heat transfer correlation data. The question now arises, however, as to the applicability of this relationship to space equipment.

   Pending further investigation, a low limit to this coefficient can be evaluated by assuming that heat transfer takes place by conduction only. The relative values of h_c and h_r are given as

$$h_c = \frac{4k}{D_h} \qquad \text{(Eq.99)}$$

$$h_r = \sigma \in T^3 \text{ (for outer space at 0 °R)}$$

   Then

$$\frac{h_c}{h_r} = \frac{4k}{\sigma \in D_h T^3} \qquad \text{(Eq.100)}$$

   Reference 31 gives the numerical values of the ratio shown in Table 19. It appears that for Freon 11, the assumption of the radiating side as the controlling thermal resistance is still valid.

TABLE 19 - Minimum Ratios for Condensing Side to Radiating Side Heat Transfer Coefficients for Integral Condenser-Radiators

Fluid	Saturation Temp., °F	Condenser Tube Dia., in	$(h_c/h_r)_{min}$
Freon 11	320	0.5	3.6
Freon 11	320	2.0	0.9
Freon 11	250	0.5	1.57
Freon 11	150	2.0	3.25
Mercury	400	0.5	640
Mercury	400	0.5	160
Sodium	800	0.5	1120
Sodium	1250	0.5	396
Sulfur	400	2.0	2.0
Sulfur	1100	2.0	0.5

4.6.1.6 (Continued):

2. Size and Weight of Condenser-Radiators – To arrive at the size and weight of a radiator using tapered tubes, the following assumptions are made:

   a. Condensation in the tube is uniform, and 90% or more of the entering saturated vapor is condensed in the tube. This condition must exist to produce the situation pictured in Figure 67, which permits easy coalescing and collecting of the liquid condensate in a zero g environment.

   b. The thickness of the condensate film in this tube is negligible compared with the tube diameter. The vapor velocity and the tube length are constant.

   c. The physical dimensions of a radiator element consisting of a tapered tube and the corresponding fin area are shown in Figure 68. Mean arithmetic values have been taken wherever integration of a variable dimension is required. Hence, referring to the nomenclature of Figure 68,

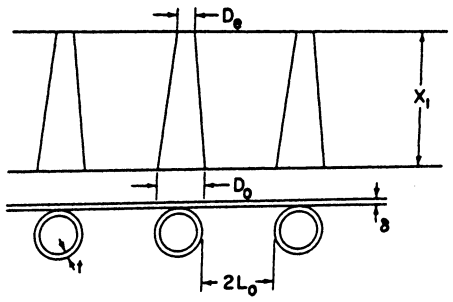

FIGURE 68 - Geometry of Tapered Tube Condenser-Radiator

4.6.1.6 (Continued):

$$a = 1 - \frac{D_e}{D_0}$$

$$\bar{D} = \frac{D_0 + D_e}{2} \qquad \text{(Eq.101)}$$

$$\bar{L} = L_0 + \frac{D_0 - D_e}{2}$$

d. The elemental radiator is designed around a fin of light weight (such as aluminum) which, according to Reference 33, is characterized by

$$\eta_f \cong 0.575; \quad \sqrt{\frac{48\sigma \in T^3}{K\delta}}\bar{L} \cong 18 \qquad \text{(Eq.102)}$$

The equations for determining the required length of the tube to condense a fraction F of the entering mass of vapor is given by

$$\frac{Q_R}{N} = g\rho V\left(\frac{\pi}{4}D_0^2\right)FL_e = \in \sigma T^4 X_1\left[\bar{D} + 2.07\sqrt{\frac{K\delta}{48\sigma \in T^3}}\right] \qquad \text{(Eq.103)}$$

The weight of the radiator element is calculated from the expression

$$\frac{W_{NT}}{N} = g\rho_f X_1 \frac{\delta}{12}\left(\bar{D} + 2\bar{L}\right) + g\rho_t X_1 \pi\left(\bar{D} + \frac{t}{12}\right)\frac{t}{12} \qquad \text{(Eq.104)}$$

The specific weight of the radiator is given by combining Equations 103 and 104 as follows:

$$\frac{W_T}{Q_R} = \frac{g\rho_f\left(\delta/12\right)\left(\bar{D} + 2\bar{L}\right)}{\in \sigma T^4\left(\bar{D} + 2.07\sqrt{K\delta/48\sigma \in T^3}\right)} + \frac{g\rho_t \pi\left[\bar{D} + \left(t/12\right)\right]\left(t/12\right)}{\in \sigma T^4\left(\bar{D} + 2.07\sqrt{K\delta/48\sigma \in T^3}\right)} \qquad \text{(Eq.105)}$$

With this design approach, the specific weight is seen to be independent of the rate of heat transfer. It depends only on the physical dimensions of the passages and the radiator temperature.

4.6.1.6 (Continued):

From Reference 33, the pressure drop in the elemental radiator is

$$\frac{\Delta P}{X_1} = \frac{1}{12}\left[\frac{4-11a+10a^2-3a^3}{(1-a)^4}\right]\frac{dP}{dX_0} \qquad \text{(Eq.106)}$$

$$\frac{dP}{dX_0} = 0.1007\,\frac{f}{\sigma g}\left(\frac{W}{N}\right)^2 \qquad \text{(Eq.107)}$$

The friction factor is that of a two-phase flow given by the correlation of Martinelli, Bergland-Gazley, or Koster in Reference 34.

As an illustration of this design procedure, Figure 69 presents the characteristics of a condenser-radiator for Freon 11 at 150 °F and 250 °F, where 95% of the entering vapor is assumed to be condensed. The specific weight shown applies also to other refrigerants operating at the same temperatures, in accordance with the previous analytical expression. The pressure drop, calculated with extrapolated data of Bergland-Gazley, is of small magnitude, a condition that satisfies the assumptions used in the design approach presented here.

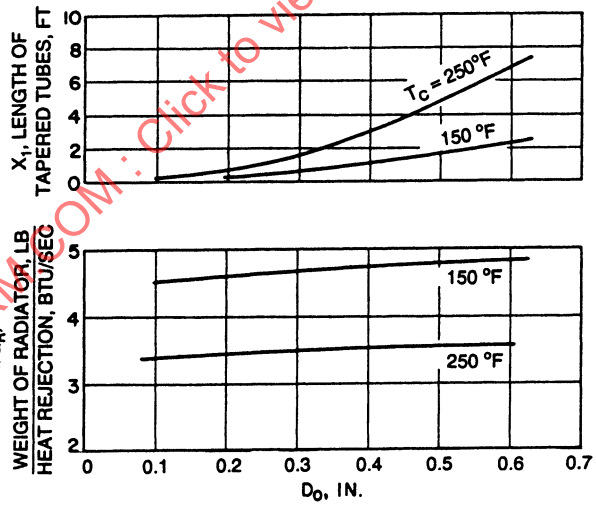

FIGURE 69 - Condenser-Radiator Characteristics with Freon 11

From Figure 69 it is seen that the specific weight changes little with tube diameter. Proper diameter is determined by the space available for the radiator length and also the taper angle of the tube. For instance, very small tubes have considerable taper angle, which precludes all the assumptions used in the calculation. In Figure 69, for a tapered tube radiator:

4.6.1.6 (Continued):

1. Emissivity, 0.9
2. Tube thickness, 0.020 in
3. Fin thickness, 0.020 in
4. Tube material, aluminum, 173 lb/ft^3
5. Fin material, aluminum, 173 lb/ft^3
6. Condensation in tube, 95%
7. Vapor velocity: 1 ft/s at 250 °F condenser; 10 ft/s at 150 °F condenser

4.6.1.7 Condensers with Curved Passages – Curved passages have been proposed for space condensers to provide a force similar to that of gravity. Here, the entire mass of the condensing refrigerant flows over a helicoidal path. At any point along its trajectory, the fluid is subject to centrifugal force due to local acceleration, defined by the tangential speed and the corresponding radius of curvature of the path.

Two contributions account for the heat transfer in curved passages of the condensing refrigerant shown in Figure 70. Since the condensate layer on wall B is relatively thin, owing to centrifugal action, there is good heat transfer. On wall A, the condensate layer is thicker. The heat transfer rate is compensated, however, by mixing due to the secondary flow inherent in curved passages, and the fluid temperature will be closer to that of wall A. As a result, heat transfer rates are practically the same on both walls. Usually these rates are taken as those of flat plates (Reference 35).

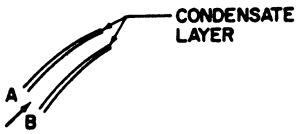

FIGURE 70 - Flow in Curved Passages

A conceptual design of a condenser with curved passages is given in Reference 31 and shown in Figure 71. This spiral condenser consists of curved layers in which the coolant and condensing refrigerant flow is countercurrent. For some typical operations of vapor cycle systems, Reference 31 reports a preliminary design study yielding the characteristics of spiral condensers. The heat transport fluid was taken as an alloy of sodium and potassium (22% Na, 78% K) that melts at 12 °F and has a high conductivity.

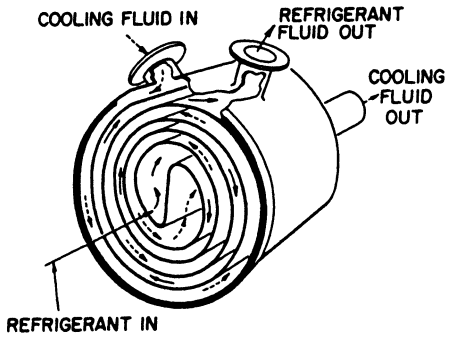

FIGURE 71 - Spiral Condenser (Fluids in Counterflow) (Reference 31)

4.6.1.7 (Continued):

Pending further experimental work, the feasibility study used the same design procedure as for a ground-use condenser. A relatively good vapor velocity (20 ft/s) and a resulting condensing heat transfer coefficient of 275 Btu/h-ft^2-°F have been used. Flat plate data have been applied without consideration of the stability of flow or the slugging under zero g operation.

The computed characteristics of the spiral condenser derived from this study are shown in Figures 72 through 74.

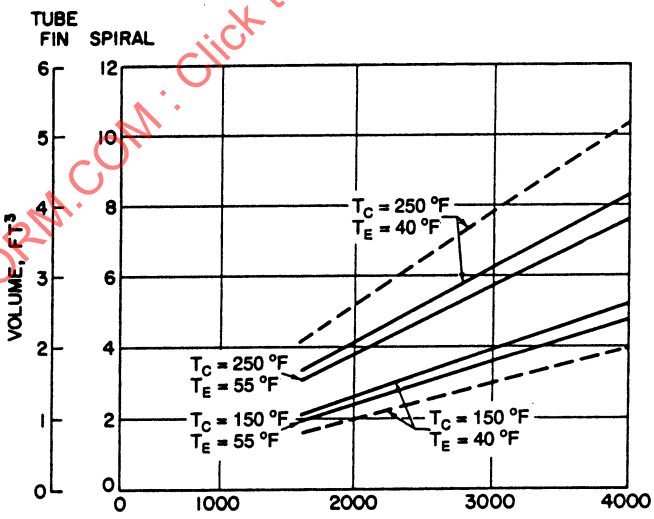

FIGURE 72 - Comparison of Volumes of Freon 11 Spiral Condenser (Zero g) with Large Tube-Fin Condensers (1 g); Staggered Circular Finned Tubes, NaK Side Pressure Drop = 0.5 psia, Tube ID = 0.55 in, Fin Thickness = 0.10 in, Number Fins/in = 8.7, Freon Flow Length = 1.0 ft Dashed Curves Represent Spiral Condensers and Solid Curves the Tube-Fin Condensers

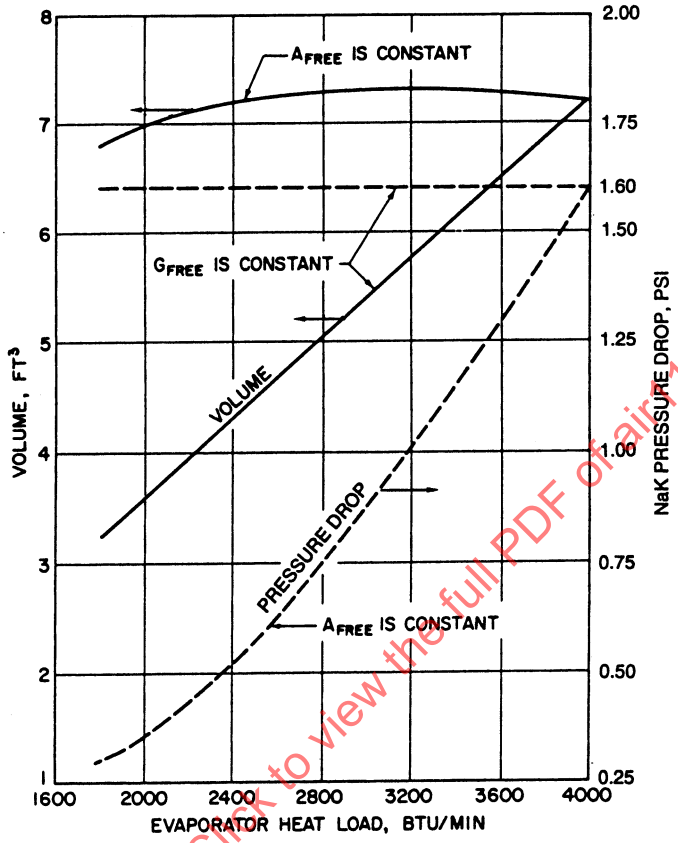

FIGURE 73 - Volume and Pressure Drop for Freon 11 Spiral Condenser; T_c = 250 °F, T_E = 40 °F, Freon Plate Spacing = 0.25 in, NaK Plate Spacing = 0.75 in (Reference 31)

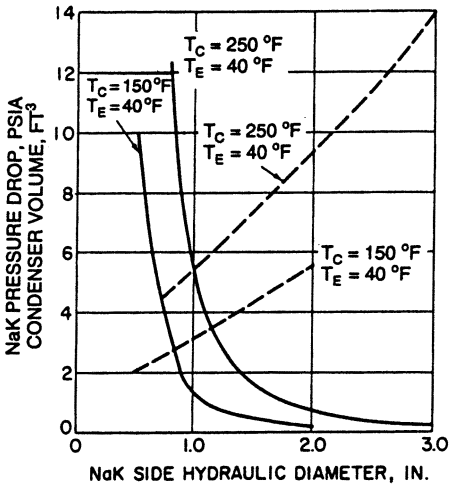

FIGURE 74 - Variation of Freon 11 Spiral Condenser Volume and Pressure With NaK Side Hydraulic Diameter; Freon Plate Spacing = 0.25 in, Condenser Length = 1.0 ft, Evaporator Heat Load = 4000 Btu/min; the Dashed Curves Represent Volume and the Solid Curve the Pressure Drop (Reference 31)

4.6.1.8 Rotating Condensers: Another method for providing the body forces required for satisfactory condensation in zero gravity environment is to use a centrifugal force supplied by rotating the equipment itself, which is the principle of operation in a rotating condenser.

Figure 75 illustrates a rotating condenser design. Vapor from the compressor is sprayed on a series of rotating hollow discs cooled by coolant flow. The vapor condenses in these discs and the liquid condensate, in the form of droplets or thin film, is centrifuged outward by the rotation of the discs. The liquid is collected in an annular channel from which it is returned to the liquid main as a result of a pressure difference.

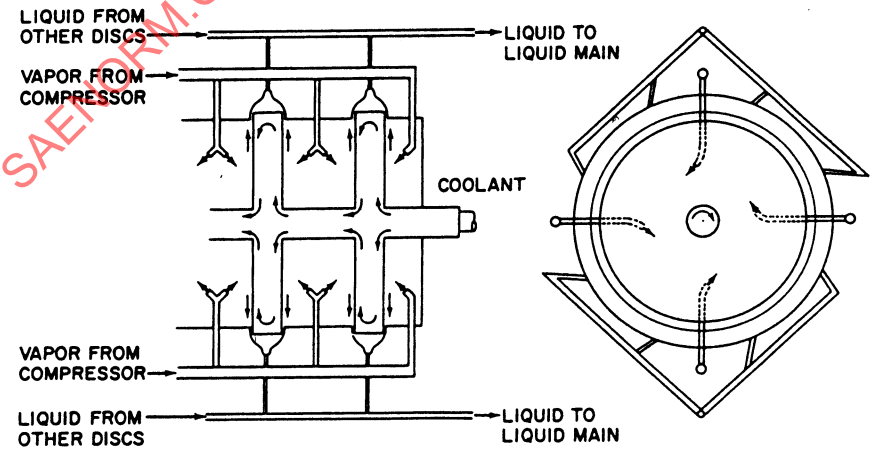

FIGURE 75 - Rotating Condenser (Reference 31)

4.6.1.8 (Continued):

Though a rotating condenser, with its extra power requirements and complex design, is thought to offer little advantage over other approaches, a fully detailed design study has been carried out in Reference 31. The weight and power requirements of vapor cycle systems using Freon 11 are shown in Figures 76 and 77 for some typical operating conditions.

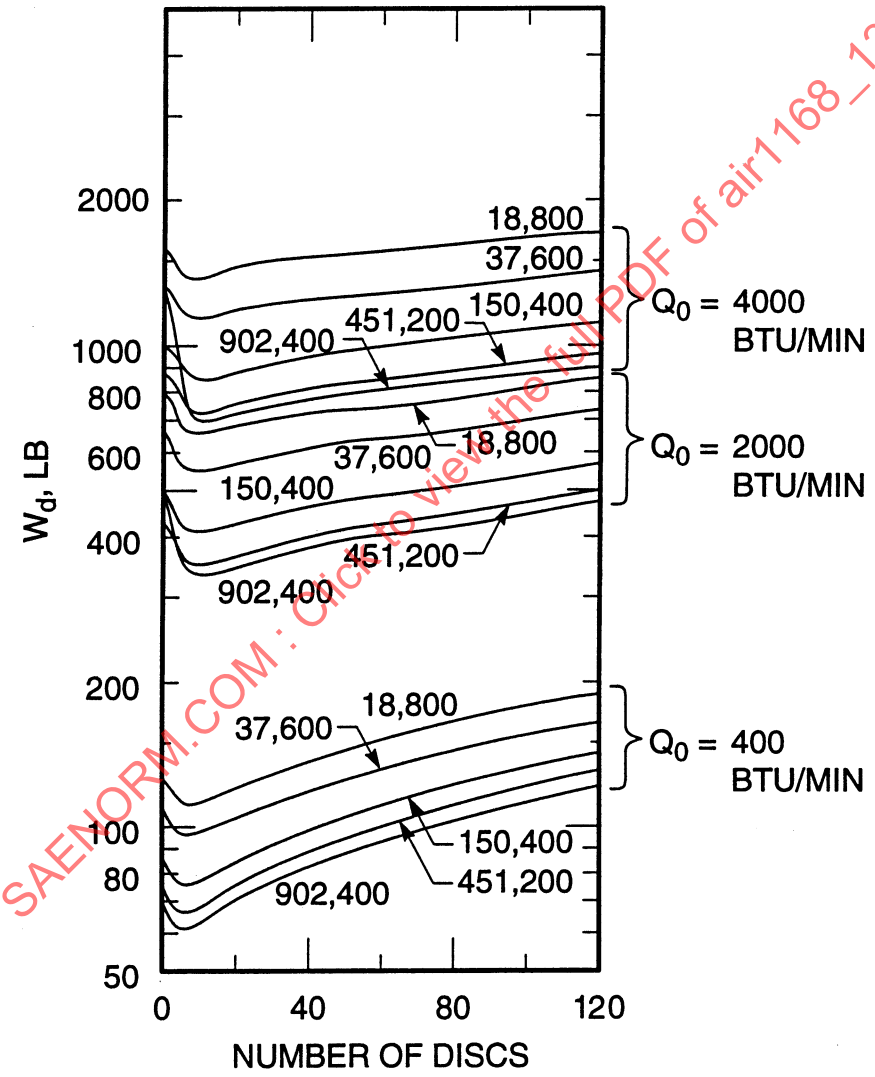

FIGURE 76 - Condenser System Dead Weight Versus Number of Discs;
Evaporation Temperature = 40 °F, Condensation Temperature = 250 °F;
the Condenser Angular Velocity and System Capacity are the Parameters (Reference 31)

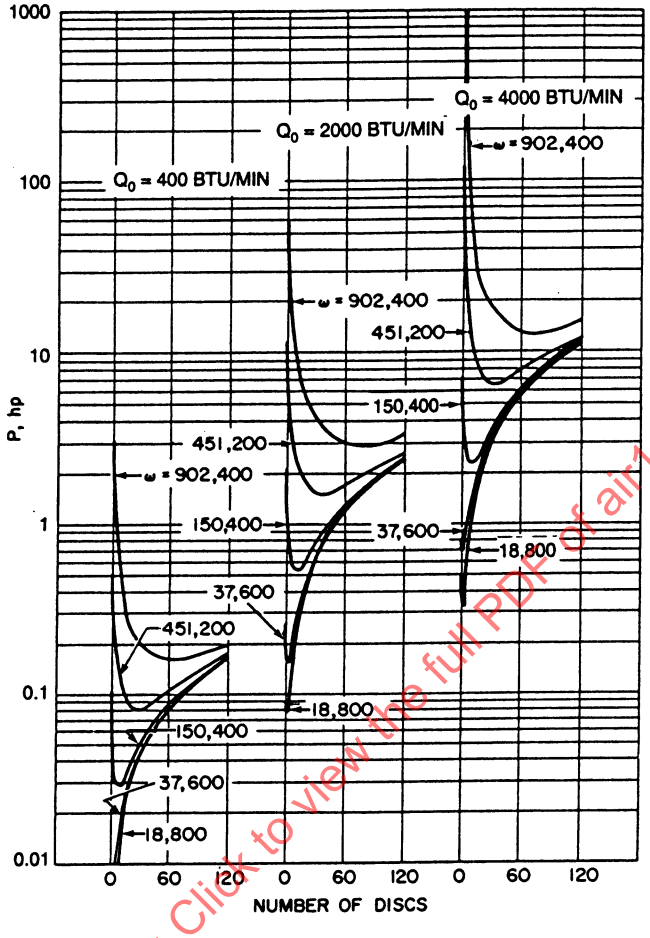

FIGURE 77 - Total Power Requirement Versus Number of Discs;
Condenser Angular Velocity and System Capacity are the Parameters;
ω Given in Radians/h; Evaporation Temperature = 40 °F and Condensation Temperature = 250 °F

4.6.2 Actual Performances of Vapor Cycle Systems: Actual performances of vapor cycle systems are often needed for comparative studies such as system analysis. While system performance can be calculated from that of the components, it is desirable to get a rapid approximation of the actual value without detailed calculation. This is best handled by the introduction of a cycle efficiency, defined as

$$\eta_{cycle} = \frac{\text{Actual COP of cycle}}{\text{Ideal COP of cycle}} \qquad \text{(Eq.108)}$$

4.6.2 (Continued):

The actual COP is calculated, accounting for the performance of all the components, while the ideal COP is evaluated from purely thermodynamic processes. For illustrative purposes, Figure 78 presents the cycle efficiency achieved on a high-speed aircraft vapor cycle system as derived from preliminary calculations found in Reference 19. In this case, the refrigerant was Freon 11, evaporator temperature was 40 °F, and heat load was 2000 to 3000 Btu/min.

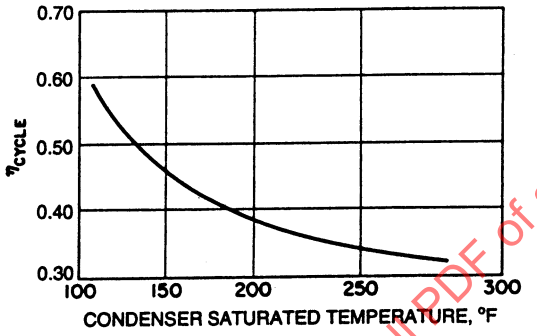

FIGURE 78 - Performance of Vapor Cycle (Reference 36)

4.6.2.1 Demonstration of Vapor Cycle System Analysis: Consider a vapor cycle system to be designed for space application. The requirements are as follows: evaporator temperature 40 °F; condenser temperature, 150 to 250 °F; cooling capacity, 1000 to 2000 Btu/min. A simple cycle with a superheat of 20 °F and a compressor efficiency of 60% will be assumed.

4.6.2.2 Selection of the Refrigerants: Following the steps presented in this study, the factors governing the refrigerant selection are evaluated. The COP of the common refrigerants, the refrigeration effect Q/V_1, and the pressure ratios of the compressor cycle are shown in Figures 79, 80, and 81. Table 20 lists these refrigerants in order of COP for a condenser temperature of 250 °F.

There appears to be little to chose from when the relative standings of each refrigerant are added on a basis of 1, 2, 3, 4. Other factors, such as state-of-the-art in component development, must be taken into consideration in a final selection. For illustrative purposes, Freon 11 has been chosen in this example.

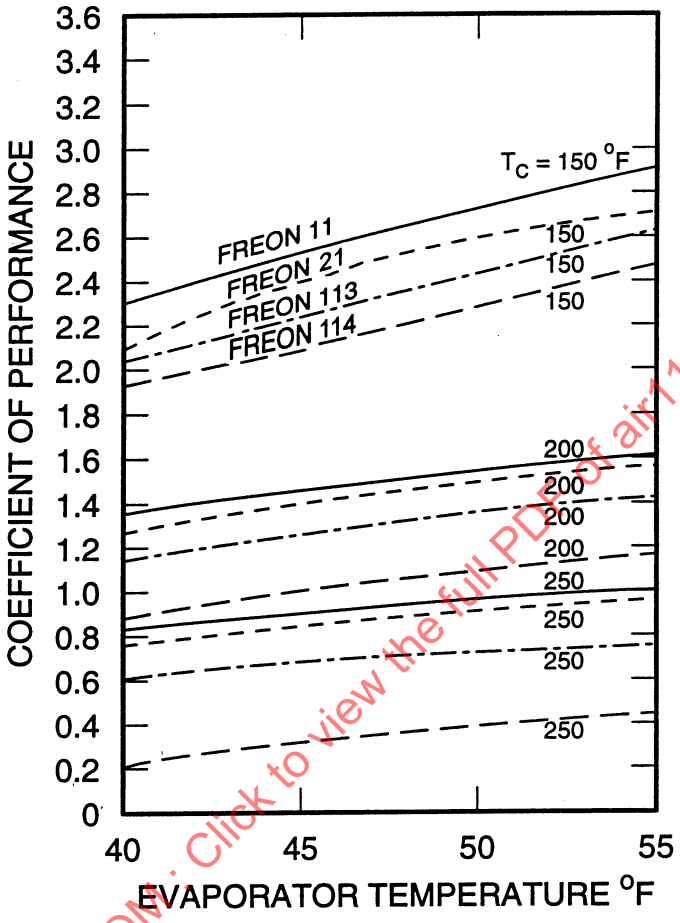

FIGURE 79 - Coefficient of Performance of Freon Refrigerants;
20 °F Superheat and 60% Compressor Efficiency (Reference 31)

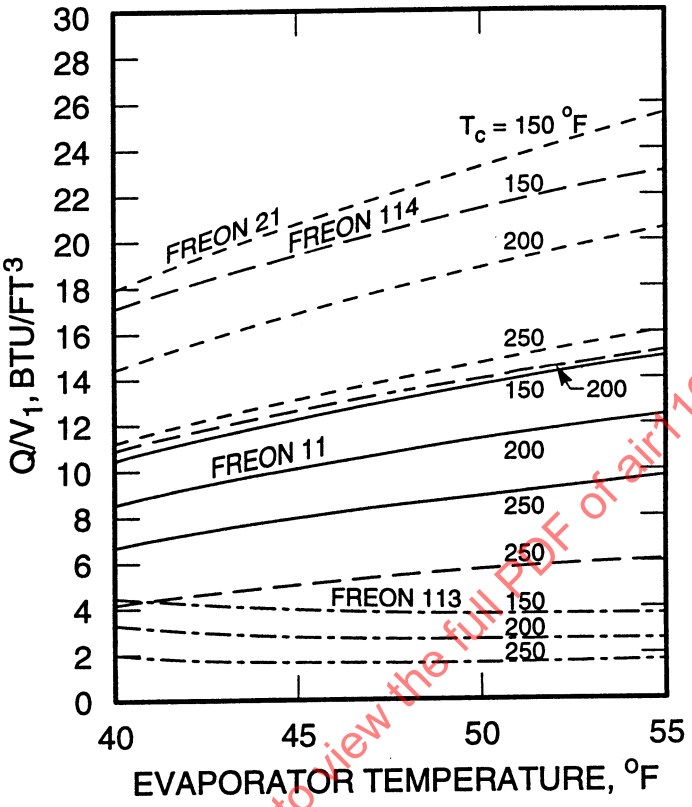

FIGURE 80 - Refrigeration Effect Per Unit Volume for Freon Refrigerants; 20 °F Superheat and 60% Compressor Efficiency (Reference 31)

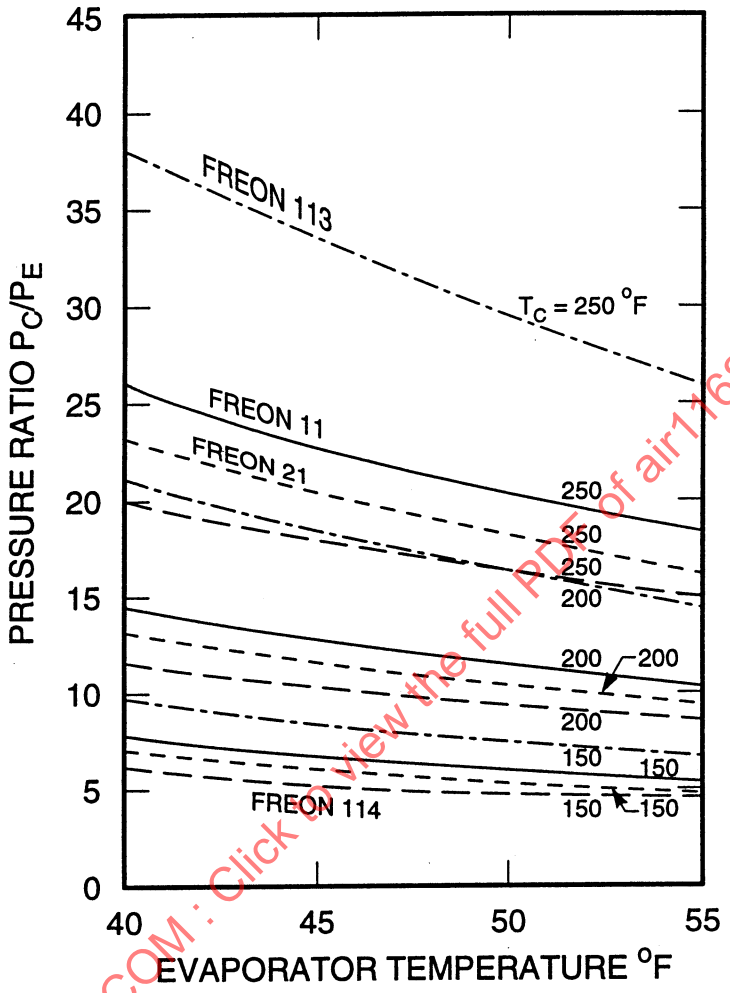

FIGURE 81 - Ratio of Condenser Pressure to Evaporator Pressure for Freon Refrigerants; 20 °F Superheat, 60% Compressor Efficiency (Reference 31)

TABLE 20 - Summary of Properties of Selected Refrigerants[1]

Coefficient of Performance, COP		Refrigeration Effect, Q/V_1, Btu/ft^3		Pressure Ratio, P_c/P_e		Condenser Pressure P_c, psia		Evaporator, $\Delta T/\Delta P$		Σ of Relative Positions in Preceding Columns
F-11	0.85	F-113	2.06	F-114	20.4	F-113	102	F-114	3	12
F-21	0.77	F-114	4.15	F-21	23.2	F-11	182	F-21	3.5	13
F-113	0.63	F-11	6.7	F-11	26	F-21	295	F-11	6	13
F-114	0.28	F-21	11.1	F-113	28.5	F-114	310	F-113	13	12

[1] Evaporator temperature, 40 °F; condenser temperature, 250 °F.

4.6.2.3 Performance Characteristics and Estimate of System Weight: Conditions of systems operating at 250 °F and 150 °F condenser temperatures are as follows:

1. Condenser Temperature 250 °F – Table 21 represents the characteristics of a Freon 11 system operating at a condenser temperature of 250 °F. With a COP of 0.85, the compressor power required for a system with a cooling capacity of 2000 Btu/min (10 tons) is 55.4 hp. The radiator accounts for 69% of the total. The estimated radiator weight would be considerably higher with protection from meteoritic damage.

TABLE 21 - Vapor Cycle System Weight and Performance Characteristics[1]

Characteristic	Weight, lb for Cooling Capacity, in Btu/min 1000	Weight, lb for Cooling Capacity, in Btu/min 2000	Source of Information
Evaporator, Plate-Fin Design			
P = 0.3 psia			Data from Reference 32
$T_{air\ side}$ = 25 °F	7.5	13.5	25% for header
Superheater	7	10	Reference 31
Expansion Valve	3	5	Reference 31
Receiver	3	4	Reference 31
Refrigerant	7	10	Reference 31
Temperature Control	6	6	Reference 31
Centrifugal Compressor and			
400 cycle AC Electric Motor	35	50	AiResearch Mfg. Co.
Condenser Radiator with			
Tapered Tubes and			Figure 69
Conventional Design	104	218	W_T/Q_R = 3 lb-s/Btu
Total	172.5	316.5	
COP	0.85	0.85	
Compressor hp Required	27.7	55.4	

[1] Conditions of operation, using Freon 11: evaporator, 40 °F; radiator condenser, 250 °F; 20 deg superheat; 60% compressor efficiency.

Table 21 also shows the weight estimate for a system with 1000 Btu/min in cooling capacity. It can be seen that the system weight variation relates principally to radiator weight. Thus, for a reasonable range of cooling capacities, the system weight can be written as

$$W_{T2} = W_{T1} + Q_c\left(1+\frac{1}{COP}\right)\left(\frac{W_{T2}+W'}{Q_R}\right) \qquad \text{(Eq.109)}$$

4.6.2.3 (Continued):

where:

W_{T1} = Weight of system components, compressor, refrigerants, evaporators, and others except condenser-radiator, lb
W_{T2} = Condenser radiator weight (such as given in Figure 80), lb
W' = Increment in radiator weight for meteoritic protection, lb

and Q_c and Q_R are given in Btu/s.

Equation 109, valid within a given range of capacities, is predicated upon a radiator weight that is large compared with that of other components. For a wide range of capacities, variation with capacity of the evaporator weight, electric motor weight, and of other component weights must be taken into account.

2. Condenser Temperature 150 °F – Table 22 presents the characteristics of a Freon 11 system operating with a condenser temperature of 150 °F. With the thermodynamic properties of Freon, a COP of 2.3 is achieved as compared with 0.85 for the 250 °F condenser. Thus, a 10 ton cooling system requires a compressor power of only 20.5 hp.

TABLE 22 - Vapor Cycle System Weight and Performance Characteristics[1]

Characteristic	Weight, lb for Cooling Capacity in Btu/min 1000	Weight, lb for Cooling Capacity in Btu/min 2000	Source of Information
Evaporator, Plate-Fin Design			Data from Figures
P = 0.3 psia			60 and 61
$T_{air\ side}$ = 25 °F	7.5	13.5	25% for header
Superheater	7	10	Reference 31
Expansion Valve	3	5	Reference 31
Receiver	3	4	Reference 31
Refrigerant	7	10	Reference 31
Temperature Control	6	6	Reference 31
Centrifugal Compressor and			
400 cycle AC Electric Motor	25	35	AiResearch Mfg. Co.
Condenser Radiator with			
Tapered Tubes and			Figure 69
Conventional Design	129	258	W_T/Q_R = 5.4 lb-s/Btu
Total	187.5	341.5	
COP	2.3	2.3	
Compressor hp Required	10.25	20.5	

[1] Conditions of operation, using Freon 11: evaporator, 40 °F; radiator condenser, 150 °F; 20 deg superheat; 60% compressor efficiency.

4.6.2.3 (Continued):

Because of operation at a lower temperature level, the radiator specific weight (weight per unit of heat rejection rate, lb-s/Btu) increases. Relatively, resulting radiator weight is even larger than in the previous case.

4.6.2.4 Condenser Temperature for Optimum Vapor Cycle System Weight: The demonstration estimate indicates reasons for high condenser temperature operation to decrease the system weight. The examples indicate a difference of only 6.5% between 150 °F and 250 °F operation. With the 150 °F condenser, this difference would be further reduced with a compressor of higher efficiency (compatible with 1965 year technology).

Retaining Freon 11 as a refrigerant, operation at a temperature higher than 250 °F will not be advantageous, from the weight viewpoint, because the COP begins to deteriorate considerably, introducing a large amount of heat to be rejected to the environment. This problem must be considered in addition to that of refrigerant stability. Thus the feasibility of higher condenser temperature operation is to be sought in the high temperature refrigerants mentioned earlier in this study.

4.6.2.5 Vapor Cycle Subsystem in the Thermal Environmental Control System: If integration of the vapor cycle subsystem in an environmental control system is considered, an optimum weight of both the vapor cycle and power systems may require a condenser operating temperature different from the optimum of the vapor cycle system alone. From the previous numerical examples, the ratio

$$\frac{hp_{250\ °F}}{hp_{150\ °F}} = \frac{55.4}{20.5} = \frac{COP_{150\ ëF}}{COP_{250\ ëF}} = \frac{2.3}{0.85} = 2.71 \qquad \text{(Eq.110)}$$

indicates that operation at 250 °F requires 2.71 times more power. The energy rejected due to inefficiency in the generation of the necessary compressor power is then much more.

In Reference 37, the optimization of this system assumes that the energy associated with the inefficiency of power generation is rejected to the environment at the same temperature as that of the condenser of the vapor cycle system. For optimization, this study calls for a high condenser temperature, even beyond the limits of existing refrigerants.

While the weight consideration is of prime importance, the integrity of the vapor cycle system must still be considered. Previous numerical examples consider Freon 11 for operation at 250 °F. Practically, such a system would require a change in refrigerant after short periods of operation. There also exists the possibility of using a refrigerant with a lower COP, a higher system weight, and a considerable improvement in reliability.

4.6.3 Gas Cycle Method: Gas cycle cooling methods should be considered for space application for several reasons. For example, the problems usually associated with vapor cycles, such as toxicity, leakage, and availability of the refrigerant, can be avoided by proper selection of the working fluid. More important, however, is the absence of problems associated with weightlessness and with two-phase flow.

Gas cycle cooling can operate in an open or a closed loop. In the open circuit, the gas circulating through the cooling loop is supplied directly from the source. After being processed in the cooling system, it is then returned to the same source. In the closed cycle, the same amount of refrigerant, continuously circulated through the cooling system, absorbs heat from the environment through a heat exchanger.

4.6.3.1 Thermodynamics and Operation: Gas cycle cooling systems usually operate on the reversed Brayton cycle, though cooling systems using Stirling and other cycles have been successful. The Brayton cooling cycle is shown on the T-S diagram of Figure 82. The system diagram of this closed cycle is shown schematically in Figure 83. The cycle consists of four major components: compressor, turbine, radiator, and heat exchanger. In an open cycle, the heat exchanger is eliminated, since the cooling fluid is allowed to flow directly to the environment.

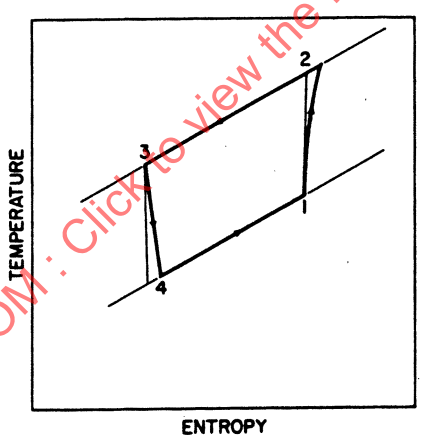

FIGURE 82 - Temperature Entropy Diagram of the Brayton Cycle

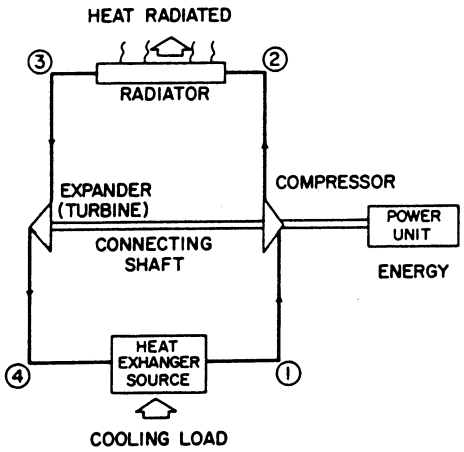

FIGURE 83 - A Gas Cycle Cooling System

4.6.3.1 (Continued):

The gas entering the compressor is at condition 1 and relatively warm (Figure 83). In going through the compressor during process 1–2, its temperature and pressure are raised. This gas then flows at constant pressure through the radiator, rejecting heat to the sink, which must be at a lower temperature, during process 2–3. The cooled gas is then expanded in a turbine during process 3–4, where work is extracted from the fluid. At the turbine exit, the gas temperature is low enough to absorb heat from the environment, as it does during the constant pressure process 4–1.

4.6.3.2 Performance Characteristics: Gas cycle system performance is measured by its coefficient of performance, defined in the same way for gas as for vapor cycles:

$$\text{COP} = \frac{\text{Heat extracted}}{\text{Cycle work}} \qquad \text{(Eq.111)}$$

In making a generalized study of the influence on the performance of the cycle, it is assumed that the circulating fluid is a perfect gas and that the evaporator and radiator operate with 100% efficiency. Pressure drops in these components are not taken into account. (Effects of the inefficiency of the components on cycle performance are discussed in Reference 30.) The COP of the cycle of Figure 82 can then be written as

$$\text{COP} = \frac{\Delta T_E / T_4}{\left(\Delta T_E / T_4\right) - \left(\Delta T_c / \Delta T_t\right)} \qquad \text{(Eq.112)}$$

4.6.3.2 (Continued):

where:

ΔT_E = Temperature rise in source heat exchanger, °R
ΔT_c = Temperature rise in compressor, °R
ΔT_t = Temperature drop in turbine, °R
T_4 = Temperature of turbine exit, °R

The ratio $\Delta T_E/T_4$ is of interest to the designer of cooling systems, for it establishes the heat transfer from the environment to the system. The effects of temperature differences on operating conditions are described as follows:

1. Effect of the Adiabatic Exponent – The temperature ratios of Equation 112 can be calculated in terms of the cycle pressure ratio r, the turbine and compressor efficiencies η_t and η_c, and the adiabatic exponent of the gas γ (that is, $r = P_2/P_1$):

$$\frac{\Delta T_1}{T_4} = \frac{\eta_t Y_t}{(1-\eta_t)Y_t + 1} \quad \text{(Eq.113)}$$

$$\frac{\Delta T_c}{T_4} = \left(1 + \frac{\Delta T_c}{T_4}\right)\frac{Y_c}{\eta_c} \quad \text{(Eq.114)}$$

where:

$$Y = r^{(\gamma-1)/\gamma} - 1$$

For a given value of the design ratio of temperatures, $\Delta T_E/T_4$, it can be seen that the nature of the fluid influences COP only through the exponent γ. Figures 84 and 85 present the COP that can be achieved for two typical values of the ratio $\Delta T_E/T_4$ and assumed values of the compressor and turbine efficiency. In addition, these figures carry the lines of constant T_m/T_4, where T_m is the arithmetic mean of the inlet and exit radiator temperatures.

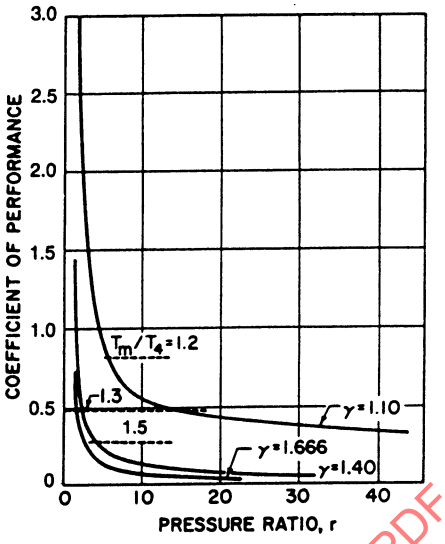

FIGURE 84 - Relationship of Gas Cycle Coefficient of Performance to Pressure Ratio; $\Delta T_E/T_4 = 0.0588$, $\eta_c = \eta_t = 0.85$, $\Delta P = 0$; T_m/T_4 Values on the Curves are the Arithmetic Mean of Inlet and Exit Temperatures

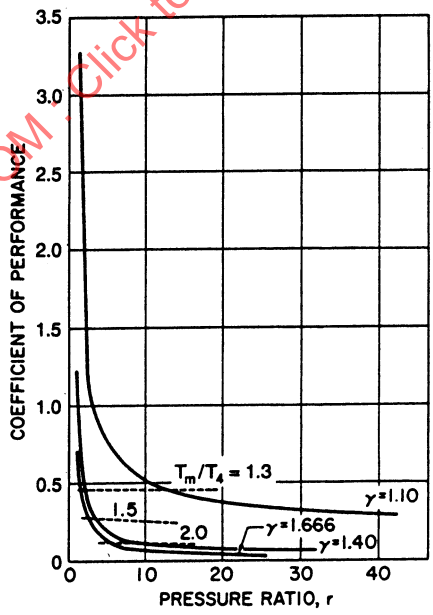

FIGURE 85 - Relationship of Gas Cycle Coefficient of Performance to Pressure Ratio; $\Delta T_E/T_4 = 0.0492$, $\eta_c = \eta_t = 0.85$, $\Delta P = 0$

4.6.3.2 (Continued):

Air, a refrigerant that has many advantages in the gas cycle, shows a low COP compared to that of conventional vapor cycles. To achieve comparable COP values, air cycles would have to operate between pressure ratios of 1 and 2, with a resulting low value of T_m/T_4, a characteristic indicating the requirement for a larger radiator area. These figures also show that the coefficient of performance does improve with fluids of lower values of γ, and that there is not an appreciable difference in COP for γ values between 1.4 and 1.666.

2. Effect of Specific Heat, c_p – From the analytical expression for COP, it appears that the specific heat of the gas does not affect cycle performance. In a gas refrigeration system it does influence the flow rate through the system in accordance with the relationship

$$w = \frac{Q_c}{c_p \Delta T_E} \qquad \text{(Eq.115)}$$

where Q_c is given in Btu/s and the temperature rise in the source heat exchanger, ΔT_E, is in °F or °R.

To introduce the concept of specific flow rate, that is, the flow rate required per unit of cooling load, Equation 115 is written as

$$\frac{w}{Q} = \frac{1}{c_p T_4 \left(\Delta T_E / T_4\right)} \qquad \text{(Eq.116)}$$

It can be seen that the specific flow rate, w/Q, is inversely proportional to the specific heat c_p. This flow rate is often used as an approximate measure of the size of the equipment required for the cooling system.

Besides the flow rate, the specific heat also establishes the boundaries of practical application of the gas cycle using compressors and turbines. For this type of equipment, the energy input per unit mass rate of flow is given by relationships such as the head rise in the compressor:

$$H_{ad} = \frac{Jc_p T_{in}\left[r^{(\gamma-1)/\gamma} - 1\right]}{\eta_c} \qquad \text{(Eq.117)}$$

The head, H_{ad}, represents a temperature rise and cannot be taken above the limits set up by the physical properties of the material. It follows, then, that for a given inlet temperature T_{in}, the specific heat establishes a maximum value of the pressure ratio usable in the gas cycle.

4.6.3.2 (Continued):

3. Radiator Area – In this comparative study, it will be assumed for simplicity that the radiator rejects heat at the mean temperature T_m to outer space having a temperature of 0 °R. The radiator area required for a cooling capacity Q_c is given by

$$Q_c\left(1+\frac{1}{COP}\right)=A\sigma e T_m^4 \qquad \text{(Eq.118)}$$

where:

$$T_m=\left(\frac{T_{in}+T_{ex}}{2}\right) \qquad \text{(Eq.119)}$$

The area A* of a radiator required to handle the heat rejection rate Q at the turbine exit temperature T_4 is now defined as

$$Q = A^*\sigma \in T_4^4 \qquad \text{(Eq.120)}$$

Using Equation 118, a nondimensional relation is now established:

$$\frac{A}{A^*}=\frac{1+(1/COP)}{(T_m/T_4)^4} \qquad \text{(Eq.121)}$$

This dimensionless area ratio is shown in Figures 86 and 87 superimposed on various values of pressure ratios, COP and γ. For a large number of gases with $\gamma = 1.4$, operation at a COP of 0.5 requires an increase in radiator area of 30% over that of a system having a COP of 0.2.

The variation of the radiator area with pressure ratio is presented in Figures 88 and 89. Starting with small pressure ratios, the radiator area increases as it must reject the mechanical energy input in addition to the cooling load. As the pressure ratio increases, the radiator temperature rises, permitting a higher rate of heat rejection with a consequent decrease in required area.

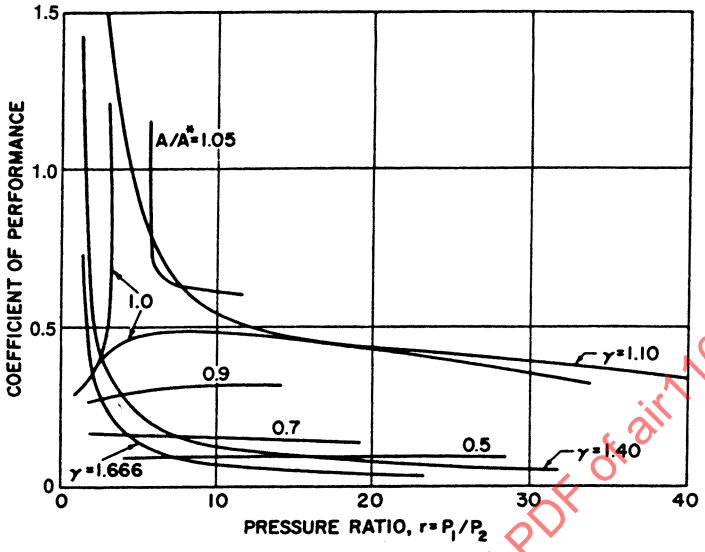

FIGURE 86 - Radiator Requirements of Gas Cycle Systems;
$\Delta T_E/T_4 = 0.0588$, $\eta_t = \eta_c = 0.85$

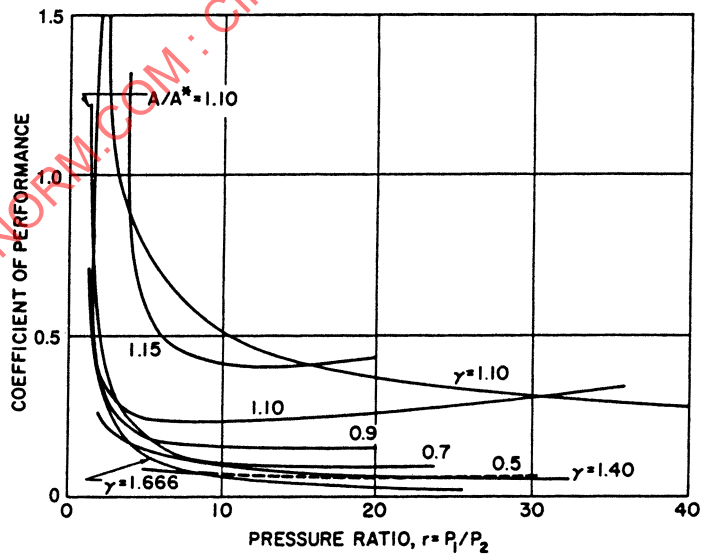

FIGURE 87 - Radiator Requirements of Gas Cycle Systems;
$\Delta T_E/T_4 = 0.0492$, $\eta_c = \eta_t = 0.85$

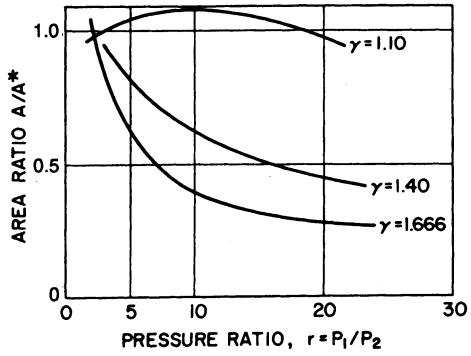

FIGURE 88 - Relationship of Radiator Area Ratio to Cycle Pressure Ratio;
$\Delta T_E/T_4 = 0.0588$, $\eta_c = \eta_t = 0.85$

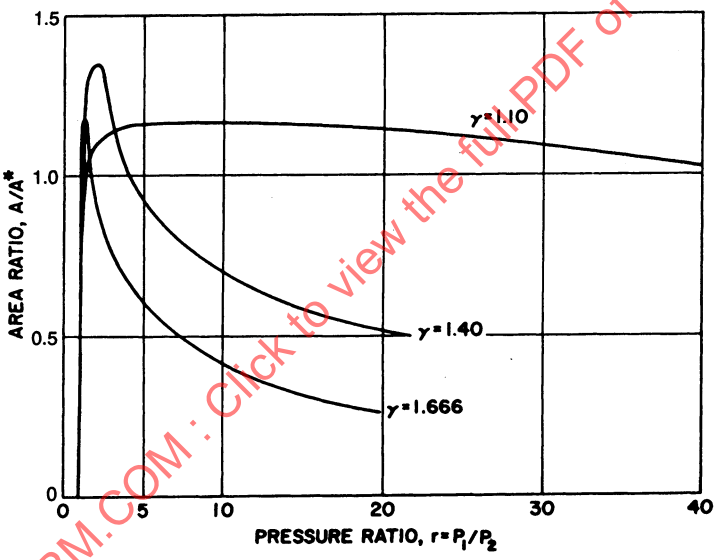

FIGURE 89 - Relationship of Radiator Area Ratio to Cycle Pressure Ratio;
$\Delta T_E/T_4 = 0.0492$, $\eta_c = \eta_t = 0.85$

4.6.3.3 Fluids for Gas Cycle Systems: Among the fluids usable in a gas cycle, air has the most advantages. A major advantage is the possibility of its application in a nontoxic open cycle in an environmental control system for human use. The components for the cycle are well developed and available today. Extensive studies of both air and hydrogen gas cycles may be found in Reference 38.

Hydrogen deserves consideration because its γ value of 1.4 yields the same COP as air. Its high specific heat, however, dictates a lower flow rate for any given refrigeration load. The advantage of hydrogen lies, then, in a reduction in the size of the system components when large cooling requirements are encountered. One disadvantage is its high combustibility.